# SYNTHESIS AND CHARACTERIZATION OF SOLUTION AND MELT PROCESSIBLE POLY(ACRYLONITRILE-*CO*-METHYL ACRYLATE) STATISTICAL COPOLYMERS

Padmapriya Pisipati

Dissertation submitted to the faculty of the Virginia Polytechnic Institute and State University in partial fulfillment of the requirements for the degree of

Doctor of Philosophy
in
Macromolecular Science and Engineering

**James E. McGrath, Chair**
**Judy S. Riffle, Acting Chair**
**Eugene G. Joseph**
**Sue J. Mecham**
**Donald G. Baird**

02/20/2015
Blacksburg, VA

Keywords: melt processability, polyacrylonitrile, carbon fibers, methyl acrylate, acrylic fibers, plasticizer, solution processing, high tensile modulus

Copyright 2015, Padmapriya Pisipati

# SYNTHESIS AND CHARACTERIZATION OF SOLUTION AND MELT PROCESSIBLE POLY (ACRYLONITRILE-*CO*-METHYL ACRYLATE) STATISTICAL COPOLYMERS

## ABSTRACT

**Padmapriya Pisipati**

Polyacrylonitrile (PAN) and its copolymers are used in a wide variety of applications ranging from textiles to purification membranes, packaging material and carbon fiber precursors. High performance polyacrylonitrile copolymer fiber is the most dominant precursor for carbon fibers. Synthesis of very high molecular weight poly(acrylonitrile-*co*-methyl acrylate) copolymers with weight average molecular weights of at least 1.7 million g/mole were synthesized on a laboratory scale using low temperature, emulsion copolymerization in a closed pressure reactor. Single filaments were spun via hybrid dry-jet gel solution spinning. These very high molecular weight copolymers produced precursor fibers with tensile strengths averaging 954 MPa with an elastic modulus of 15.9 GPa (N = 296). The small filament diameters were approximately 5 µm. Results indicated that the low filament diameter that was achieved with a high draw ratio, combined with the hybrid dry-jet gel spinning process lead to an exponential enhancement of the tensile properties of these fibers.

Carbon fibers for polymer matrix composites are currently derived from polyacrylonitrile copolymer fiber precursors where solution spinning accounts for ~40 % of the total fiber production cost. To expand carbon fiber applications into the automotive industry, the cost of the carbon fiber needs to be reduced from $8 to ~$3-5. In order to develop an alternative melt processing route several benign

plasticizers have been investigated. A low temperature, persulfate-metabisulfite initiated emulsion copolymerization was developed to synthesize poly(acrylonitrile-*co*-methyl acrylate) copolymers with acrylonitrile contents between 91-96 wt% with a molecular weight range of 100-200 kg/mol. This method was designed for a potential industrial scale up. Furthermore, water was investigated as a potential melting point depressant for these copolymers. Twenty-five wt% water lead to a decrease in the $T_m$ of a 93/7 wt/wt % poly(acrylonitrile-*co*-methyl acrylate) of $M_w$ = 200 kg/mol to 160 $^0$C as measured via DSC.

Glycerin, ethylene glycol and glycerin/water combinations were investigated as potential plasticizers for high molecular weight (~200,000 g/mol), high acrylonitrile (93-96 mole:mole %) content poly(acrylonitrile–*co*-methyl acrylate) statistical copolymers. Pure glycerin (25 wt %) induced crystallization followed by a reduced "$T_m$" of about 213 $^0$C via DSC. However this composition did not melt process well. A lower $M_W$ (~35 kg/mol) copolymer did extrude with no apparent degradation. Our hypothesis is that the hydroxyl groups in glycerin (or water) disrupt the strong dipole-dipole interactions between the chains enabling the copolymer endothermic transition ($T_m$) to be reduced and enable melting before the onset of degradation. Additionally high molecular weight ($M_w$ = 200-230 kg/mol) poly(acrylonitrile–*co*-methyl acrylate) copolymers with lower acrylonitrile content (82-85 wt %) were synthesized via emulsion copolymerization and successfully melt pressed. These materials will be further investigated for their utility in packaging applications.

## ACKNOWLEDGEMENTS

I would like to express my sincerest and deepest gratitude to my late advisor Dr. James McGrath for his persistent guidance, support and help throughout the four years that I have worked in his research group. I could not have asked for a better advisor and this dissertation would most certainly not be possible without him. I would also like to express my sincerest thanks to Prof. Riffle for her help, support and tremendous patience in seeing me through the rest of my Ph.D. after the passing of Dr. McGrath. In addition I would like to thank my committee members: Dr.Sue Mecham, for sharing her scientific knowledge, help with the experiments and for playing a huge role in helping the research projects run smoothly; Dr. Eugene Joseph, for his scientific advice and for being a constant source of support and encouragement; Dr.Turner and Dr.Baird for their valuable scientific insights and support.

Furthermore I would like to thank my labmates, especially Matt for his meticulously planned and executed research work, and both Matt &Ali for the helpful research discussions, advice and more importantly their friendship and light heartedness that has kept me sane. I would be remiss to not thank Ozzie for her generosity in helping me edit my technical work and for her support.

Lastly, I would like to thank my family-my mom Pisipati Rajeswari, my brother Pawan and sister-in-law Shaama, for always being there and for showing me every day what it is to be wonderful and compassionate human beings. Most of all I would like to thank my late father Pisipati Lakshmi Narasimha Swamy, for his unconditional love and support, no matter what. This is for you.

## ATTRIBUTION

Several of my colleagues aided in the research behind some of the chapters presented here in my dissertation. A brief description of their contribution is given below:

**CHAPTER 2 Synthesis, Spinning, And Properties Of Very High Molecular Weight Poly(Acrylonitrile-Co-Methyl Acrylate) For High Performance Precursors For Carbon Fiber**

Ashley Morris, Ph.D. is a Senior Research Engineer at University of Kentucky Center for Applied Energy Research. Ashley served as a co-author and designed and oversaw the hybrid-jet gel spinning, mechanical testing and characterization, of the copolymers discussed in the chapter.

Stephanie Bradley, B.S. is currently an Application Engineer at Lectrodryer, LLc,. Stephanie served as a co-author and was involved in the processing and characterization of the copolymers fibers discussed in the chapter.

Matthew C. Weisenberger, Ph.D. is an Engineer Associate at University of Kentucky Center for Applied Energy Research. Dr.Weisenberger served as a co-author and oversaw the project and is the principal investigator.

Mohamed G. Abdallah, Ph.D., PE. is a fiber consultant for Oak Ridge National Laboratories. He served as a co-author on this paper and aided in design of the experiments.

Sue J. Mecham, Ph.D. is a Research Associate in the department of Chemistry at the University of North Carolina. Sue served as a co-author and oversaw and ran SEC experiments for the copolymers that were discussed in this chapter.

James E. McGrath, Ph.D. (Macromolecular Science and Engineering) is a co-author on this paper and was the advisor of the author and oversaw the project.

**CHAPTER 3 Low Temperature Synthesis And Characterization Of Poly(Acrylonitrile-Co-Methyl Acrylate) Statistical Copolymers And Their Water Blends**

R. Matthew Joseph, B.S. is a graduate student in the department of Macromolecular Science and Engineering at Virginia Tech. Matt is a co-author and performed the synthesis of the poly (acrylonitirile-*co*-methyl acrylate) copolymers listed in Table 3-3.

Ann Norris, Ph.D. is a lab technician in the department of Sustainable Biomaterials at Virginia Tech. Ann is a co-author and performed the X-ray diffraction experiments on the poly(acrylonitirile-*co*-methyl acrylate) copolymers for the plots shown in Figure 3-8 of Chapter 3.

Judy Riffle, Ph.D.; is a Professor in the department of Chemistry at Virginia Tech. Prof. Riffle, a co-author is the author's advisor and oversaw the project.

James E. McGrath, Ph.D.; was a Professor in the department of Chemistry at Virginia Tech for the first years of this project and co-author. He unfortunately passed away in May of 2014. Prof. McGrath was the author's advisor and oversaw the project.

**CHAPTER 4 Thermal Characterization Of Poly(Acrylonitrile-Co-Methyl Acrylate) Statistical Copolymers And Their Water And Alcohol Plasticizer Blends**

Sue Mecham, Ph.D. is a Research Associate in the Department of Chemistry at the University of North Carolina. Sueis a co-author, oversaw much of the work and ran SEC experiments for the copolymers that were discussed in this chapter. Those molecular weights are listed in Table 4-3.

Judy Riffle, Ph.D. is Professor in the department of Chemistry at Virginia Tech. Prof. Riffle, who served as a co-author is the author's advisor and oversaw the project.

James E. McGrath, Ph.D. is a co-author and was a Professor in the department of Chemistry at Virginia Tech. Prof. McGrath was the author's advisor and oversaw the project during the first few years.

**Chapter 5 Melt Processable Poly (Acrylonitrile-Co-Methyl Acrylate) Copolymers: Effect Of The Comonomer Content**

Judy Riffle, Ph.D. is a co-author and a Professor in the department of Chemistry at Virginia Tech. Prof. Riffle is the author's advisor and oversaw the project.

James E. McGrath, Ph.D. is a co-author and was a Professor in the department of Chemistry at Virginia Tech. Prof. McGrath was the author's advisor and oversaw the project.

TABLE OF CONTENTS

CHAPTER 1 LITERATURE REVIEW ..... 1
1.1 Introduction ..... 1
1.1.1 Acrylonitrile Synthesis ..... 1
1.1.2 Polyacrylonitrile Based Fibers ..... 3
1.1.3 Polymerization ..... 11
1.1.4 Kinetics of Free Radical Addition ..... 12
1.1.5 Kinetics of Free Radical Copolymerization ..... 20
1.1.6 Emulsion Polymerization ..... 23
1.7 Prior Art in Melt Processable PAN ..... 39
1.7.1 Comonomers for Melt Processible PAN ..... 39
1.7.2 Plasticizers for Melt Processible PAN ..... 42
Chapter 2 : SYNTHESIS, SPINNING, AND PROPERTIES OF VERY HIGH MOLECULAR WEIGHT POLY(ACRYLONITRILE-CO-METHYL ACRYLATE) FOR HIGH PERFORMANCE PRECURSORS FOR CARBON FIBER ..... 45
2.1 Introduction ..... 45
2.1 Experimental ..... 46
2.1.1 Copolymer Synthesis ..... 46
2.1.2 Polymer Characterization ..... 49
2.3 Spinning of VHMW PAN-co-MA Precursor Fibers ..... 53
2.3.1 Dope Preparation ..... 53
2.3.2 Rheological Analysis ..... 54
2.3.3 Fiber Spinning Equipment ..... 55
2.4 As-Spun Fiber Analysis ..... 58
2.4.1 Optical Microscopy ..... 58
2.4.2 Scanning Electron Microscopy (SEM) ..... 58
2.4.3 Mechanical Measurements ..... 59
2.5 Results and Discussion ..... 59
2.5.1 Polymer Composition and Molecular Weight ..... 59
2.5.2 Viscoelastic Properties of the VHMW PAN-co-MA Dope ..... 71
2.5.3 VHMW PAN-co-MA Fiber Spinning Conditions ..... 77

2.5.4 As-Spun Fiber Structure and Physical Properties ..... 79
2.5.5 Effect of Polymer Molecular Weight on As Spun Fiber Properties ..... 86
2.6 Conclusions ..... 89
Chapter 3 LOW TEMPERATURE SYNTHESIS AND CHARACTERIZATION OF POLY(ACRYLONITRILE-co-METHYL ACRYLATE) STATISTICAL COPOLYMERS AND THEIR WATER BLENDS ..... 91
3.1 Introduction ..... 91
3.2 Experimental ..... 96
3.2.1 Materials ..... 96
3.2.2 Synthesis ..... 96
3.2.3 Characterization ..... 97
3.2.4 Preparation of the copolymer and plasticizer blends ..... 100
3.3 Results and Discussion ..... 101
3.3.1 Low Temperature Emulsion Synthesis of the Poly(acrylonitrile-co- ..... 101
methylacrylate) Copolymers ..... 101
3.3.2 Composition analysis by $^{1}$H NMR ..... 103
3.3.3 Thermal Analysis of the Poly (acrylonitrile-*co*-methylacrylate) Water Blends ..... 106
3.3.4 X-Ray Diffraction ..... 109
3.4 Conclusions ..... 112
Chapter 4 THERMAL CHARACTERIZATION OF POLY(ACRYLONITRILE-*co*-METHYL ACRYLATE) STATISTICAL COPOLYMERS AND THEIR WATER AND ALCOHOL PLASTICIZER BLENDS ..... 114
4.1 Introduction ..... 114
4.2 Experimental ..... 119
4.2.1 Materials ..... 119
4.2.2. Synthesis ..... 119
4.3 Characterization ..... 121
4.3.1 Composition Analysis by 1H NMR ..... 121
4.3.2 Molecular Weight Analyses ..... 122
4.3.3 Thermal Analysis ..... 122
4.4 Preparation of copolymer-plasticizer blends ..... 123
4.4.1 Glycerin, 1,4-butanediol, diethylene glycol blends ..... 123

4.4.2 Water and Ethylene glycol blends ..... 124
4.4.3 Glycerin-Water Blends ..... 124
4.5 Results and Discussion ..... 125
4.5.1 $^{1}$H NMR Characterization of the Poly(acrylonitrile-co-methylacrylate) ..... 125
copolymers ..... 125
4.5.2 Thermal properties of blends of poly(acrylonitrile-co-methyl acrylate) with water and alcohol plasticizers ..... 126
4.5 CONCLUSION ..... 137
Chapter 5 : MELT PROCESSABLE POLY (ACRYLONITRILE-CO-METHYL ACRYLATE) COPOLYMERS: EFFECT OF THE COMONOMER CONTENT ..... 139
5.1 Introduction ..... 139
5.2 Experimental ..... 142
5.2.1 Materials ..... 142
5.3 Characterization ..... 144
5.3.1 Composition analysis by $^{1}$H NMR ..... 144
5.3.2 Thermal analysis ..... 144
5.3.3 Molecular Weight Analyses ..... 145
5.3.4 Melt pressing the poly(acrylonitrile-*co*-methyl acrylate) copolymers ..... 146
5.4. Results and Discussion ..... 146
5.4.1 Synthesis of 80/20 wt/wt% poly(acrylonitirile-*co*-methyl acrylate) random ... 146
copolymers ..... 146
5.4.3 Composition and molecular weight analysis ..... 148
5.4.4 Thermal Properties ..... 151
5.5 Conclusion ..... 153
Chapter 6 Conclusions and suggested future research ..... 155
BIBLIOGRAPHY ..... 157

TABLE OF FIGURES

Figure 1-1. Wet spinning of PAN fibers[31] Ismail, A. F.; Rahman, M. A.; Mustafa, A.; Matsuura, T., The effect of processing conditions on a polyacrylonitrile fiber produced using a solvent-free free coagulation process. Materials Science and Engineering: A 2008, 485 (1-2), 251-257. Used under fair use, 2015..... 10
Figure 1-2. Kinetic events in an ab initio emulsion polymerization[73]..... 30
Figure 1-3. Intervals I, II and III in emulsion polymerization.[52] Thickett, S. C.; Gilbert, R. G., Emulsion polymerization: State of the art in kinetics and mechanisms. *Polymer* 2007, *48* (24), 6965-6991. Used under fair use, 2015..... 31
Figure 1-4. Polymerization rate vs monomer conversion in Intervals I, II, III [61] Chern, C. S., *Progress in Polymer Science* 2006, *31* (5), 443-486. Used under fair use, 2015. ... 31
Figure 1-5. (a) Micellar Nucleation Mechanism[61] (b) Homogeneous Nucleation Mechanism[61]. Chern, C. S., *Progress in Polymer Science* 2006, *31* (5), 443-486. Used under fair use, 2015. ..... 36
Figure 2-1. Schematic of the custom fabricated dope mixer for full dissolution of polymer into the solvent ..... 55
Figure 2-2. Nascent filament jets passing through an air gap, accelerating and attenuating from an applied spin draw, and entering the coagulation bath during dry-jet solution spinning ..... 57
Figure 2-3. Schematic of solution spinning line ..... 58
Figure 2-4. $^{1}$H NMR of a 96 wt% AN and 4 wt% MA copolymer..... 61
Figure 2-5. SEC chromatograms of a 97/3 AN/MA copolymer in NMP at 50°C where the sample was filtered through a 1.6 µm filter (SEC analysis results are provided in Table 2-3)..... 64
Figure 2-6. Aggregation is apparent in the comparison of the normalized MALLS chromatograms of 97/3 AN/MA copolymer run in NMP with and without LiBr salt added…….. ..... 69
Figure 2-7. Normalized light scattering chromatograms of a Virginia Tech synthesized VHMW 97/3 AN/MA compared to a commercially prepared 93/7 AN/MA copolymer run in NMP with 0.05 M LiBr..... 69
Figure 2-8 Light Scattering chromatograms of the 85/ 15 wt/ wt% Poly(acrylonitrile-co-methyl acrylate) samples at different time points ..... 70
Figure 2-9. Steady state shear viscosities of VHMW polymer dopes as a function of shear rate at 25 °C ..... 72
Figure 2-10. The storage and loss shear moduli as a function of temperature with an angular frequency of 10 rad/s for dope showing the crossover point of G' and G"..... 73
Figure 2-11. Spinnable windows for rheological properties determined experimentally 74
Figure 2-12. Oscillatory rheology of a VHMW polymer solution ($M_w$ = 1.3M) ..... 76

Figure 2-13. Oscillatory rheology of a LMW PAN-*co*-MA polymer solution ($M_w$ = 200k) showing marked differences in the storage and loss shear moduli as a function of temperature compared to the VHMW PAN (Figure2-11). ..... 76
Figure 2-14. 560 m of hybrid dry-jet, gel spun VHMW PAN-*co*-MA fiber in 100 filament count tow (5.7 ± 0.4 µm filament diameter, 1037 ± 101 MPa tensile strength, and 17.9 ± 1 GPa elastic modulus) ..... 78
Figure 2-15. Reflected light optical microscopy of VHMW PAN-*co*-MA fiber ends embedded in epoxy, magnification 1000x ..... 79
Figure 2-16. Precursor fiber cross section imaged using SEM (a) Fibers at 1000x magnification (bean-shape highlighted by arrows). (b) Fibers at 3000x magnification (bean-shape highlighted by arrows). (c) 10kx magnification shows smooth fiber surface, typical of dry-jet spun fibers. (d) High magnification (100kx) shows striations in the fiber surface, typical for fibers produced using a diffusion coagulation process ..... 80
Figure 2-17. SEM images of dry-jet spun VHMW PAN-*co*-MA fiber. ..... 81
Figure 2-18. Tensile properties of precursor dry-jet, gel spun fibers in this work from VHMW PAN-*co*-MA ..... 85
Figure 2-19. Fiber tensile properties for filament diameters in the 4-6 µm range, showing the average values for break stress and modulus ..... 85
Figure 2-20. Results shown in Figure 17 separated into high vs. low molecular weight to show the impact of molecular weight on tensile strength ..... 87
Figure 3-1. (a) Antiparallel arrangement giving rise to maximum attraction. ..... 92
Figure 3-2. (a) refractive index vs concentration plot of a 93/7 wt/wt % poly(acrylonitrile-co-methyl acrylate) copolymer (b) dn/dc calibration curve as a function of copolymer composition. ..... 99
Figure 3-3. Structure of Poly(acrylonitrile-*co*-methylacrylate) ..... 104
Figure 3-4. $^1$H NMR spectrum of a 94/6 wt/wt % poly(acrylonitrile-co-methyl acrylate) 104
Figure 3-5. Light scattering chromatograms of poly(acrylonitrile-co-methyl acrylate) entries 1-4 ..... 105
Figure 3-6. Thermal characterization of the 94/6 wt/wt % poly(acrylonitrile-*co*-methylacrylate copolymer ..... 107
Figure 3-7. Thermal characterization data of the poly(acrylonitrile-*co*- methylacrylate) copolymers ..... 109
Figure 3-8 . X-ray diffractograms of poly(acrylonitrile-co-methylacrylate) copolymers (a)full scale (b) zoomed region between $2\theta$ = 12 and 20. ..... 111
Figure 4-1. $^1$H NMR spectrum of a 95:5 mole:mole % poly(acrylonitrile-*co*-methyl acrylate) copolymer ..... 125
Figure 4-2. DSC plot of the 95:5 mole:mole % poly(acrylonitrile-*co*-methylacrylate) at two different heat scans: (1) 10 $^0$C/min and (2) 80 $^0$C/min. ..... 126
Figure 4-3. DSC thermogram of the 95:5 mole:mole % poly(acrylonitrile-*co*-methylacrylate) and water blends (1) 50 mole % water (2) 56 mole%water ..... 127

Figure 4-4. DSC overlay of the (95:5 mole:mole % poly (acrylonitrile-*co*-methylacrylate) + glycerin) blends of various ratios ..... 130
Figure 4-5. DSC thermograms of the glycerin-water and 95:5 mole:mole %poly(acrylonitrile-*co*-methylacrylate) copolymer blends G= glycerin and W = water 131
Figure 4-6. Transition temperatures of glycerin/water (mole:mole % ) blends with the 95:5 mole:mole % poly(acrylonitrile-*co*-methylacrylate) ..... 132
Figure 4-7. DSC overlay of the 95:5 mole:mole % poly(acrylonitrile-*co*-methyl acrylate) copolymer and plasticizer blends: (1)95:5 mole:mole% copolymer (2) 25 mole % *1,4*-butanediol (3) 16 mole % glycerin(4) 22 mole % ethylene glycol ..... 133
Figure 4-8. DSC thermogramsof the ethylene glycol blends with the 95:5 mole:mole % poly(acrylonitrile-*co*-methylacrylate) ..... 134
Figure 4-9. Effect of moles OH/CN ratio on the thermal transitions ..... 135
Figure 4-10. SEC chromatograms of the AN/MA mole:mole % copolymer (1) 95:5 (2) 90:10 (3) 97:3 ..... 136
Figure 5-1. $^{1}$H NMR of an 82/18 wt/wt % poly(acrylonitrile-*co*-methyl acrylate) copolymer prepared by emulsion copolymerization ..... 149
Figure 5-2. Light scattering chromatograms of the poly(acrylonitrile-*co*-methyl acrylate) copolymers ..... 150
Figure 5-3. Intrinsic viscosity of the 82/18 wt/wt % poly(acrylonitrile-*co*-methyl acrylate) emulsion copolymer ..... 151
Figure 5-4 DSC thermograms of the poly(acrylonitrile-*co*-methyl acrylate) copolymers: (1) 82/18 AN/MA wt/wt% suspension, (2) 85/15 wt/wt % emulsion, and (3) 82/18 wt/wt % emulsion ..... 152
Figure 5-5. Melt pressed discs of poly(acrylonitrile-*co*-methyl acrylate) copolymers:1) 82/18 wt/wt% AN/MA, suspension (2) 85/15 wt/wt% AN/MA, emulsion (3) 82/18 wt/wt% AN/MA, emulsion ..... 153

LIST OF TABLES

Table 1-1. Polymer compositions of acrylic fibers[9] ..... 4
Table 1-2. Composition for Emulsion Polymerization of Styrene-Butadiene[36] ..... 25
Table 2-1. Statistical analysis of 24 batches of polyacrylonitrile-co-methyl acrylate copolymers ..... 61
Table 2-2. Dilute solution viscosity measurements of a sample of very high molecular weight polyacrylonitrile-co-methyl acrylate ..... 63
Table 2-3. SEC analysis of the same 97/3 AN/MA polymer sample in NMP with and without 0.05 M LiBr at 50 °C using two different columns shows the impact of losing the high molecular weight fraction of sample on the molecular weight results. ..... 67
Table 2-4. The product of spin draw and fiber stretch give the total drawdown ratio (DDR) ..... 78
Table 2-5. Summary of precursor fiber diameters and tensile strengths produced with reference to commercial manufacturer ..... 83
Table 3-1 Carbon fiber production in tons[152] ..... 91
Table 3-2 Reaction scheme and reaction components ..... 101
Table 3-3. Synthesis and Characterization of random poly (acrylonitrile-*co*-methylacrylate) copolymers ..... 102
Table 3-4 Molecular weight data of the poly (acrylonitrile-*co*-methylacrylate) ..... 106
Table 3-5. Relative % crystallinity values of the poly (acrylonitrile-*co*-methylacrylate) copolymers ..... 112
Table 4-1. Thermal transitions in poly(acrylonitrile-co-methylacrylate) copolymer-water blends ..... 128
Table 4-2. Boiling points of glycerin and water solutions estimated from Dühring ..... 130
Table 4-3. Characteristics of the high AN content copolymers and their 25 mole:mole % glycerin blends ..... 136
Table 5-1. Synthetic parameters used in the suspension and emulsion copolymerization ..... 147

## LIST OF SCHEMES

Scheme 1-1. Propylene ammoxidation route to synthesize acrylonitrile..... 2
Scheme 1-2. Reactions taking place during the stabilization step[16] ..... 7
Scheme 1-3. Chemistry of formation of PAN based carbon fibers[12]..... 9
Scheme 1-4. Formation and reaction of primary and secondary initiator radicals[40] ..... 14
Scheme 1-5. Thermal decomposition of persulfates[43, 44]..... 15
Scheme 1-6. Decomposition of persulfate in the presence of metabisulfite anion ..... 16
Scheme 1-7. Termination of polyacrylonitrile chains by a) Disproportionation and b) Combination..... 17
Scheme 1-8 Reactions of the persulfate anion in alkaline, neutral and acidic media[55] . 19
Scheme 1-9. Inhibiting Reaction of Oxygen[57]..... 20
Scheme 1-10. Maxwell Morrison mechanism for radical entry into particles ..... 33
Scheme 5-0-1. Representative reaction scheme and reaction components ..... 146

# CHAPTER 1 LITERATURE REVIEW

## 1.1 Introduction

Polyacrylonitrile (PAN) is a homopolymer of acrylonitrile. It is industrially copolymerized with various comonomers which include styrene, butadiene, methyl acrylate and vinyl acetate among others. Polyacrylonitrile is a versatile polymer and has many applications ranging from high end carbon fibers used in reinforced composites and for making acrylic fiber clothing.

### 1.1.1 Acrylonitrile Synthesis

Acrylonitrile is mainly used for the production of polyacrylonitrile for acrylic fiber production and apart from that it is also used for the synthesis of acrylamide, adiponitrile and in high performance plastic resins like ABS (acrylonitrile-butadiene-styrene) and SAN (styrene-acrylonitrile). Acrylonitrile is currently industrially synthesized via propylene ammoxidation, i.e. the reaction of stoichiometric amounts of propylene and ammonia in the presence of oxygen; a route developed by Sohio.[1] This reaction is exothermic (Scheme1-1). The cost of the raw materials for this reaction is high due to the heterogeneous catalysts like bismuth molybdate that increased selectivity of acrylonitrile and lowered the percentage of side products. Other routes include the use of nitric oxide in place of air and propylene or acetylene as the starting material.[2]

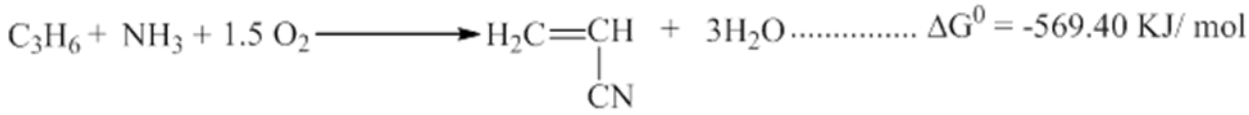


**Scheme 1-1. Propylene ammoxidation route to synthesize acrylonitrile**

### 1.1.1.1 Polyacrylonitrile Copolymers and their Uses

Polyacrylonitrile contains polar, pendent nitrile groups which have strong electrostatic interactions between one another. As a result the PAN chain is very rigid and stiff and has a high crystalline melting point of 317 $^0$C, which is above its degradation temperature of about 300 $^0$C. Due to this PAN is insoluble in most solvents except for a few like DMF and DMAc, and some inorganic salt solutions like aqueous zinc chloride solution and sodiumthiocyanite solution. Polyacrylontirile is hence copolymerized with a suitable comonomer which disrupts the long range order in the chain and improves its solubility in solvents by lowering its melting point, also enabling it to be melt processed.[3]

Acrylonitrile is a versatile polymer and its copolymers have many applications ranging from high end applications like carbon fiber precursors to acrylic fibers used in textiles and in plastics including poly(styrene-*co*-acrylonitrile) (SAN) and poly(acrylonitrile-butadiene-styrene) rubber, and in membranes for water and gas separation.[4] This versatility in uses is due to its attractive properties like rigidity, chemical resistance, and gas barrier properties.

Polyacrylonitrile films have excellent barrier properties towards oxygen and carbon dioxide, due to the presence of the nitrile group which allows for good packing due to the dipole-dipole interactions between the nitrile groups. However the high polarity of the nitrile groups cause it to have high water vapor uptake.[5] Copolymers of

acrylonitrile and vinylidene chloride are used to make low permeability films. Polyacrylonitrile laminates are used in food containers to enhance their barrier properties against oxygen ingression.[6] Acrylonitrile copolymers with 2-dimethylaminoethyl methacrylate have potential medical applications which include dialysis ultrafiltration membranes and adsorbent coatings.[7]

### 1.1.2 Polyacrylonitrile Based Fibers

Fibers made from polyacrylonitrile were first reported in 1938, though the commercial production of polyacrylonitrile began much earlier. Acrylonitrile fibers were not produced on a large scale earlier because suitable solvents for wet/dry spinning had not been found. Polyacrylonitrile was first developed and marketed commercially as Orlon®. It was not until 1955 that a suitable solvent (*N,N*-dimethylformamide) was found. Polyacrylonitrile was soon copolymerized with methyl acrylate and vinyl acetate.[8]

There are two kinds of fibers made from polyacrylonitrile for textile applications which are acrylic and modacrylic fibers and there is a third kind of fibers used in high strength applications, which are carbon fibers.

**Acrylic fibers** have been the major end use for acrylonitrile for a number of years. However the demand for these has been on the decline due to competition from polyester and nylon fibers. Acrylic fibers are fibers that typically contain at least 85 % of acrylonitrile by weight. The different types of comonomers used in the copolymerization of acrylonitrile are listed in **Table 1-1**.

| Monomer | Neutral Comonomer | Acid comonomer |
|---|---|---|
| Acrylonitrile, 85-100 %, typically 90-94 % | 0-14 %, typically 6- 9 % Methyl acrylate, Vinyl acetate, Methyl methacrylate, Acrylamide | 0-1% Sodium styrene sulfonate Sodium methallyl sulfonate Sodium 2-methyl 2-acryamidopropane Itaconic acid |

**Table 1-1. Polymer compositions of acrylic fibers[9]**

**Modacrylic fibers** contain between 35-85 % by weight of acrylonitrile. These can be flame retardant fibers or acid dyeable fibers. The precursors for flame retardant fibers are copolymers of acrylonitrile and an unsaturated halogen containing compound such as vinyl chloride, vinylidene chloride or vinyl bromide. Flame retardant fibers are all industrially wet spun. Acrylic and modacrylic copolymers containing a sulfonate comonomer can also be precursors for bicomponent fibers with water reversible crimp.[10]

**Acrylic Fiber Properties**

There are a number of parameters that are key to spinning good fibers and for obtaining the final end-use properties that are desired. Textile grade acrylic polymers typically require weight average molecular weights in the range of 90,000 – 170,000 g/mol. The molecular weight of the copolymer is adjusted such that the solution of the copolymer is viscous enough to be able to spin fibers but not too viscous. The molecular weight and molecular weight distribution are affected by a number of synthetic variables including initiator type and concentration, comonomer type and concentration, surfactant type and concentration, polymerization temperature and polymerization time.[8] The number average molecular weight is also an important property that affects the dyeability. In polymerization methods that use redox initiator systems, any sulfate and sulfonate end groups provide dye sites and consequently the number of dye sites is inversely proportional to $M_n$. Hence it is necessary to determine the optimum molecular weight for the required rheological properties and the distribution necessary for dyeability. Initiating systems like pottasium persulfate combined with sodium bisulfite are inexpensive and very low concentrations are required in order to achieve the acid end groups.[11] Sulfonic acid dye sites have also been shown to be more thermally stable than carboxylic acid dye sites.

**Carbon fibers** are used as a structural reinforcement material in composites including fiber-reinforced polymer matrix composites and cement. Due to their properties such as high strength, low coefficient of thermal expansion and light weight, carbon fibers are mainly used in the aerospace and automobile industry for making the

body parts of aircrafts and automobiles. The emerging applications of carbon fibers include their use in prosthetics and in composite core wires to replace steel. Carbon fibers can be made from polyacrylonitrile, mesophase pitch, rayon, high performance polymers, or from vapor deposition of hydrocarbons such as benzene or methane. PAN based carbon fibers are by far the most commercially used precursors for carbon fibers mainly due to their high tensile strength. However in applications that require more molecular and structural order, the pitch based carbon fibers are preferred. PAN carbon fibers account for the majority of carbon fiber production in the world (>70%).[12]Polyacrylonitrile cyclizes and degrades along the chain before it can melt and therefore needs to be copolymerized with a suitable comonomer to reduce its melting point, also improving its oxidative stability. Comonomers like vinyl acetate, methyl acrylate or acrylic acid are commonly used.[13, 14] The precursors used for high modulus and high tensile strength applications usually have very high molecular weights and high acrylonitrile contents (>90%).[15] Carbon fibers derived from mesophase pitch can be graphitized. However, PAN carbon fibers are preferred due to the high costs involved in the purification of mesopitch for pitch based carbon fibers.[16]

The production of carbon fibers from PAN precursors involves the following steps.

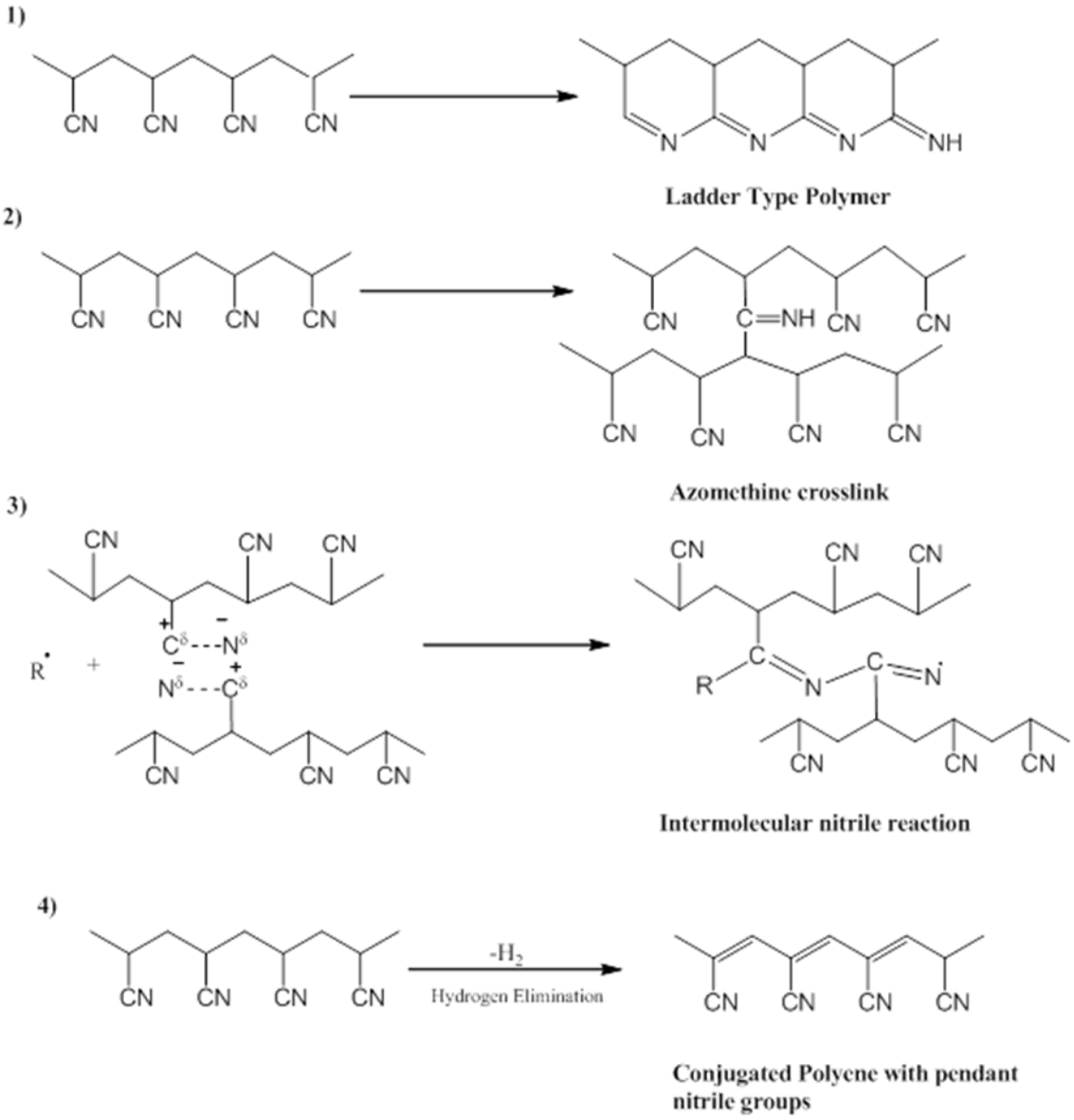


**Scheme 1-2. Reactions taking place during the stabilization step[17]**

**1) Low Temperature Oxidative Stabilization:** PAN-based acrylic fibers are subjected to temperatures between 200 and 300 $^{0}$C in air[14, 18] to convert them to an infusible and non-flammable state. The stabilization process involves physical as well as chemical changes. The physical changes include changes in color, crystallinity, entropy, density and tensile strength and the chemical changes include chain scission and the formation of carbonyl, carboxyl and peroxide groups on the backbone that aid in faster cyclization

and degradation. Much research has been done for over 40 years on the reactions that take place during stabilization of the PAN fiber.[17] After much debate, the consensus is that the following reactions take place during stabilization: 1) Intermolecular cyclization along the chain to form a cyclized ladder type polymer,[19-21] 2) Crosslinking due to azomethine formation, 3) Formation of a conjugated backbone chain caused by hydrogen abstraction that can undergo further reaction, and 4) Crosslinking caused by intermolecular nitrile reactions (Scheme 1-2). However, the cyclization mechanism in PAN is significantly influenced by the composition of the comonomer.[22, 23] Carboxylic acid comonomers such as itaconic acid are incorporated in order to decrease the temperature of stabilization, thus controlling the exotherm. Acrylate and methacrylate comonomers are neutral comonomers that do not inhibit or initiate the cyclization.[24, 25]

**2) Carbonization and Graphitization:** The fibers are then treated at elevated temperatures between 1500 and 2000 $^0$C to remove any inorganic material or impurity. This process is known as carbonization. This process eliminates all atoms except for carbon, achieving about 92-95 % carbon in the material.[26, 27]Goodhew *et al.*[28] showed that the cyclied rings undergo hydrogenation reactions to give a graphitic structure. The dehydrogenation occurs between 400 to 600 $^0$C, followed by denitrogenation to ultimately form the graphite layers. Volatile gases like HCN, $H_2O$, $O_2$, $H_2$, CO, $NH_3$, $CH_4$, are evolved between 200 to 1000 $^0$C, along with some other high molecular weight compounds and tar. Other condensation reactions occur until 1600 $^0$C, forming the turbostatic carbon phase which is responsible for the high tensile strength of the carbon fibers.The final heat treatment step is called graphitization which during which the

carbon fibers are further heated at 3000 $^{0}$C, to orient the turbostatic crystallites in the direction of the fiber axis.[15]

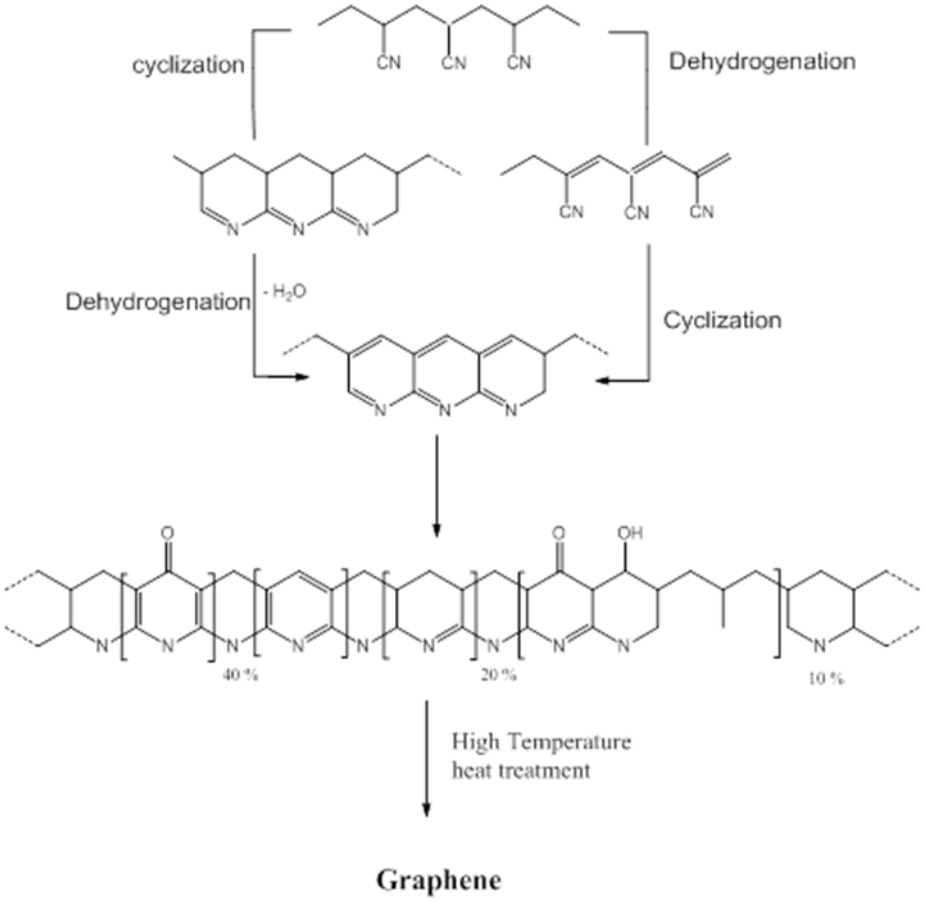


**Scheme 1-3. Chemistry of formation of PAN based carbon fibers[13, 29]**

The strength and modulus of the precursor fibers are directly related to the strength and modulus of the carbon fiber, and this is one reason that polymers with high molecular weights are synthesized for the precursors.[9] The production of carbon fibers is limited due to the high costs involved in the stabilization process that is required for both pitch and PAN based fibers. Current processing methods for polyacrylonitrile include wet and dry spinning. In both wet and dry spinning, the polymer is partially dissolved in a

suitable solvent like DMF or DMSO at low temperatures of ~5 $^{0}$C to prevent gel formation, after which it is completely dissolved by use of heat and shear mixers.[30] The dope is then filtered and deaerated prior to spinning. Any necessary additives like pigments are mixed in at this point. Wet spinning is a process in which fiber formation occurs by exchange of solvent with a non-solvent. A filtered dope is spun through a spinneret into a dilute solvent or coagulation bath to produce the acrylic fibers (Figure 1-1).

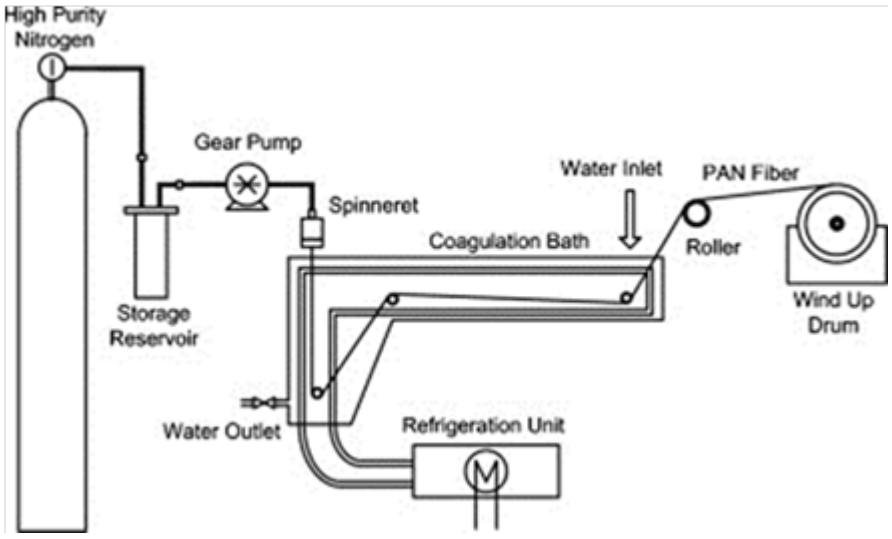


**Figure 1-1. Wet spinning of PAN fibers[31] Ismail, A. F.; Rahman, M. A.; Mustafa, A.; Matsuura, T., The effect of processing conditions on a polyacrylonitrile fiber produced using a solvent-free free coagulation process. Materials Science and Engineering: A 2008, 485 (1-2), 251-257. Used under fair use, 2015.**

Dry spinning is a process in which fibers are drawn from a solvent by removing the solvent in hot air. A suitable solvent for dry spinning would be one that is low boiling, is stable at the boiling point, does not react with the polymer, has a low heat of

vaporization and is non-toxic. The most commonly used commercial solvent is DMF, generally used in concentrations70-93 wt% which allows for processing below the cyclization temperature of PAN.[32-34]

### 1.1.3 Polymerization

Acrylonitrile can be polymerized via a variety of techniques which include bulk, solution, or heterogeneous free radical polymerization techniques like suspension, emulsion and aqueous dispersion polymerization. Unlike some other monomers acrylonitrile does not homopolymerize readily in the absence of an initiator. Aqueous dispersion polymerization is a widely preferred method for industrial synthesis of PAN due to ease of control, good heat transfer, ease of polymer recovery and absence of an organic solvent. The monomer is dispersed in the aqueous phase as droplets with the help of a dispersant or stabilizer, similar to suspension polymerization. However in this case, the initiator and dispersant used are water soluble and not oil-soluble as in suspension polymerization.[8, 35, 36] Hence, akin to emulsion polymerization, when inorganic water-soluble initiators like persulfates are used, initiator radical generation takes place in the aqueous phase, however propagation in the aqueous phase is limited due to insolubility of the polymer in water. Polymerization in the monomer droplet phase dominates as the number of particles increases.[35] Heterogeneous polymerization techniques like emulsion and suspension have the same advantages with regards to good heat transfer and low viscosity of the reaction media. However, emulsion polymerization of high content polyacrylonitrile is complicated because of the considerable partitioning of acrylonitrile into the aqueous phase and the insolubility of

polyacrylonitrile in its monomer.[37, 38] These aspects make the formation of latex particles difficult. While emulsion polymerization is more commonly used for modacrylic fibers, solution and aqueous dispersion polymerization are more commonly used in the industry for acrylic fiber production.[39] Bulk polymerization of acrylonitrile is not preferred due to its autocatalytic nature. Due to high viscosity of the reaction medium, there is little or no termination and this can lead to a highly uncontrollable exothermic reaction that can be explosive.[40, 41] However, it has been shown to be possible to control the heat of reaction by stopping the polymerization at low conversions of about 40-50 % and by using initiators that have an extremely high decomposition rate. Control over the rate of polymerization is achieved by controlled addition of the initiator.[42]

### 1.1.4 Kinetics of Free Radical Addition

Polyacrylonitrile is commercially produced via free radical polymerization due to ease of control and incorporation of various comonomers that impart mechanical properties and dye sites in the fibers. The same reaction mechanisms apply for all types of polymerizations: bulk, solution or emulsion. Steric and electronic (resonance, inductive) effects play an important role in deciding if a monomer will undergo free radical addition. The relief of strain from $sp^2$ to $sp^3$ hybridization of the carbon is a major driving force for the cleavage of the double bond to undergo addition. Some of the initiators used in free radical addition are peroxides, two-component redox systems, azo compounds, light and high energy radiation. The three main steps of free radical addition are i) initiation ii) propagation and iii) termination.

### 1.1.4.1 Initiation

The structure of the repeating unit along with any defects and end groups present in the chain play an important role in governing the final polymer properties. It is for this reason that selection of a suitable initiator and knowledge of the rate, efficiency and mechanism of initiation is important. Initiation of the polymer chains involves two steps. One is the decomposition or activation (in case of a redox system) of the initiator and the second is the addition of the initiator free radical to a monomer unit. Upon thermolysis or activation by a reducing agent (as in the case of redox polymerization) the polymer chains are initiated by either the primary radicals or initiator derived secondary radicals. The primary radicals formed may a) react with the monomer, b) react with the solvent or an impurity, c) undergo cage reactions, d) undergo fragmentation producing secondary radicals which in turn react with the monomer and initiate a chain (Scheme 1-4). Upon dissociation, not all radicals that are formed initiate chains and hence the initiator efficiency is never 100 %. Initiator efficiency is the mole fraction of initiator that actually reacts with monomer to give polymer chains and is given by

$$F = \frac{[Rate\ of\ initiation\ of\ propogating\ chain]}{n\ [Rate\ of\ initiator\ disappearance]}$$

where, n is the number of moles of radicals produced per mole of initiator.

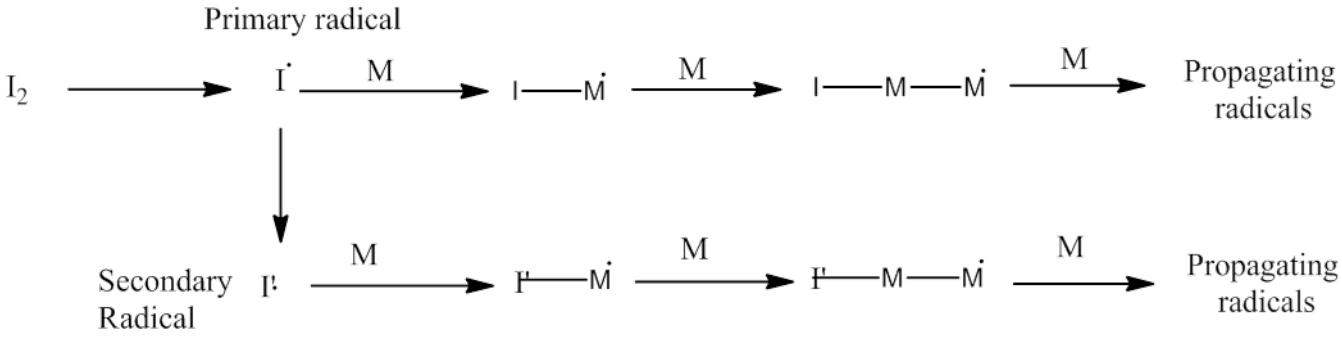


**Scheme 1-4. Formation and reaction of primary and secondary initiator radicals[43]**

The rate of initiation is given by $R_i = 2 f k_d[I]$……..(1)

where $k_d$ = the rate constant of initiator decomposition, f = initiator efficiency, and [I] = the molar concentration of the initiator. For a two-component redox initiating system this can be written as $R_i = 2f k_d$ [reductant] [oxidant] ……(2)

The initiator adds to a monomer unit and begins to propagate the chain, thus giving the equation for rate of initiation as:

$R_i = 2 f k_d [I] + k_i [M] [I^{\cdot}]$……..(3)

The rate constant for propagation of the initiator radical is extremely high, and there is almost immediate capture and propagation with the monomer in the aqueous phase.

**1.1.4.1.1 Persulfate initiation: Thermal decomposition and Redox initiation**

Persulfate initiators are widely used in emulsion polymerizations and other aqueous polymerization techniques due to their high water solubility and poor organic solubility (80 g/100 mL of water at 25 °C for ammonium persulfate[44]). The persulfate or peroxydisulfate bond has a high bond energy (~ 131.6 kJ/mol for ammonium persulfate at 70 $^0$C[45]) and can only undergo decomposition thermally, photochemically and in the presence of a reducing agent at low temperatures (redox catalysis). The relative

hydrophilic/hydrophobic character of the persulfate radical ion is critical in determining the critical length that is required for it to attain sufficient surface activity in order to enter the micelle/particle to initiate a chain by reacting with the monomer.

**Thermal Decomposition:** The half-life $t_{1/2}$ and decomposition rate constant $k_d$ for ammonium persulfate at 60 $^0$C was found to be 38.5 hours and 4.3 x $10^{-5}$ $s^{-1}$.[45] Among the mechanisms proposed for the thermal decomposition of persulfates are unimolecular thermal decomposition and bimolecular decomposition by reaction with water (**Scheme 1-5**).

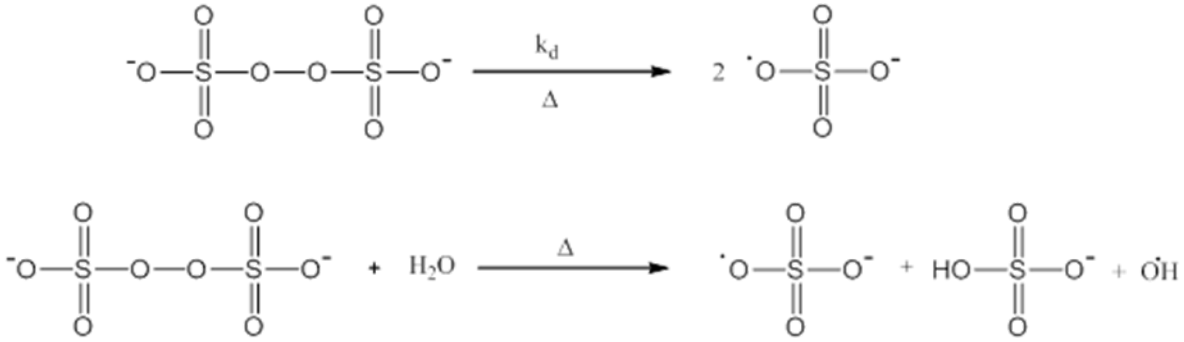

**Scheme 1-5. Thermal decomposition of persulfates[46, 47]**

The thermal decomposition of persulfates has also been shown to be accelerated in the presence of some alcohols.[48, 49] Persulfate decomposition has also been shown to be sensitive to solvent effects, ionic strength, pH and also the presence of certain vinyl monomers and surfactants.[50, 51]

**Redox Catalysis (Activation using a reducing agent**): Redox initiation is most commonly employed in emulsion and aqueous dispersion polymerization where high molecular weights and low temperatures are required. Also, the radical flux of initiator radicals produced in the redox reaction is assumed to be much higher than that of the thermal decomposition of the same system.[52] However, the initiator efficiencies are

much less than unity due to the possibility of further redox reaction of the initially formed radicals. Persulfates can be activated at room temperature by using a suitable activator or reducing agent like transition metal ions like $Fe^{2+}$, $Ag^{+}$ and $Ti^{3+}$. A commonly used redox initiation system is the persulfate-metabisulfite pair, the mechanism for which has been proposed by Bamford[53] is shown in Scheme 1-6. Other reducing agents include bisulfite, halide ions, thiols, ascorbic acid and amines.

**Scheme 1-6. Decomposition of persulfate in the presence of metabisulfite anion**

### 1.1.4.2 Propagation

Two assumptions are made while deriving the equation for rate of propagation. The first assumption is that the rate of propagation is equal to rate of polymerization assuming that all or most of the monomer is consumed in the propagation step.[54] The second assumption is that, radicals of all chain lengths have equal reactivities,thus giving the expression for rate of propagation/ polymerization as: $R_p = k_p [M^{\cdot}][M]$

While this expression for rate of propagation holds true for a homogeneous polymerization, the same can be applied to a heterogeneous polymerization by replacing overall monomer concentration with the concentration of monomer in the particle alone, since the latex particles are the main locus of polymerization.

### 1.1.4.3 Termination

Termination of the growing chains can occur either by transfer to initiator, disproportionation or combination. Termination by combination results in a product of molecular weight that is much higher than the average molecular weight of the growing

chains. Scheme 1-7 shows the two major reactions by which the growing polymer radicals terminate.

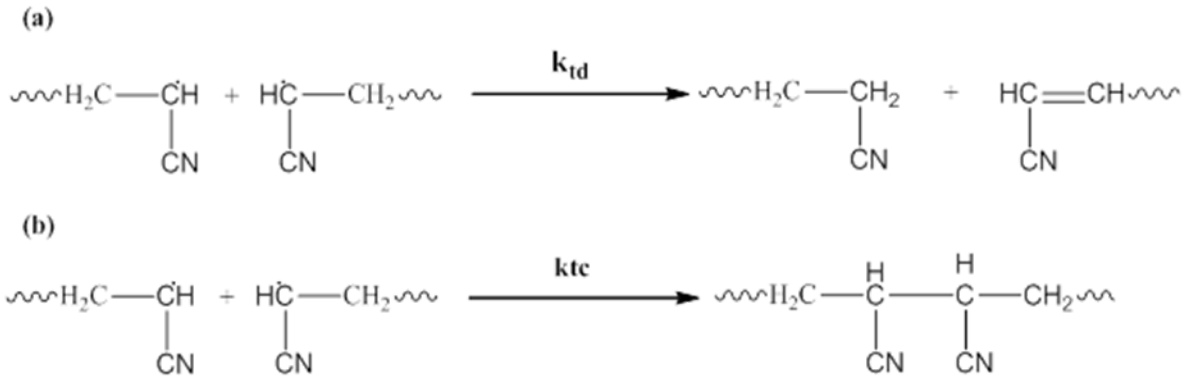


**Scheme 1-7. Termination of polyacrylonitrile chains by a) Disproportionation and b) Combination**

The rate of termination is given by

$R_t = - d[M]/dt = 2 k_t [M]^2$

$k_t = k_{td} + k_{tc}$

Applying the quasi steady state approximation that radicals are consumed at the same rate as they are formed,

$R_i = R_t$

$2 k_d f [I] = 2 k_t [M^{\cdot}]$; thus $[M^{\cdot}] = \frac{2 k_d f [I]}{2 k_t}$

Making $R_p = k_p \sqrt{\frac{k_d f I}{k_t}} * M$

Upon termination, different chains have different lengths and the distribution and averages of these different chain lengths and molecular weights are represented by number average chain length, weight average chain length and polydispersity index

(PDI). Under ideal conditions, PDI would be equal to 2 upon termination by disproportionation and 1.5 upon termination by combination.[54, 55] The kinetic chain length which is the average number of monomer units per growing chain before termination is given by

$$\vartheta = \frac{R_p}{R_i} = \frac{k_p[M]}{2\,(f\,k_d\,k_t)^{1/2}\,[I]^{1/2}}$$

The degree of polymerization is given by

$\bar{x} = 2\vartheta$ when termination is predominantly by combination

$\bar{x} = \vartheta$ , when the termination is predominantly by disproportionation.

In case of acrylonitrile polymerization, combination is the dominant termination reaction followed by chain transfer.[8]

#### 1.1.4.1.3 Initiator Efficiencies in Emulsion Polymerization

The choice of a suitable initiator for a particular type of polymerization is very important. Not all initiators are applicable for all types of polymerization. For example, in an aqueous heterogeneous system like suspension polymerization, an oil soluble initiator is used. An O/W (Oil in Water) emulsion polymerization however requires a water soluble initiator. Initiators such as ammonium persulfate which have appreciable organic and aqueous phase solubility can also be employed. In solution or suspension polymerization the initiator-derived radicals react with monomer to form polymer chains in a single phase. In emulsion polymerization, the initiator-derived radicals first react with monomer in the aqueous phase, and upon reaching a certain chain length (z), enter the micelles where polymerization occurs, thus forming the latex particles. Initiator efficiencies can be particularly low in emulsion polymerizations as compared to other

techniques like suspension, solution or bulk polymerization.The monomer concentrations in the aqueous phase where at least much of the initiator decomposes can be very low and hence there is a greater chance for the initiator radicals to undergo side reactions and terminate in the aqueous phase before they enter the micelles.[56] Controlling the pH by using a buffer helps control the initiator efficiency for the persulfate initiated systems.[57] In alkaline and neutral media, the persulfate ion generates two radical ions, whereas in acidic media there is no radical generation.[58] (Scheme 1-8)

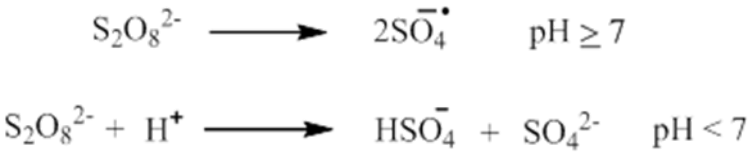


**Scheme 1-8 Reactions of the persulfate anion in alkaline, neutral and acidic media[58]**

**Inhibiting/Retarding Effects of Oxygen in Emulsion Polymerization**

The presence of oxygen in the reaction system leads to long induction periods and retards the polymerization rate. The deleterious effects of oxygen include a decrease in efficiency of the initiator and the resulting low monomer conversion. A general scheme for retardation by oxygen is shown in Scheme 1-9.Oxygen may be present as dissolved oxygen in the monomers or the continuous phase and in the headspace above the reaction mixture in the reaction flask.[59] The scheme below shows how oxygen can react with a growing chain.

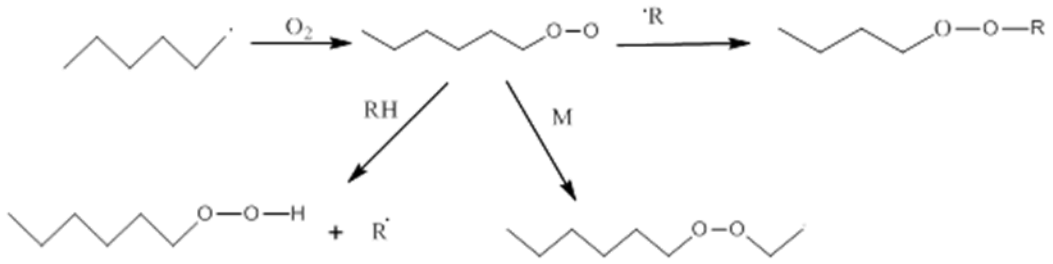


**Scheme 1-9. Inhibiting Reaction of Oxygen[59] Bruyn, H. D.; Gilbert, R. G.; Hawkett, B. S., Retardation by oxygen in emulsion polymerization. *Polymer* 2000, *41*, 8633-8639. Used under fair use, 2015.**

It has been shown through experiments that oxygen is soluble in both the aqueous and organic phases.[60] In industrial synthesis, the retardation effects of oxygen results in a significant loss in productivity and increase in cost.[61] It is hence important to understand the effect of oxygen on emulsion polymerization kinetics.

### 1.1.5 Kinetics of Free Radical Copolymerization

Many models have been used to describe the kinetics of statistical copolymerization. The simplest of these is the terminal model. The terminal model or first order Markov model of copolymerization states that the reactivity of a growing chain is independent of the chemical composition of the chain and is only dependent on the nature of the terminal monomer unit. When copolymerizing two monomers $M_1$ and $M_2$, two ends $M_1^*$ and $M_2^*$ are possible and four types of propagating reactions are possible which are shown below.

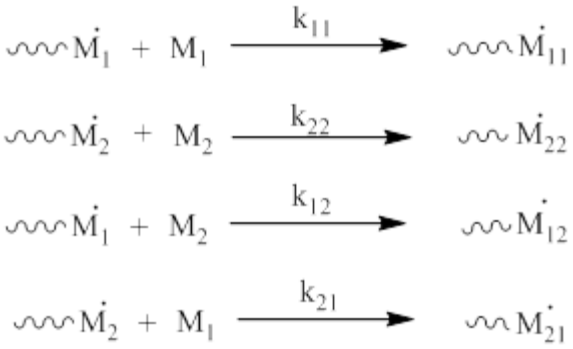

The rate constant $k_{11}$ is the rate constant for homopolymerization of $M_1$, $k_{22}$ is the rate constant for homopolymerization of $M_2$, $k_{12}$ the rate constant for the radical chain ending in $M_1$ to add on to the second monomer $M_2$ and so on.

The rates of disappearance of the two monomers are given by

$$-\frac{d[M_1]}{dt} = k_{11}[M^*_1][M_1] + k_{21}\,[M^*_2][M_1] \quad \text{.....1}$$

$$-\frac{d[M_2]}{dt} = k_{12}[M^*_1][M_2] + k_{22}\,[M^*_2][M_2] \quad \text{.....2}$$

$$\frac{d[M_1]}{d[M_2]} = \frac{k_{11}\,[M^*_1][M_1]+k_{21}\,[M_2][M_1]}{k_{12}\,[M_1][M_2]+k_{22}[M_2][M_2]} \quad \text{.....3}$$

Assuming steady state conditions,

$K_{21}\,[M_2^*]\,[M_1] = k_{12}\,[M_1^*]\,[M_2]$ .....4

Substituting the value for $[M_1^*]$ in equation 3, we get

$$\frac{d[M_1]}{d[M_2]} = \frac{\frac{k_{11}\,k_{21}\,[M^*_2][M_1]^2}{k_{12}\,[M_2]}+k_{21}\,[M^*_2][M_1]}{k_{22}\,[M_2^*][M_2]+k_{12}\,[M_1^*][M_2]} \quad \text{.....(5)}$$

Let $r_1 = \frac{k_{11}}{k_{12}}$ $\quad r_2 = \frac{k_{22}}{k_{21}}$ $r_1$ and $r_2$, known as reactivity ratios of the two monomers

$M_1$ and $M_2$, represent the ratios of rate constants for homopolymerization of a particular monomer to copolymerization with another monomer.

$$\frac{d[M_1]}{d[M_2]} = \frac{[M_1](r_1\,[M_1]+[M_2]}{[M_2]([M_1]+r_2\,[M_2]} \quad \text{.....(6)}$$

Equation (6) can be written as

$$\frac{m_1}{m_2} = \frac{[M_1](r_1[M_1]+[M_2]}{[M_2]([M_1]+r_2[M_2]} \quad \text{.....(7)}$$

where $M_1$ and $M_2$ are molar concentrations of the two monomers.

Expressing the copolymer equation in terms of mole fractions of the comonomers $M_1$ and $M_2$ which are $f_1$ and $f_2$ in the feed and $F_1$ and $F_2$ in the copolymer, we obtain

$$F_1 = \frac{d[M_1]}{d[M_1]+d[M_2]} \quad and \quad f_1 = \frac{[M_1]}{[M_1]+[M_2]} \quad \text{.....(8)}$$

Combining equations (8) and (6), we get

$$F_1 = \frac{r_1 f_1^{\,2}+f_1 f_2}{r_1 f_1^{\,2}+2f_1 f_2+r_2 f_2^{\,2}} \quad \text{and} \quad f_1 = \frac{[M_1]}{[M_1]+[M_2]} \quad \text{.....(9)}$$

where $F_1$ = the instantaneous mole fraction of $M_1$ in the copolymer and $f_1$ = the instantaneous mole fraction of monomer 1 in the feed. In case of an emulsion copolymerization,

$$f_1 = \frac{[M_1]_p}{[M_1]_p + [M_2]_p}$$

where $[M]_p$ is the monomer concentration inside the latex particle and not the overall monomer concentration in the reaction volume.

The propagation rate coefficient or polymerization rate coefficient is given by

$$\mathbf{k_p} = \frac{r1f12+2f1f2+r2f22}{(\frac{r1f1}{k110}+(\frac{r2f2}{k22})}$$

Copolymer composition is independent of the rate of copolymerization and the initiator concentration. The reactivity ratios of the monomers are dependent on temperature, pressure and solvent but independent of the concentrations or types of initiators or chain transfer agents. The mole fraction of $f_1$ is not equal to $F_1$ and with increasing

percent conversions, there is a drift, or non-homogeneity, in the copolymer composition that results in a broadened distribution of copolymer composition. This may affect the final mechanical properties of the copolymer.[62]

### 1.1.6 Emulsion Polymerization

The first attempt at emulsion polymerization dates back to 1910 by an idea conceived by Bayer during World War I. Emulsion Polymerization was mainly developed during World War II to make styrene-butadiene rubber.[63] It is now industrially used to make many commercial polymers and sometimes can directly be used as a dispersion which finds applications in paints, coatings and textiles. The method for emulsion polymerization normally utilizes a water-insoluble monomer but as in the case of acrylonitrile, the monomer can partition between the aqueous and monomer phases. It uses a water soluble initiator and a surfactant that stabilizes the micelles and monomer/polymer droplets by lowering the surface tension between the aggregates and the water. If enough surfactant is added for the concentration to be above critical micellar concentration, micelles are formed which are aggregates of about 100 molecules of surfactant in case of spherical micelles which are the most commonly formed micelles.[64] These micelles are far greater in number as compared to the monomer droplets and are the primary loci during the early stages of these polymerizations. As the reactions progress, the micelles grow into polymer particles that will become swollen with monomer (the micelles will be depleted) and the loci of polymerization primarily shifts to those particles. Emulsion polymerization is a technique where, in the early reaction stages, polymerization primarily occurs in surfactant-stabilized micelles. Other possible loci of polymerization are the aqueous phase, the

monomer droplets, the water-particle interphase and the latex particles. In the case of monomers such as vinyl acetate and acrylonitrile, which have appreciable solubility in water, an intermediate between emulsion and solution polymerization is thought to take place.

Some advantages of emulsion polymerization over other techniques like solution and bulk polymerization are 1) the use of environmentally friendly dispersion media i.e. water, 2) high rates of polymerization, 3) high molecular weights obtainable due to compartmentalization of growing radicals giving rise to little or no termination, 4) small particle size of about 100s of nm and latex that can be readily used as coatings, adhesives etc., 5) good heat transfer to the medium, and 6) low viscosity of the dispersion media-water. A few shortcomings of this type of polymerization include the difficulty of complete removal of surfactant that has adsorbed on the latex particles which may lead to deleterious performance of the polymer, and water-removal costs can be high.

#### 1.1.6.1 Emulsion Polymerization

Emulsions can be oil in water (O/W) or water in oil (W/O). Most industrial polymers are oil in water emulsions. A typical emulsion polymerization consists of water insoluble monomer, water soluble initiator/activator, surfactant/emulsifying agent, buffers/electrolytes and chain transfer agents as required. A typical emulsion recipe for styrene-butadiene random copolymers is shown in **Table 1-2**.

| Component | Parts by weight |
|---|---|
| Styrene | 25 |
| Butadiene | 75 |
| Water | 180 |
| Emulsifier | 5 |
| n-Dodecyl Mecaptan | 0.5 |
| NaOH | 0.061 |
| Cumene hydroperoxide | 0.17 |
| $FeSO_4$ | 0.017 |
| $Na_4P_2O_7.10\ H_2O$ | 1.5 |
| Fructose | 0.5 |

i

**Table 1-2. Composition for Emulsion Polymerization of Styrene-Butadiene[36]**

**Monomer**: The monomer is a liquid that is immiscible with the continuous aqueous phase but has partial solubility forming an equilibrium solution. Emulsion polymerization is commonly used to copolymerize monomers like ethylene, styrene, acrylonitrile, vinyl acetate and acrylates.

**Choice of Initiator:** Water soluble initiators are normally used, as the continuous phase is water. Commonly used initiators are persulfates (potassium, sodium and ammonium salts of persulfates) and azo compounds. These initiators can also be employed for low temperature polymerization when used in conjunction with a suitable activator, which is known as redox initiation as the mechanism of initiation involves a reduction-oxidation reaction. Other low temperature initiator systems include hydroperoxides and Fe(II). Redox initiation is useful when polymerization at low temperatures is desired, especially on an industrial scale where good control over the reaction exotherm is required. Other initiation systems are $\gamma$-radiolysis, photoinitiators

and high energy electron beams which have been used to obtain rate coefficients.[63, 65, 66]

**Choice of Surfactant / Emulsifier:** The function of a surfactant is to reduce the interfacial tension between the micelles and monomer/polymer particles with the aqueous medium. Surfactants are classified on the basis of their hydrophilic end which can be anionic, cationic, amphoteric (hydrophilic end function depends on the pH) or non-ionic. Cationic and anionic surfactants also known as electrostatic surfactants include sodium lauryl sulfate, sodium dodecyl sulfate and Dowfax 8390 which is a sulfonic acid salt. These types of surfactants provide colloidal stability by forming an electric double layer around the latex particles. The droplets are prevented from coagulating due to like charge repulsion of the adsorbed surfactant. Steric, non-ionic surfactants can include polymeric surfactants such as poly(ethylene oxide-*b*-propylene oxide)s**.** The negatively charged end groups of the persulfate initiator may also help in stabilizing the polymer particles, hence enabling polymerization in the absence of surfactant in select cases.

**Electrolytes, buffers, Dispersion agents:** Other additives such as electrolytes may be added to control the pH,and prevent surfactant hydrolysis. Chain transfer agents such as mercaptans are often used as molecular weight modifiers, i.e. to lower the molecular weight since emulsion polymerization often results in extremely high molecular weights.

#### 1.1.6.2 Monomer Reactivity Ratios and Process Strategies

Monomer reactivity ratios are affected by synthetic parameters including the reaction medium, temperature, pressure and resonance effects. Using the nonlinear least squares method of analysis, reactivity ratios of acrylonitrile and methyl acrylate

have been determined to be 1.29 and 0.99 with a 95 % joint confidence limit, utilizing analytical techniques like in situ FTIR and $^{1}$H NMR.[67] The reactivity ratios of monomers in heterogeneous systems like suspension and emulsion copolymerization tend to differ from those in homogeneous medium like solution copolymerization. In the case of emulsions, the relative solubilities of the monomers in micelles may be different from that in the dispersion medium or the relative diffusion rate of the monomers into the micelles may be different.[68, 69] The dependence of reactivity ratios with temperature is a function of the activation energies and is given by

$$r_1 = \frac{k_{11}}{k_{12}} = \frac{A_{11}}{A_{12}} = exp\left(\frac{E_{12} - E_{11}}{RT}\right)$$

where $k_{11}$ is the propagation rate constant for monomeric radical $M_1$ to add on to a chain with a terminal radical $M_1$, $A_{11}$ is the frequency factor, and $E_{11}$ is the activation energy barrier for propagation. The temperature effect on reactivity ratios is more predominant in cases where reactivity ratios are far from 1. This is particularly true for ionic copolymerization rather than free radical polymerization because the activation energy required for radical propagation is as low as 10 kJ/mol for most monomer pairs.[36] Difference in reactivity ratios can lead to non-uniform copolymer compositions and sequence distributions. Process strategies such as rate of addition of monomers and initiators/ activators have an effect on the rate of polymerization and final copolymer product properties such as molecular structure and particle morphology. A starved method of addition of monomer is used in copolymerizations where one monomer is faster reacting than the other, in order to achieve uniform copolymer composition.[65] It gives additional flexibility over the batch process in copolymerizations where reactivity ratios of the comonomers are not close to 1. This also affects the colloidal properties of

the latex, the, surface charge density and particle size during the copolymerization. In order to conduct the polymerization at high rates to complete monomer conversion, the individual components of the redox system are introduced during polymerization, or a third component which limits the rate of radical formation is used in the redox system. It has been shown by conducting styrene emulsion polymerization under starved monomer feed conditions that the number of particles formed had a higher dependence on surfactant and initiator concentrations than in batch emulsion polymerization. The particle size distribution is expected to be broader, however, due to the lower rate of particle growth.[70]

### 1.1.6.3 Kinetics of Emulsion Polymerization

The same basic reaction mechanisms apply for solution and emulsion polymerization, except for that the necessary adjustments for monomer concentration must be made. In emulsion polymerization each latex particle is a micro reactor and the monomer concentration inside the latex particle is to be considered while writing the equation for rates. The various kinetic events that take place during the course of emulsion polymerization are shown in Figure 1-2. A good understanding of the kinetic and mechanistic aspects of emulsion polymerization is required in order to be able to have good control over the process. The first mechanistic theories were reported in 1947. The kinetic model put forth by Smith and Ewart [71, 72] is by far the most referenced.

#### 1.1.6.3.1 Ab Initio Emulsion Polymerization

A typical ab initio emulsion polymerization consists of three intervals, each corresponding to a certain state of the system.[72] Interval I is where particle formation takes place and consists of monomer droplets, micelles and colloidally unstable

particles which eventually grow to mature stable particles due to the swelling of the polymer chains in it. Two to ten percent of the monomer conversion takes place in this interval. Particle formation ends in Interval I. Interval II is characterized by a constant number of particles $N_p$ and a drop in the free surfactant concentration below the critical micelle concentration. As the particle grows, the surfactant becomes adsorbed onto the particle surface and the concentration of the surfactant in the medium falls below the critical micellar concentration. The monomer concentration in the particles is maintained constant by a continuous supply from the monomer droplets by diffusion through the aqueous phase across the particle interface. Conversions of about 30-70 % can be achieved in this interval depending on the monomer system. Upon exhaustion of the monomer droplets, Interval III begins where the remaining monomer within the polymer/monomer particles is polymerized and this drop in concentration corresponds to a decrease in the rate of polymerization. However, there may be an increase in

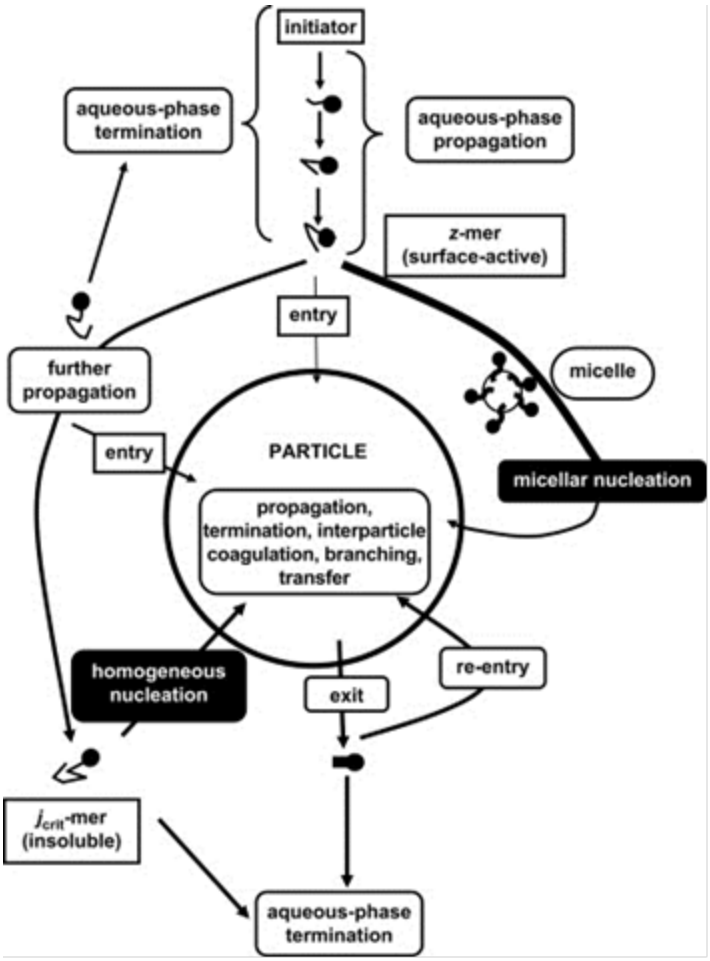


**Figure 1-2. Kinetic events in an ab initio emulsion polymerization[73]**

**Stuart C. Thickett, R. G. G., Emulsion Polymerization : State of art in kinetics and mechanisms. *Polymer* 2007, *48*, 27. Used under fair use, 2015.**

the rate of polymerization due to increasing monomer conversion and a drop in bimolecular termination due to the reaction medium becoming too viscous (gel effect). Figure 1-3 shows the three intervals of emulsion polymerization. Conversion increases as a function of time (Figure 1-4).

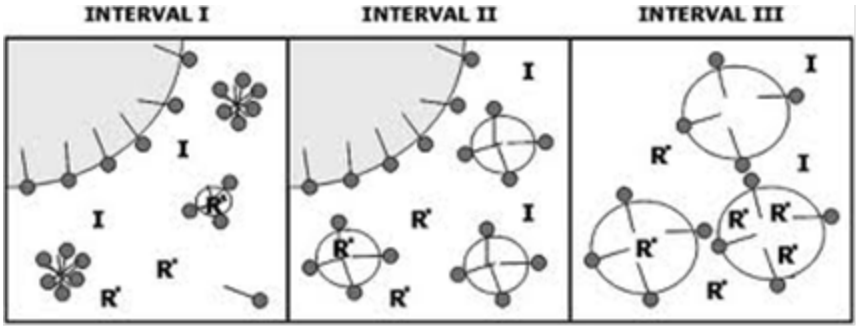


**Figure 1-3. Intervals I, II and III in emulsion polymerization.[52] Thickett, S. C.; Gilbert, R. G., Emulsion polymerization: State of the art in kinetics and mechanisms. *Polymer* 2007, *48* (24), 6965-6991. Used under fair use, 2015.**

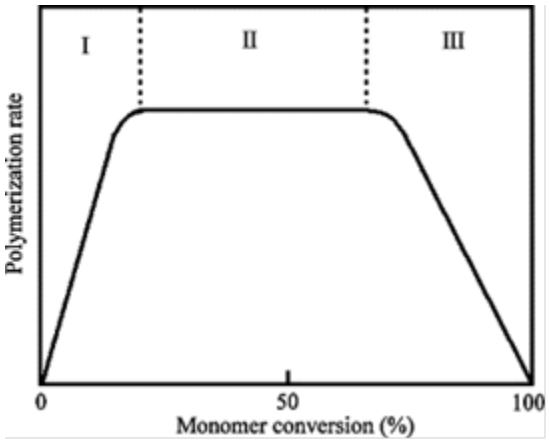


**Figure 1-4. Polymerization rate vs monomer conversion in Intervals I, II, III [61] Chern, C. S., *Progress in Polymer Science* 2006, *31* (5), 443-486. Used under fair use, 2015.**

The rate of polymerization varies as a function of the number of particles, particle size and initiator concentration.[52]

#### 1.1.6.3.2 Radical Entry in Emulsion Polymerization

It was originally proposed that all of the aqueous radicals formed upon the dissociation of initiator entered the micelles/polymer particles[71] but this was proven incorrect by the work of Gilbert *et al.*[74-76] They showed that efficiencies of radical entry into the micelles from the aqueous phase were much less than 1, thus suggesting that termination occurs in the aqueous phase before the radicals enter the particles. Subsequently, an alternative hypothesis describing radical entry, the diffusive entry model, was proposed.

##### 1.1.6.3.2.1 Diffusive Entry Model

According to this model, the mechanism of radical entry into a micelle is by simple diffusion of the oligomeric radical onto the particle surface, thus making it the rate determining step.[77] Another theory suggested that a radical enters the particle interior by displacing a surfactant molecule from the surface of the particle. This however, was shown to be incorrect by the work of Adams *et al*.[78] The currently accepted mechanism for radical entry is the Maxwell Morrison entry mechanism.[79]

##### 1.1.6.3.2.2 Maxwell-Morrison Entry Mechanism

This theory states that formation of latex particles occurs upon the formation and diffusion of radicals of a certain critical degree of polymerization *z* into the micelles. The diffusion of the z-mer is assumed to be so fast that it is not the rate-determining step. The reaction Scheme for radical entry is shown below (Scheme 1-10).

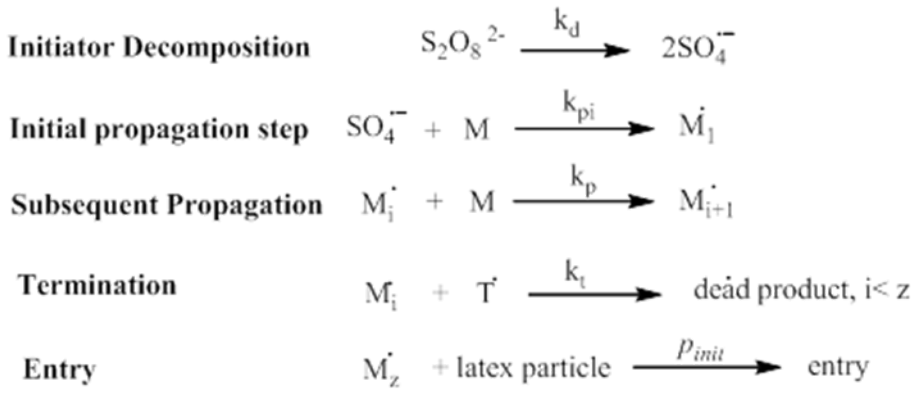


**Scheme 1-10. Maxwell Morrison mechanism for radical entry into particles**

The model also states that there is no charge effect on the kinetics with regards to the entry of a charged radical through a charged particle surface and this was supported by experiments conducted by Van Berkel *et al.*[79] Experiments conducted with electrostatically stabilized systems are all in agreement with this model. The parameter z however is not known for every system.

#### 1.1.6.3.2.3 Maxwell-Morrison Model: Thermodynamic Rationalization

The Maxwell-Morrison model for radical entry states that entry of an oligomeric radical takes place upon reaching a critical length z which imparts the radical surface activity in order to diffuse in to the particle. For aliphatic alkyl sulfate initiator and styrene monomer system, it was seen that the minimum value of hydrophobic free energy ( $\Delta G^{hyd}$) needed to impart surface activity was 23 KJ $mol^{-1}$ where,

$$\Delta G^{hyd} = RT \ln C_w^{sat}$$

The value of z depends upon the ionic group on the initiator. The sulfate and persulfate groups are extremely hydrophilic. The value of z for persulfate initiated systems can be

calculated using the formula:

$$z = 1 + int\left(\frac{-23\,KJ\,mol^{-1}}{RT\ln C_w{}^{sat}}\right)$$

Dong and Sundberg[80] developed a lattice model that can be used to estimate the critical length z for comonomer systems. It shows that the sequence distribution of the comonomers in the aqueous phase oligomer has no effect on the value of *z*. It has been shown that while persulfate derived primary radicals can directly diffuse and lead to particle formation[81], this is negligible in comparison to aqueous phase propagation.[82]

Radical entry in redox initiated polymerization has also been investigated and a model describing radical entry kinetics has been proposed.[83] It is assumed that the radical flux resulting from a redox reaction is much higher than the radical flux due to thermal decomposition and the initiating radicals have been classified into hydrophilic and hydrophobic types. The initiator efficiencies for hydrophilic species are low at high initiator concentrations due to the requirement for aqueous phase propagation prior to entry into micelles. The hydrophobic initiating species however have 100 % entry efficiency.[83]

**1.1.6.3 Particle Formation and Particle Growth and Nucleation**

As the active micelles in which polymerization occurs grow, they become polymer particles. Particle nucleation can be homogeneous or heterogeneous (Figure 1-5). When particle nucleation occurs upon the entry of oligomeric radicals that initiate polymerization from the aqueous phase into micelles, this is known as heterogeneous or micellar particle nucleation. Homogeneous particle nucleation is where the oligomeric radicals formed in the aqueous phase precipitate onto themselves and absorb

surfactant from the micelles or the solution and eventually become polymer particle equivalents upon absorption of monomer. This usually happens in cases where the free surfactant concentration in the medium is below the critical micelle concentration or in the absence of surfactants. Depending upon the aqueous solubility of the monomers and the surfactant concentration, either of the two nucleation mechanisms can predominate. For example, homogeneous nucleation is predominant for relatively hydrophilic monomers such as vinyl acetate and methyl methacrylate. Another significant phenomenon that occurs below the critical micelle concentration besides homogeneous nucleation is “coagulative nucleation”, which involves the coagulation of smaller polymer particles to form larger mature particles that subsequently grow via polymerization.[52] Particle formation ends when enough particles are available to capture all of the surface active *z*-mers formed in the aqueous phase. The number of particles is given by $N_p = \frac{m_p}{\frac{4}{3}\pi\ r^3\ d_p}$ where, $m_p$ = mass of the polymer per unit volume of the continuous phase, r = unswollen radius of the seed latex, and $d_p$ = density of the polymer.

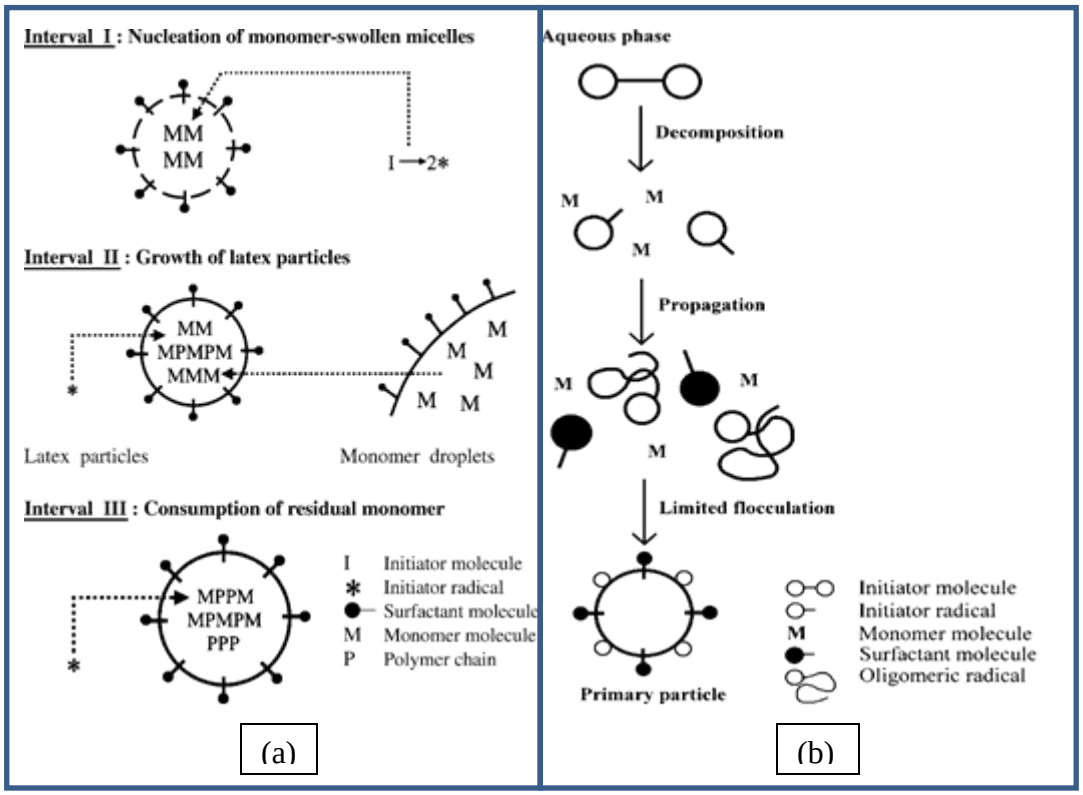


**Figure 1-5. (a) Micellar Nucleation Mechanism[61] (b) Homogeneous Nucleation Mechanism[61]. Chern, C. S., *Progress in Polymer Science* 2006, *31* (5), 443-486. Used under fair use, 2015.**

It is necessary to understand aqueous phase events such as radical entry and exit in order to be able to understand the particle formation mechanism. The mechanism of particle formation helps understand the relation between number of particles $N_p$ and surfactant concentration, initiator concentration and temperature. Smith and Ewart[84] put forth a mathematical expression for the dependence of particle number on initiator and surfactant concentration at the end of Interval I. $N_p$ is dependent on surfactant concentration and a strong variation can be observed especially at the critical micellar concentration.

$$N_p = k \left(\frac{R_i}{\mu}\right)^{2/5} (a_s S)^{3/5}$$

Particle number can be calculated from experimentally determined values of particle diameter through dynamic light scattering and transmission electron microscopy.

The rate of polymerization is given by $\frac{d[M]}{dt} = k_p\ [M]_p[R]$, which can be written as

$$R_p = \frac{k_p\,[M]_p\,N_p\,\bar{n}}{N_A}$$

where $[M]_p$ = monomer concentration in the particle, $N_A$= Avogadro's number, $k_p$ = propagation rate constant, and $\bar{n}$ = average number of radicals per particle. In emulsion polymerization the rate of propagation obeys the zeroeth law with respect to monomer concentration, unlike suspension and other homogeneous polymerizations which have a first order dependence. All emulsion polymerizations can be classified as zero-one or pseudo bulk as put forth by the Smith and Ewart kinetic model.[84]

**Pseudo Bulk System:** The radicals rapidly move from particle to particle, where the polymer particles have been described as being equivalent to a pseudo bulk system. Here intraparticle termination is rate determining and the particle at any time can contain a very large number of $\bar{n}$, because the high viscosity in the particle interior allows for coexistence of more than 2 radicals without rapid termination. In this case, rate of polymerization is independent of particle size due to the absence of the radical compartmentalization effect.

**Zero-one System:** The particles contain either zero or one radical at any given time. Any radical entering a particle that already contains a growing chain results in rapid termination. Radical exit and transfer reactions are negligible. Since the timescale on which this intraparticle termination occurs is really fast it is not rate determining. The value of $\bar{n}$ is never more than 0.5.

The systems whose kinetics are in between pseudo bulk and zero-one are complex. These are termed as the zero-one-two systems where it is assumed that the entering oligoradical has a finite lifetime in the particle and instantaneous termination does not take place, but upon entry of a radical into a particle containing two radicals, instantaneous termination takes place. Chain length and radical compartmentalization are taken into account when determining the expression for the termination rate constant $k_t$.[65]

Termination rate coefficients have been shown to be chain length dependent. Termination is said to involve 3 steps: a) The encounter of end groups of two chains with each other, i.e. the end groups should be in close proximity with one another, caused by segmental diffusion, b) Center of mass diffusion leading to the chains bearing the end groups collide with one another, and 3) Termination which is very fast on the timescale of the diffusion controlled events.[85]

Radical exit is another phenomenon that cannot be excluded when modeling emulsion polymerization kinetics. Radical exit usually occurs upon chain transfer to monomer. This monomer radical can easily diffuse through the breadth of the latex particle and desorb into the aqueous phase before it can propagate. An exception is when the particles are extremely large and glassy in which case propagation is diffusion controlled. If the monomer radical propagates and forms a dimer, it may become too hydrophobic to re-renter the aqueous phase. The desorbed radical may undergo aqueous phase termination or re-enter another latex particle causing termination / re-exiting before termination.

## 1.7 Prior Art in Melt Processable PAN

Polyacrylonitrile homopolymer melts at 317 $^{0}C$[86] which is higher than the temperature at which degradation occurs. The production of carbon fibers involves the following steps: Synthesis of the acrylic fiber precursor, spinning of the acrylic fiber, thermoxidative stabilization of the fiber at ~200 $^{0}C$ and carbonization at elevated temperatures. Currently acrylic fibers are drawn by wet spinning from a suitable solvent such as DMAc or DMF at relatively low wt % of solids (about 5-30 %) so the throughput per pound of solid is not very high. It is for this reason and for eliminating the need for environmentally unfriendly solvents that melt spinning is preferred. Also, the melt spun fibers are believed to be void free which means lesser time is required in the stabilization and carbonization steps, thus reducing the cost compared to traditional solution spinning. However, due to the degradation by intra and inter chain crosslinking of the PAN chain at temperatures below its melting point, the PAN precursors cannot be melt spun.

### 1.7.1 Comonomers for Melt Processible PAN

High performance acrylic precursors for carbon fibers are generally very high molecular weight and have high acrylonitrile content. The atactic polyacrylonitrile that is produced via free radical polymerization does not have a three dimensional crystalline structure but rather exhibits lateral order that is known as paracrystallinity. Comonomers aid in disrupting this long-range order by acting as defects, thus improving solubility. Flory and Eby have put forth two different theories explaining this phenomenon. Flory

suggested that the comonomer is incorporated in the amorphous regions, thus reducing the length of sequences of acrylonitrile units.[87] Eby's theory states that the comonomer becomes incorporated in the crystalline lattice as a defect.[88]

#### 1.7.1.1 Effect of Comonomer Type and Content

The most commonly used comonomers are methyl acrylate and vinyl acetate. Acidic comonomers like methacrylic acid and itaconic acid can be used to control the exotherm during the stabilization step. Rangarajan *et al.* have shown the effect of various comonomers on the melt stability of polyacrylonitrile.[89] They investigated the amount of comonomer and copolymer molecular weight required to achieve the desired melt stability to melt spin the polyacrylonitrile copolymers that have applications in carbon fiber and textile fiber industry. Two different kinds of polymerization techniques, solution and redox aqueous dispersion polymerization, were used to synthesize copolymers of acrylonitrile and methyl acrylate with different compositions. The melt stability, time stability and char yield of these copolymers at 220 $^{0}$C was investigated. It was determined that at least 10 mol% of methyl acrylate was required to disrupt the long-range order in the polyacrylonitrile chains. Below that temperature, no flow was observed with the copolymers even at low molecular weights of 20,000 g/mol.

It has been demonstrated through investigation of three comonomers, methyl acrylate, acrylamide and isobutyl acrylate, that the size and nature of the comonomer affect the $T_g$ of the final copolymer. Isobutyl acrylate is bulkier and occupies more free volume, thus leading to a greater decrease in $T_g$ as compared to methyl acrylate for the same amount of comonomer loading. On the other hand, in accordance with the Fox-Flory equation, the incorporation of acrylamide increases the $T_g$ of the copolymer, as

the $T_g$ of polyacrylamide is greater than that of polyacrylonitrile. The acrylonitrile/acrylamide copolymer also had a high char yield of 65 wt% as compared to a theoretical char yield of 50 wt % for the polyacrylonitrile homopolymer.[90] However, due to the extremely viscous nature of the copolymer at the stabilization temperature (200 – 220 $^0$C) that was caused by extensive crosslinking, melt spinning was reportedly not feasible.

The amount of methyl acrylate in the copolymer is crucial to melt processing since a sufficient amount is required to disrupt the long-range order in the polyacrylonitrile chains and yet too much methyl acrylate would decrease carbon yield and lead to a more difficult stabilization step. Also, adding enough methyl acrylate increases polyacrylonitrile chain mobility, giving it more orientation when the fibers are drawn, thus enhancing the mechanical properties. Hence it is important to determine the optimum amount of methyl acrylate in the copolymer. DSC thermograms of copolymers with methyl acrylate contents ranging from 5 to 20 mol % in comparison with a polyacrylonitrile homopolymer showed a progressive decrease in $T_g$ as expected. Increasing the methyl acrylate content increases the amorphous region in the copolymer making the transition and shape of the curve better defined. However, in the range of copolymer content investigated (5-15 mol % of methyl acrylate), there was no evidence for a threshold value of methyl acrylate that disrupted long-range order in the polyacrylonitrile chains, which would be characterized by a large drop in $T_g$. This was better observed in the dynamic melt viscosity experiments where there was a large drop in the dynamic melt viscosity at 10 mol % of methyl acrylate and not much change with further increase in comonomer content to 15 mol%. Similar observations in the storage

and loss modulus were made. A fourfold drop in storage and loss modulus at 90 mol% methyl acrylate proved the existence of a critical amount of comonomer required to disrupt the crystalline nature of polyacrylonitrile. Wide angle X-ray diffraction also showed that the long-range order in the polyacrylonitrile chains was disrupted by increasing comonomer content, but quantitative information is unavailable. It has also been shown through dynamic melt viscosity measurements that by increasing the amount of comonomer, the molecular weight window for melt processing the copolymer becomes broader. Thus, it was determined that 90 mol% and 85 mol % of acrylonitrile in acrylonitrile/methyl acrylate systems are melt processible. The 85 mol % acrylonitrile copolymer had better flexibility with respect to the molecular weight window for processing[91]. However, these precursors with high comonomer content relax and/or fuse in the stabilization step while making carbon fibers, rendering them unsuitable for stabilization.

### 1.7.2 Plasticizers for Melt Processible PAN

One of the routes used to achieve melt spinnable polyacrylonitrile is the addition of 10-60 wt% of polar low molecular weight additives (plasticizers) that aid in reducing the melting point. It is expected that the dipolar interactions between the CN groups in the polymer will be decoupled and replaced by the interaction between the CN groups and dipoles of the additive. The choice of additive is partly governed by its ease of extraction from the spun fibers, level of toxicity and boiling point, all of which impact the overall cost of melt spinning and in some cases impact the fiber morphology.

Water has been investigated and patented as a plasticizer for these copolymers. It has been shown to reduce the melting point of polyacrylonitrile. Coxe was the first to report the melt extrusion of polyacrylonitrile hydrates under pressure.[92] Since water boils at 100 $^0$C, which is well below the melt processing temperature, the Coxe process failed due to foaming of the fiber at the die end. Frushour showed that a minimum of 20 wt% water was sufficient to lower the melting point of polyacrylonitrile to 200 $^0$C.[93-95] Porosoff modified the process and developed a melt spinning apparatus for the polyacrylonitrile-water mixtures using a pressurized chamber, but their process was not commercialized because Grove *et al.* later found that the fibers contained voids.[96, 97] Daumit *et al.* at BASF patented a procedure that used 23-48 wt% mixtures of water, acetonitrile and a monohydroxy alcohol and successfully achieved melt spun carbon fiber precursors.[98] Acetonitrile was later replaced by nitromethane and nitroethane.[99] Although the BASF process used significantly lower amount of solvents than commercial wet or dry spinning (70-80 wt%), the cost associated with the extraction and recovery of the toxic solvent prevented it from being commercialized.

Bashir and Atureliya reported the melt extrusion of propylene carbonate plasticized polyacrylonitrile where the crystallization of polyacrylonitrile from the plasticizer caused the extruded fibers to cool during fiber uptake, eliminating the additional step of using a coagulation bath. However, in spite of having eliminated the need to use a pressure chamber due to the high boiling point of propylene carbonate (240 $^0$C), there was a lack of chain orientation in the fibers which is critical to achieving good mechanical properties in acrylic and carbon fibers. The amount of plasticizer used to generate polyacrylonitrile copolymer melts with good shear thinning behavior has

been as high as 50 wt%.[100-102] Min *et al.* reported that mixtures of water and ethylene carbonate were synergistic in reducing the melting point, with water being the more effective component.[103]

In the 1990's, workers at British Petroleum developed a series of high acrylonitrile thermoplastic polyacrylonitrile copolymers and claimed that by using a starved monomer feed strategy the incorporation of comonomer in polyacrylonitrile can be manipulated to impart melt processability.[104, 105] However, the rate of extrusion was deemed too slow to achieve cost effective production.

Glycerin is a non-toxic plasticizer with a relatively high boiling point of 290 $^0$C. It was first reported by Alves *et. al.*[106] The mixture of glycerin and glycol additives was reported to depress the melting point of a high acrylonitrile content polyacrylonitrile/vinylacetate copolymer ($M_n$ = 270 kg/mol) from 390 $^0$C to 217 $^0$C, and successful extrusion of fibers of low diameter was reported. Furthermore, the dregradation enthalpy of a poly(acrylonitrile-*co*-vinyl acetate) copolymer that was melt processed using glycerin was shown to be lower than that of a poly(acrylonitrile-*co*-methyl acrylate-*co*-itaconic acid) copolymer.[107] It appears though that glycerin alone has not been shown to impart melt processability to polyacrylonitrile without the use of other additives. In addition, methyl acrylate is preferred over vinyl acetate as a comonomer for polyacrylonitrile precursors for carbon fibers due to greater melt stability of the copolymer. Small amounts of acid comonomer aid in controlling the exotherm during the stabilization step. Methyl acrylate also has more favorable reactivity ratios with acrylonitrile as compared to vinyl acetate, which enables uniform distribution of the comonomer in the polymer chain.[67]

## CHAPTER 2 : SYNTHESIS, SPINNING, AND PROPERTIES OF VERY HIGH MOLECULAR WEIGHT POLY(ACRYLONITRILE-CO-METHYL ACRYLATE) FOR HIGH PERFORMANCE PRECURSORS FOR CARBON FIBER

Used with the Permission of Elsevier, 2015 as:

" Chapter 2: Synthesis, Spinning and Properties of Very High molecular weight Poly(Acrylonitrile-co-methyl acrylate) for high performance precursors for carbon fibers, Morris, A.E.;Weisenberger, M.C.; Bradley, S.B.;Abdallah, M.G.; Mecham, S.J.; McGrath, J.E., *Polymer* **2014**, 55(25), 6471-6482."

### 2.1 Introduction

Due to their unique properties, carbon fibers are one of the leading reinforcing fibers for lightweight, high strength and stiffness composite materials [8, 108, 109]. The quality of the precursor fiber from which the carbon fibers are derived contributes to the properties of the resultant carbon fibers [8, 108, 110-112]. Polyacrylonitrile (PAN) precursor derived carbon fibers dominate the market due to their good strength and modulus properties [27] and high toughness. In order to increase ease of processing and minimize cost, the molecular weights targeted are usually lower than optimal for producing the highest strength precursor fibers. Currently, most carbon fiber is produced from acrylonitrile copolymer precursor fiber with acrylonitrile content of 95 weight % or higher and molecular weights in the range of 70,000 to 200,000 g/mole [14]. Polymer in this molecular weight range provides fibers, which have sufficient strength for textile applications, but the strength may not be optimal in precursor fibers for high performance carbon fiber. It is known that there is a strong impact of increasing molecular weight on increasing mechanical properties [113]. It has been reported that very high molecular weight (VHMW), high acrylonitrile (AN) content polymers estimated

at > 1,000,000 g/mole can provide significant increases in precursor fiber strength and modulus [114-116]. This paper tests and confirms that hypothesis. VHMW polymer leads to a reduced solids content necessary to produce a spinnable dope viscosity. Therefore smaller diameter filaments can be produced using VHMW polymer. These very small diameter filaments have been shown to provide a corresponding increase in tensile strength [27, 115]. The primary goal of this research was to investigate the development and implementation of a commercially feasible approach to synthesize and spin VHMW, high AN content (95-97 weight %) copolymers and analyze the resulting precursor fiber tensile properties as a function of decreasing filament diameter.

## 2.1 Experimental

### 2.1.1 Copolymer Synthesis

Very high molecular weight (VHMW) copolymer was synthesized at Virginia Tech using the following procedure.

#### 2.1.1.1 Materials

The monomers, acrylonitrile, ≥ 99+ % (AN) and methyl acrylate, 99 % (MA), the initiator, ammonium persulfate, and the activator, sodium metabisulfite, along with magnesium sulfate used in the workup of the emulsion, were all purchased from Sigma-Aldrich. The surfactant, Dowfax 8390 (35% in water), was kindly provided by the Dow Chemical Company. Acrylonitrile was eluted through an activated alumina column to remove the stabilizer immediately before use. Methyl acrylate was washed three times with 0.1 N aq sodium hydroxide to remove the stabilizer immediately before use.

#### 2.1.1.2. Copolymerization

The free radical emulsion copolymerization of AN and MA was conducted in a Parr pressure reactor under a nitrogen atmosphere. A representative procedure for a 97/3 wt% AN/MA copolymer is as follows. Deionized (DI) water (200 mL) was stirred and boiled for 20 minutes and then cooled without stirring immediately prior to its use in the reaction to remove dissolved oxygen. Dowfax 8390 solution (5.714 g solution, 1.7 wt % active surfactant) was diluted in 100 mL of the deoxygenated DI water at room temperature with vigorous stirring and then transferred to the Parr vessel. Acrylonitrile (97 g, 182.8 mmol) and methyl acrylate (3 g, 34.8 mmol) were weighed into beakers and each added to the Parr reactor followed by a 40 mL water wash with the deoxygenated DI water for each addition. The ammonium persulfate initiator (0.212 g, 0.05 mol % based on total monomers), and sodium metabisulfite activator (0.106 g, 0.03 mol % based on total monomers) were individually weighed and dissolved in 5 mL of deoxygenated DI water each, and then added to the Parr vessel. The reactor head was placed securely on top of the vessel after addition of the remaining deoxygenated DI water to bring the total % solids to 25%. The headspace of the Parr reactor was purged with nitrogen for 1 min and then sealed under a slight nitrogen pressure. The reaction temperature was automatically controlled via an internal cooling loop connected to a circulating cold water line. The reaction was stirred at 600 rpm and maintained at 25 $^{\circ}$C for 24 h. The resultant emulsion was added to 2000 mL of a 1 % aq $MgSO_4$ solution at 65 $^{\circ}$C and stirred briefly to break the emulsion, then the solid polymer was filtered. The solid powder was washed by stirring in 1500 mL of DI water at 65 $^{\circ}$C twice, and after the final filtration it was dried at 100 $^{\circ}$C under vacuum overnight. The recovered yield was 89 %.

#### 2.1.1.2.1 Copolymerization procedure for the time study

The free radical emulsion copolymerization of 85 wt% AN and 15 wt% MA was conducted in a Parr pressure reactor under a nitrogen atmosphere, in order to observe the progress of the reaction with time and the molecular weight or appearance of aggregation by SEC at different time points. Deionized (DI) water (200 mL) was stirred and boiled for 20 minutes and then cooled without stirring immediately prior to its use in the reaction to remove dissolved oxygen. Dowfax 8390 solution (5.714 g solution, 1.7 wt % active surfactant) was diluted in 100 mL of the deoxygenated DI water at room temperature with vigorous stirring and then transferred to the Parr vessel. Acrylonitrile (85 g, 160.2 mmol) and methyl acrylate (15 g, 174.4 mmol) were weighed into beakers and each added to the Parr reactor followed by a 40 mL water wash with the deoxygenated DI water for each addition. The ammonium persulfate initiator (0.212 g, 0.05 mol % based on total monomers), and sodium metabisulfite activator (0.106 g, 0.03 mol % based on total monomers) were individually weighed and dissolved in 5 mL of deoxygenated DI water each, and then added to the Parr vessel. The reactor head was placed securely on top of the vessel after addition of the remaining deoxygenated DI water to bring the total % solids to 25%. The headspace of the Parr reactor was purged with nitrogen for 1 min and then sealed under a slight nitrogen pressure. The reaction temperature was set to 20 $^{0}$C. The reaction exothermed to 39 $^{0}$C and the temperature automatically controlled via an internal cooling loop connected to a circulating cold water line. Three mL aliquots were drawn by opening the sampling valve, every 1 hour for 9 hours. Each emulsion sample was broken with 1 mL of 1 %

$MgSO_4$ solution, filtered, vacuum dried and weighed. After 24 h, reaminder of the emulsion was added to 2000 mL of a 1 % aq $MgSO_4$ solution at 65 °C and stirred briefly to break the emulsion, then the solid polymer was filtered. The solid powder was washed by stirring in 1500 mL of DI water at 65 °C twice, and after the final filtration it was dried at 100 °C under vacuum overnight. The recovered yield was 86 %.

### 2.1.2 Polymer Characterization

#### 2.1.2.1 Composition Analysis by $^1$H NMR

$^1$H NMR in deuterated dimethylsulfoxide (DMSO-$d_6$) was used to measure AN/MA copolymer compositions using a 400 MHz Varian NMR spectrometer. Copolymer composition was determined by comparing the integrals of the proton signals in the repeat units. The signal at 3.2 ppm (Y) corresponds to the methine (CH) protons from AN and MA. The signal at 2.1 ppm (X) corresponds to the methylene ($CH_2$) protons from AN and MA repeat units. The signal at 3.7 ppm corresponds to the methyl ($CH_3$) protons of the MA units. The copolymer composition was calculated from the integral values of the methylene protons using the following equations:

$$\text{Moles MA } \alpha \left(\frac{\int \text{CH}_3}{3}\right)$$

$$(\text{Moles MA}) \times \left(86.04 \frac{g}{mole}\right) = \text{relative weight MA}$$

$$\text{Moles AN } \alpha \left[\left(\frac{\int \text{X}}{2}\right) - \left(\frac{\int \text{CH}_3}{3}\right)\right]$$

$$(\text{Moles AN}) \times \left(53.06 \frac{g}{mole}\right) = \text{relative weight AN}$$

$$\text{Weight Percent AN} = \frac{\text{relative weight AN}}{\text{relative weight AN} + \text{relative weight MA}} \times 100$$

$$\text{Weight Percent MA} = 100 - \text{weight percent AN}$$

#### 2.1.2.2 Molecular weight analysis

Dilute solution viscosity measurements were used to analyze the relative molecular weights and estimate the viscosity average molar mass ($M_v$) of each copolymer prepared for spinning trials. Size exclusion chromatography with multiple detectors was utilized to determine the weight average molar mass ($M_w$) of polyacrylonitrile-*co*-methyl acrylate copolymers based on light scattering measurements.

#### 2.1.2.3 Inherent Viscosity in DMF

Inherent viscosity measurements were performed using a Cannon Ubbelohde viscometer, according to ASTM D445, at 35 °C in dimethylformamide (DMF). DMF was filtered through a 0.45 µm PTFE filter prior to preparation of the samples. Solutions with a concentration of 0.1 g/dL were prepared by dissolving 20 mg of the sample in 20 mL of pre-filtered DMF. The sample solutions were stirred at room temperature for 16-24 hours prior to testing to ensure complete dissolution. The polymer solutions were not filtered in order to avoid filtration of high molecular weight fractions. The solvent and solutions were allowed to equilibrate to 35 °C for 20 min in the viscometer and a total of 5 efflux times were recorded for the solvent and for the sample solutions. The inherent viscosity was calculated from the natural log of the average sample efflux time divided

by the average solvent efflux time all divided by the sample concentration to provide a value in dL/g.

#### 2.1.2.4 Intrinsic Viscosity in DMF and in DMF with 0.05 M LiBr

Intrinsic viscosity measurements were performed using a Canon Ubbelohde viscometer according to ASTM D445, at 35 °C in DMF with and without 0.05 M LiBr added. DMF was filtered through a 0.2 μm PTFE filter prior to preparation of the samples and the polymer solutions were not filtered before they were run. A solution of 500 mL of DMF with 0.05 M LiBr was prepared by dissolving 2.17 g of LiBr in 500 mL of the prefiltered DMF and stirring at room temperature for 24 h. Polymer solutions of concentration 0.25 g/dL were prepared by dissolving 50 mg of the sample in 20 mL of the solvent. The solutions were stirred for 1 hour at 50 °C and 1 hour at room temperature immediately prior to testing to ensure complete dissolution. Both the solvent and copolymer solutions were added to the viscometer in the temperature controlled bath and allowed to equilibrate for at least 20 minutes before efflux times were recorded. The copolymer solution was subsequently diluted inside the viscometer by addition of 4 mL of solvent to the original 8 mL of solution with manual mixing being accomplished through repeated manipulation of the solution in the viscometer with the pipette bulb. The solutions that were diluted in the viscometer were allowed to equilibrate for 15 minutes before efflux times for the new concentration were recorded. A series of six dilutions were performed in this manner, for which efflux times were recorded. The inherent and reduced viscosity was calculated for each concentration and then each was plotted versus concentration in order to determine the y-intercepts, which were evaluated, averaged, and reported as the intrinsic viscosity.

### 3.2.2.3 Size Exclusion Chromatography (Molecular Weight Analysis)

The SEC system utilized for the analysis of the polyacrylonitrile copolymers consisted of an Agilent Infinity 1260 pump, degasser, autosampler, and column oven for managing the solvent and injecting the samples. Tosoh alpha-M columns, 10 µm particle size mixed bed hydrophilic vinyl resin based columns with a broad distribution of pore sizes suitable for use with polar solvents and capable of separating polystyrene molecules up to 5,000,000 Daltons, were used for the separations. Data is also reported for alternative mixed bed columns based on polystyrene and designated as capable of separating polymers up to 2,000,000 Daltons. The detectors, from Wyatt Technologies, consisted of a DAWN Heleos II multi-angle laser light scattering (MALLS) detector, a Viscostar II viscosity detector, and a t-REX refractive index detector. The solvent system utilized was NMP, which was vacuum distilled over $P_2O_5$, degassed, and filtered through a 0.2 µm PTFE filter before use. In cases where salt was added to the solvent, dried LiBr (0.05 M) was added to the distilled solvent before it was degassed and filtered. Typically, SEC samples were prepared in concentrations ranging from 1.0-5.0 mg/mL as necessary to obtain good signal to noise ratio in all detectors used for analysis. The sample solutions were filtered to remove any dust or insoluble particles and typically a 0.22 µm PTFE syringe filter was used. In cases where it was suspected that large polymer molecules may have been filtered out, a larger filter size of 1.6 µm was used to minimize filtration of the sample molecules.

## 2.3 Spinning of VHMW PAN-co-MA Precursor Fibers

### 2.3.1 Dope Preparation

Spinning solutions (dopes) were prepared using a custom fabricated dope mixer, purposely-built for heating and slow stirring of the dope at controlled rates while maintaining zero-head gas space above the contained dope through means of a floating piston (analogous to a hydraulic accumulator), as shown in Figure 2-1. To prepare the dope, 51 g of VHMW polymer was hand-mixed with 800 g of Fisher Chemical reagent grade, dry *N,N*-dimethylacetamide (DMAc) to create a suspension. The suspension was placed under a rotor-stator, Silverson lab mixer (L4RT) operated at 3000 rpm for 10 minutes with a 2-inch diameter high shear screen in order to ensure a homogeneous mixture. The suspension was then vacuum degassed at a reduced pressure of 29.9 inHg for 20 minutes, poured into the dope mixer, sealed with the floating piston, and subjected to a 0.25 °C/min temperature ramp to 110 °C while stirring at 8 rpm. Thorough mixing of the suspension while heating ensured full dissolution of the polymer into the solvent and a homogeneous solution viscosity with minimal gel formation. Maintaining zero head gas space while mixing mitigated both the inclusion of air bubbles into the solution and the formation of a surface skin from dried polymer solution.

The fully dissolved dope was then slowly cooled to room temperature for extraction from the mixer. Dope extraction was completed using four KD Scientific 200 mL stainless steel syringes, fitted with Kalrez O-rings, that were filled from the bottom of the mixer through a 140 µm Swagelok in-line screen filter by locking the floating piston from rising and pressurizing the internal volume with nitrogen. The open syringes were then placed

in a vacuum box at 29.9 inHg for 4 h at room temperature to de-gas the dope. After the syringes were degassed, they were ready for integration into the dope metering pump inlet system, and sampled for rheological analysis.

### 2.3.2 Rheological Analysis

Rheological characterization of the VHMW polymer dopes was performed using a TA instruments AR-G2 parallel plate rheometer equipped with a temperature controlled Peltier plate and a 40-mm diameter upper plate geometry set at a gap of 500 µm. A thin layer of paraffin oil was applied to the gap edge circumference after the dope was loaded to prevent dope drying during the test. A conditioning step was completed at 25 °C, with a pre-shear of 1 $s^{-1}$ and equilibration of 1 minute before each step. Steady state shear viscosity analysis was completed by ramping the shear rate from 0.1 to 10 $s^{-1}$ at 25 °C. Dynamic oscillatory rheological analysis was completed using a frequency sweep step from 0.1 to 500 rad/s at 25 °C with a strain amplitude of 0.01 %. The storage shear modulus ($G'$), loss shear modulus ($G''$), complex viscosity ($|n^*|$), and tan delta (phase lag angle) were analyzed as a function of angular frequency. In addition, a temperature ramp step was completed, ramping the temperature from 25 to 100 °C at 3 °C/min, while holding the angular frequency at 10 rad/s and the strain amplitude at 0.01 %.

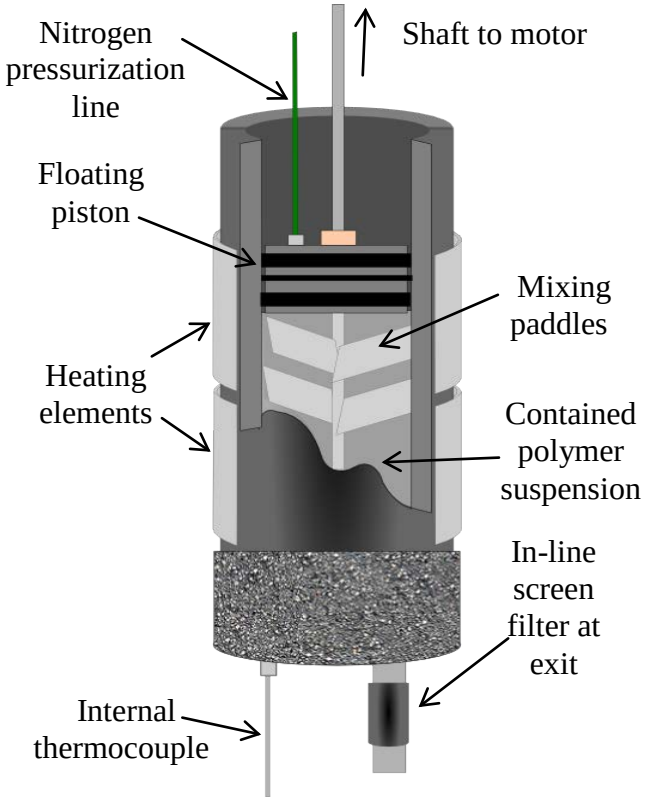


**Figure 2-1. Schematic of the custom fabricated dope mixer for full dissolution of polymer into the solvent**

### 2.3.3 Fiber Spinning Equipment

All fibers were spun utilizing the multifilament, solution fiber spinning facility at the University of Kentucky Center for Applied Energy Research. The spinning line was purposely-built to balance the production of meaningful research quantities of continuous filament tow (100-500 filament-count tow, ~ 1 km of tow) from small quantities of polymer (10s to 100s of grams), while minimizing the time and effort necessary for line preparation and change-over. The line efficiently affords itself to test the spinnability of numerous experimental dopes and enables the systematic variation of a plurality of processing parameters during spinning [117].

The spinning line was fed using four 200-mL stainless steel syringes loaded with the de-gassed dopes described above, which were pressurized using pneumatic cylinders into the dope inlet system. Sintered metal in-line filters, on the outlet of each syringe, were used to pre-filter the dope before it entered the metering pump, which provided a constant volumetric flow of dope downstream through a sintered metal filter cup, for the removal of gels and other agglomerates.

At the spinnerette head, the dope was passed through a screen pack for final filtration before flowing through the breaker plate to the spinnerette capillaries, from which jets emerged to form filaments. A variation of dry-jet (or air gap) solution spinning, in which the filament jets were extruded through a small air gap prior to being drawn into the coagulation bath, was used. Dry-jet spinning is used currently for producing high tenacity acrylic fibers [27, 118-120] and has several advantages over wet-jet solution spinning (where the polymer jets emerge from a spinnerette submerged in the coagulant), including: higher spin line speed, enhanced molecular orientation prior to coagulation (stemming from the high spin draw in the air gap), increased smoothness and luster of fiber surfaces, and discrete temperature separation between the dope and coagulation bath temperatures [27, 118-120]. The spinnerette used was a 100-filament dry-jet spinnerette, with 150 µm capillary diameter. Figure 2-2 shows forming filaments passing through an air gap and entering the coagulation bath liquid surface during dry-jet spinning at the University of Kentucky Center for Applied Energy Research.

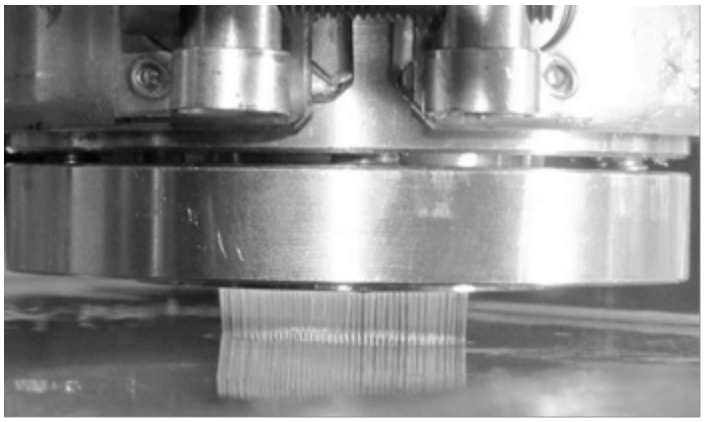

**Figure 2-2. Nascent filament jets passing through an air gap, accelerating and attenuating from an applied spin draw, and entering the coagulation bath during dry-jet solution spinning**

After passing through an air gap of 4 to 6 mm, and entering a 60 wt% DMAc/$H_2O$ coagulation bath, diffusion of solvent (DMAc) out of, and non-solvent (water) into, the forming filaments caused them to coagulate. The filaments were then passed through a sequence of wash baths, as in Figure 2-3. The coagulation bath was maintained near 0 °C, with the temperature-controlled wash baths increasing from 5 to 30 °C, followed by a hot water bath in which significant stretching occurs (to be discussed). A hot glycerol bath was used to further stretch the fiber above the polymer $T_g$, while the remaining two hot water baths provided a final level of washing prior to spin finish application, drying, and take-up using a traversing winder. The fiber tow was taken up at a rate of 56 m/min.

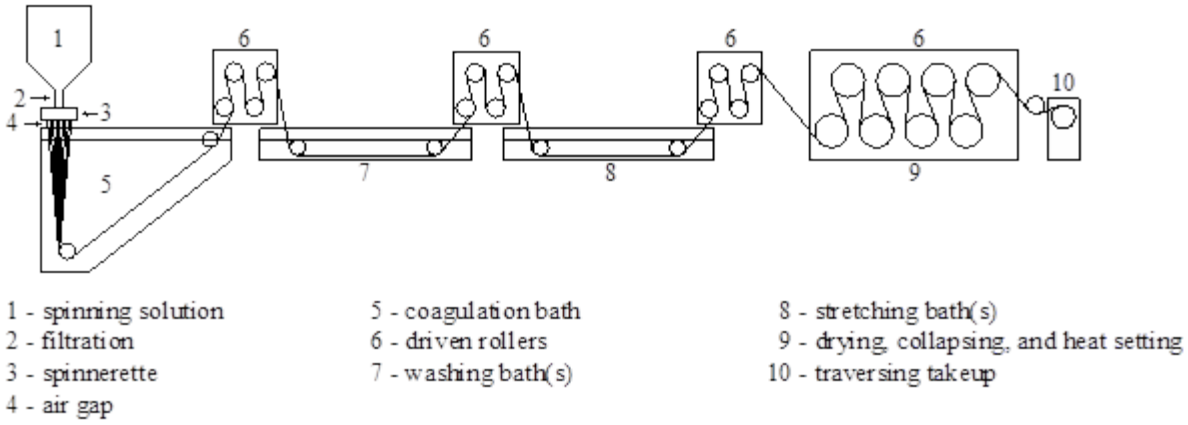


**Figure 2-3. Schematic of solution spinning line**

## 2.4 As-Spun Fiber Analysis

### 2.4.1 Optical Microscopy

Fibers were analyzed for cross sectional shape and area using optical microscopy. Collimated fiber tows were embedded vertically into epoxy, cured, and polished for optimum resolution. Fiber cross sections were viewed through a 100x objective lens with a 10x ocular through oil using reflected light. Fiber cross section perimeters were traced by hand using SPOT Imaging Solutions Microscopy software. Cross section perimeters were converted to an equivalent circular cross section diameter. A total of 50 specimens for each sample were analyzed.

### 2.4.2 Scanning Electron Microscopy (SEM)

Imaging of the precursor fiber surface and cross sectional morphology was performed using a Hitachi S-4800 field emission SEM. Low magnification samples (<100 kx) were sputter-coated with gold for 120 seconds, while high magnification samples (≥100 kx) were sputter-coated with platinum for 90 seconds, both using a Hummer 6.2 Sputter

System. Fiber cross-section samples were prepared for imaging by cutting the fiber bundle in liquid nitrogen using surgical scissors and placing the cut bundles vertically in the SEM sample holder. Fiber samples were prepared for surface imaging by adhering a short length of fiber bundle onto conductive carbon tape adhered to Al SEM sample holders. Fibers were imaged at 5 kV accelerating voltage.

### 2.4.3 Mechanical Measurements

Tensile properties of precursor fiber samples were measured using approximately 20 specimens per sample at a crosshead speed of 5 mm/min. A total of 296 specimens were tested. The specimens were prepared by bonding a single filament to a 40 mm gauge length aperture card using Easypoxy K-20. Following curing of the epoxy, the aperture card was mounted in the miniature tensile grips of an MTS Systems Q10 machine fitted with a 150 g load cell. The sides of the aperture card were then cut, leaving the filament intact.

## 2.5 Results and Discussion

### 2.5.1 Polymer Composition and Molecular Weight

Twenty-four 100-g batches of polymer were synthesized and compared for estimated $M_v$ and AN content using the inherent viscosity measurements and $^1$H NMR analyses. Figure 4 shows a representative $^1$H NMR spectrum of a 96/4 wt% AN/MA copolymer. Inherent viscosity measurements at 0.1 g/dL in DMF at 35 °C were used to estimate and compare the molar mass of polymers synthesized for spinning. It is anticipated that the inherent viscosity will be slightly higher than the intrinsic viscosity, but when comparing polymers of similar molecular weights at the same concentration,

the inherent viscosity procedure provides a good measure of comparison. The viscosity average molar mass ($M_v$) was estimated from the inherent viscosities using Mark-Houwink parameters [114]. The Mark-Houwink parameters are based upon the intrinsic viscosity. If the assumption is made that the solution concentration of 0.1 g/dL is sufficiently dilute for the polymers in question to provide a reasonable estimate of the intrinsic viscosity, then the use of the Mark-Houwink parameters can provide a reasonable estimate of the $M_v$. It was noted that there was no correlation between AN content, which varied only slightly, and inherent viscosity. Although it is expected that the Mark-Houwink parameters would be affected by a change in AN content, the range of variation between the samples being compared is very small so the effect on the estimated $M_v$ should be minimal. Table 2-1 provides the statistical analysis of the copolymers used for the spinning trials. It should be noted that one copolymer was synthesized which had a measured composition of 98% AN, and it was found to have inherent gels in the dope that inhibited spinning of that particular material.

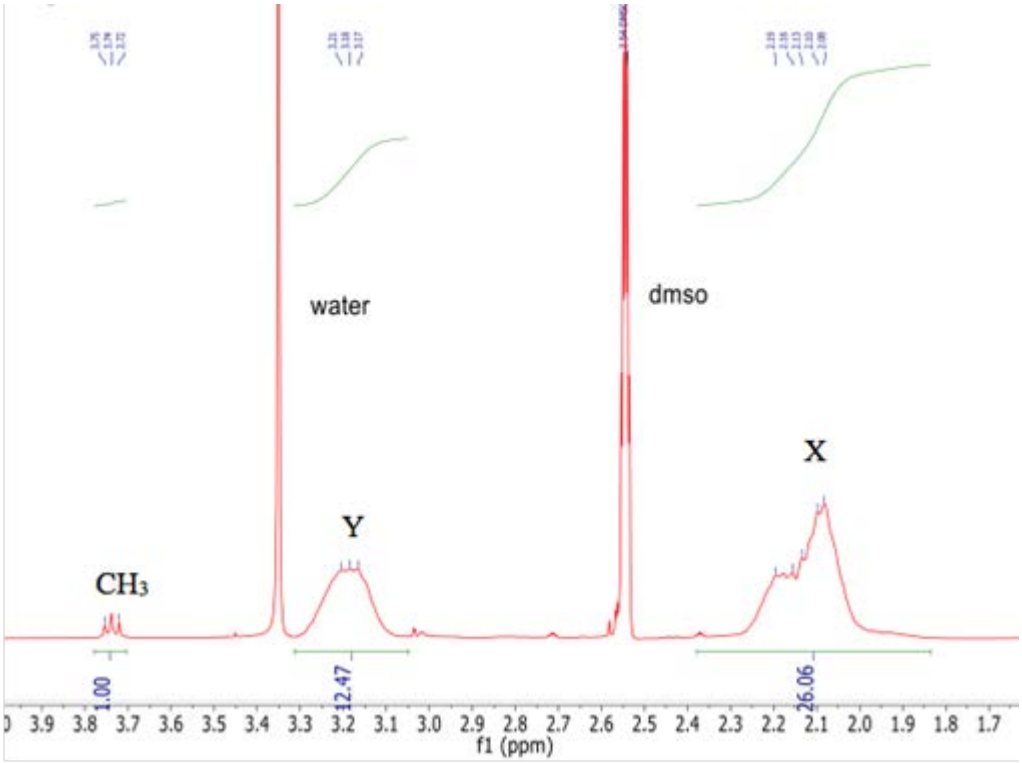


**Figure 2-4. $^{1}$H NMR of a 96 wt% AN and 4 wt% MA copolymer**

| | Acrylonitrile Content (weight %) | Inherent Viscosity (0.1 g/dL, DMF, 35 °C) | Estimated $M_v$ (g/mole) |
|---|---|---|---|
| Average | 97 | 7.8 | 775,974 |
| Standard Deviation | 1 | 1.3 | 169,617 |
| Count | 24 | 24 | 24 |
| Low | 95 | 5.9 | 529,155 |
| High | 98 | 10.9 | 1,204,817 |

**Table 2-1. Statistical analysis of 24 batches of polyacrylonitrile-co-methyl acrylate copolymers**

In order to investigate the impact of measuring the inherent viscosity at 0.1 g/dL instead of the intrinsic viscosity, a sample was tested at multiple lower concentrations, in order to determine the intrinsic viscosity for comparison. For this sample, the inherent viscosity was measured to be 10.9 (dL/g) and the intrinsic viscosity was 9.8 (dL/g), translating into calculated $M_v$ values of 1.2 and 1.04 million g/mole respectively. It was noted, however, that the sample preparation may have had the most significant impact on this observed difference. The analogous inherent viscosity value measured during the intrinsic viscosity experiment was 9.0 dL/g in the same solvent system prepared by stirring at 50 °C for 1 hour and room temperature for 1 hour. The original inherent viscosity value of 10.9 dL/g resulted from a sample prepared by stirring at room temperature overnight. The affect of the temperature of solvent preparation on the viscosity of the solution is likely due to the presence of the very high molecular weight, high acrylonitrile content, polymer chains being very slow to dissolve at room temperature, or the potential for aggregation of the polymer chains during the dissolution process. Table 2-2 provides the comparison of dilute solution viscosity measurements.

Based on the recognition that the addition of salt affected the polymer aggregation and molecular weight analysis by light scattering, the intrinsic viscosity in DMF with 0.05 M LiBr was measured to compare to the value obtained in DMF without salt. The intrinsic viscosity analysis did not show a large difference due to the addition of salt, exhibiting a value of 9.8 dL/g without salt and 9.7 dL/g with salt. Addition of the salt is proposed to break up aggregation of the polymer chains, which could affect polymer size and

viscosity. The aggregation observed in the light scattering measurements (presented in Figure 2-5) was not detected in the intrinsic viscosity results.

| Sample | $\eta_{inh}$ (DMF at 35 °C) (dL/ g) (0.1 g/dL concentration) | $[\eta]^{35}_{DMF}$ (dL/ g) | $[\eta]^{35}_{DMF}$ w/ 0.05 M LiBr (dL/g) |
|---|---|---|---|
| 97/3 VHMW AN/MA | 10.9 | 9.8 | 9.7 |

**Table 2-2. Dilute solution viscosity measurements of a sample of very high molecular weight polyacrylonitrile-co-methyl acrylate**

The samples of interest were VHMW copolymers with very high acrylonitrile content. Due to the high acrylonitrile content and high molar mass, the high viscosity of the solutions was apparent even at low concentrations. For the SEC measurements it was necessary to prepare the samples at relatively low concentrations of 0.5 to 1.5 mg/mL and use a larger than normal 1.6 µm filter for the sample solutions. Initially samples were run in NMP without added salt. Figure 5 presents the refractive index, light scattering, and viscosity chromatograms of a very high molecular weight sample run in NMP at 50 °C. This sample was a 97/3 AN/MA copolymer (by weight) prepared by emulsion polymerization. The sample was prepared at about 0.5 mg/mL and filtered with a 1.6 µm syringe filter. Light scattering was used to analyze the size of the molecules and the molar mass of the molecules. A dn/dc of 0.066 was used for the analysis. The dn/dc was calculated from an experiment where the dn/dc was determined offline in batch mode for a series of four AN/MA copolymers with varying molecular weights and AN content from 85 to 97% in NMP/0.05 M LiBr.

Figure 2-5 shows that the concentration and viscosity profiles, as shown by the refractive index and viscometer chromatographic results, differ from the light scattering profile with elution time. The light scattering peak appears to be bimodal with a very intense peak eluting first and a smaller peak that coincides with the bulk of the concentration of the sample eluting later. The very intense peak has no appreciable concentration or viscosity to it, indicating that it is a result of the presence of a relatively low concentration of very large/high molar mass species. In fact, the species in the early eluting intense light scattering peak are estimated to be on the order of 200 nm in size by the MALLS system. The same sample was run in NMP with 0.05 M LiBr added in order to eliminate or reduce polar interactions causing polymer aggregation and column exclusion [121].

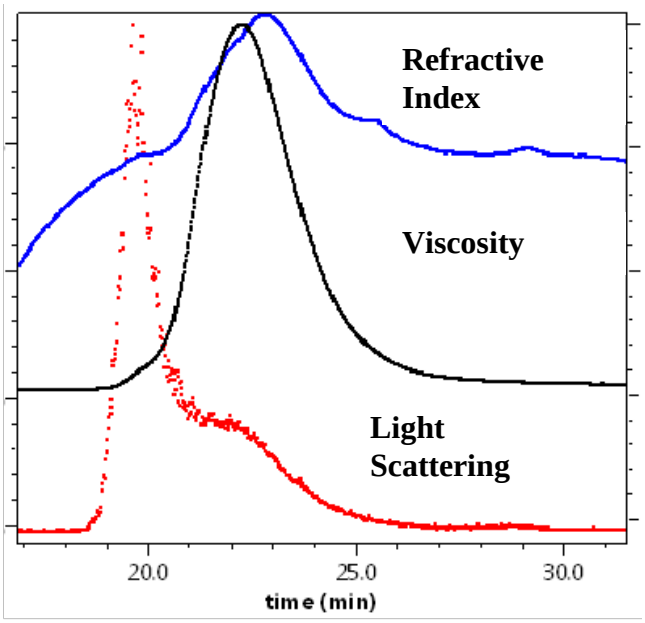


**Figure 2-5. SEC chromatograms of a 97/3 AN/MA copolymer in NMP at 50°C where the sample was filtered through a 1.6 µm filter (SEC analysis results are provided in Table 2-3)**

Table 2-3 provides a comparison of the molecular weight analysis for various solvent, concentration, and column configurations for the same sample of polymer powder. The molecular weight analysis provided in Table 2-3 consists of the molar mass averages, polydispersity, and average radius of each sample run by SEC for comparison. The injected mass is related to the concentration of a 100-microliter injection, and the mass recovery is related to the weight percent of the sample that was detected in the eluent by the refractive index detector. Loss of material is typically due either to filtration of undissolved or very large aggregated material during the sample preparation, or it can be due to polymer chains interacting with and sticking on the columns. Therefore, sample concentration, solvent composition, and column type were all found to be critical factors to the SEC measurements. The addition of the salt clearly results in a significant decrease in polymer aggregation in solution but the low mass recovery values indicate that material is still being lost during these SEC runs which may be limiting the range of the molecular weight distribution that is included in the molecular weight analysis. Higher salt compositions were prepared to further reduce the aggregation of the polymer in solution but these tests were not successful due to the limited solubility of the lithium salt in NMP.

Figure 2-6 shows the comparison of the light scattering chromatograms of the samples run through the same set of columns with and without LiBr added to the NMP. The results of the sample in NMP without added salt indicate that aggregation of the polymer molecules is occurring in this solvent system and that it can be at least reduced by the addition of LiBr salt. The results show low mass recoveries, which varies somewhat from sample to sample. The same sample preparation procedures used concentrations

ranging from 0.5 to 1.5 mg/mL. It is seen that the average molar mass values, as calculated by light scattering, decrease with decreasing mass recovery and there is an inverse correlation between sample concentration and mass recovery. This indicates that the high molecular weight fractions are being removed from the sample either by filtration of insoluble or large molecules during the sample preparation or by filtration in the columns. Therefore, it appears that the true molecular weight of this polymer is elusive because only the average molar mass of the smaller unfiltered fraction of the molecules can be measured due to the restrictions of the sample preparation and method conditions. Even with this limitation, it was possible to determine that the weight average molar mass of the polymer is at least 1.7 million g/mole.

| Solvent/ Column | $M_n$ (kDa) | $M_w$ (kDa) | Polydispersity ($M_w/M_n$) | Rz (nm) | Injected mass (µg) | Mass recovery (%) | dn/dc (mL/g) |
|---|---|---|---|---|---|---|---|
| NMP/1 high MW mixed bed PMA | 2193 | 13,844 | 6.31 | 218 | 56 | 73 | 0.066 |
| NMP0.05M LiBr/3 Mixed Bed PS | 952 | 1514 | 1.59 | 113 | 86 | 52 | 0.066 |
| NMP0.05M LiBr/2 high MW mixed bed PMA | 634 | 1268 | 2.00 | 131 | 148 | 34 | 0.066 |
| NMP0.05M LiBr/2 high MW mixed bed PMA | 1064 | 1713 | 1.61 | 111.7 | 67 | 52 | 0.066 |

**Table 2-3. SEC analysis of the same 97/3 AN/MA polymer sample in NMP with and without 0.05 M LiBr at 50 °C using two different columns shows the impact of losing the high molecular weight fraction of sample on the molecular weight results.**

The polymers of interest for this effort have significantly higher molar masses than commercially spun polymers used to produce carbon fiber precursors. SEC was used to compare a commercial copolymer, obtained by Oak Ridge National Laboratories, to the VHMW sample. The normalized light scattering chromatograms and weight average molar mass values are provided in Figure 2-7. The very high molecular weight polymer elutes earlier and the relative light scattering response is observed to be significantly larger due to the larger size of the molecules in solution.

Due to the fact that the samples appear to aggregate in NMP, it seems likely that the same behavior is present in related solvents such as DMF, DMAc, and DMSO, which are often used for solution spinning these polymers. The spinning solutions of these polymers in DMAc were prepared at a concentration of around 6 wt% solids and initially filtered through a 140 µm filter which is likely large enough to allow aggregates to pass through. It was observed that the material had a very high viscosity and the gelled fibers were mechanically very coherent, leading to high drawability. The presence of a highly aggregated/entangled component, as seen in the SEC in NMP without LiBr, could be adding to the strength of the gel phase. Molecular weight analysis of unfiltered very high molecular weight polyacrylonitrile copolymers is a subject of research in the laboratories at Virginia Tech utilizing Asymmetric Flow Field Flow Fractionation (AF4) equipment in NMP provided through an NSF-MRI.

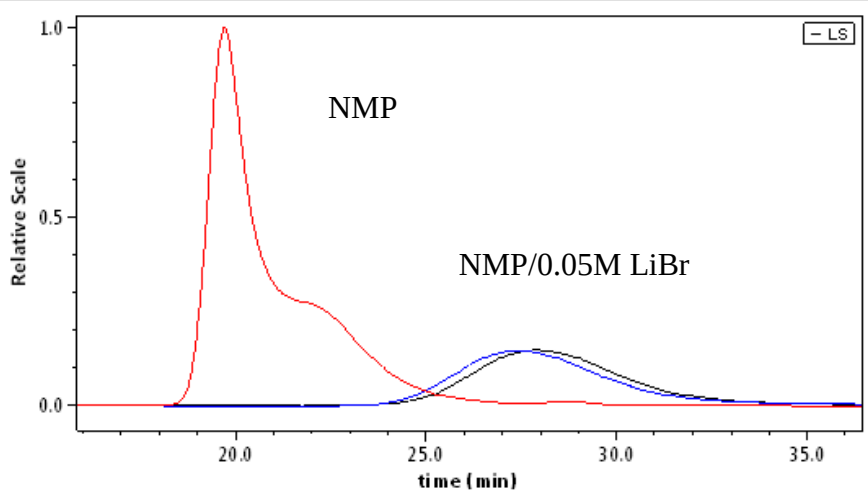


**Figure 2-6. Aggregation is apparent in the comparison of the normalized MALLS chromatograms of 97/3 AN/MA copolymer run in NMP with and without LiBr salt added.**

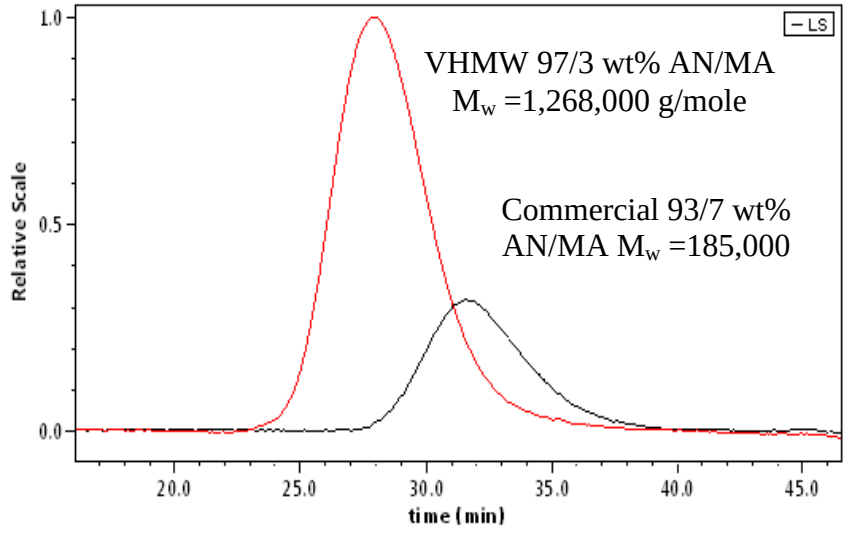


**Figure 2-7. Normalized light scattering chromatograms of a Virginia Tech synthesized VHMW 97/3 AN/MA compared to a commercially prepared 93/7 AN/MA copolymer run in NMP with 0.05 M LiBr.**

### 2.5.1.1. Molecular Weight Analysis as a function of reaction time

The free radical emulsion copolymerization of 85 wt% AN and 15 wt% MA was conducted in a Parr pressure reactor under a nitrogen atmosphere, in order to observe the progress of the reaction with time and the molecular weight or appearance of aggregation by SEC at different time points. **Figure 2-8** shows the light scattering chromatograms of the aliquots sampled from the emulsion polymerization mixtures at various reaction times, t= 1, 2, 3,4,5 and 6 hours, run in NMP with 0.05 M LiBr. The chromatograms of the different time samples are bi-modal. An intense peak with relatively low viscosity elutes at an earlier time followed by a slightly less intense peak with appreciable viscosity. An increase in the weight average molecular weight with reaction time was observed, as expected. It was also observed that the intrinsic viscosity which is a measure of the average hydrodynamic size of the polymer chains in solution, decreased with an increase in molecular weight, which is indicative of association or aggregation of these molecules, even in the presence of salt.

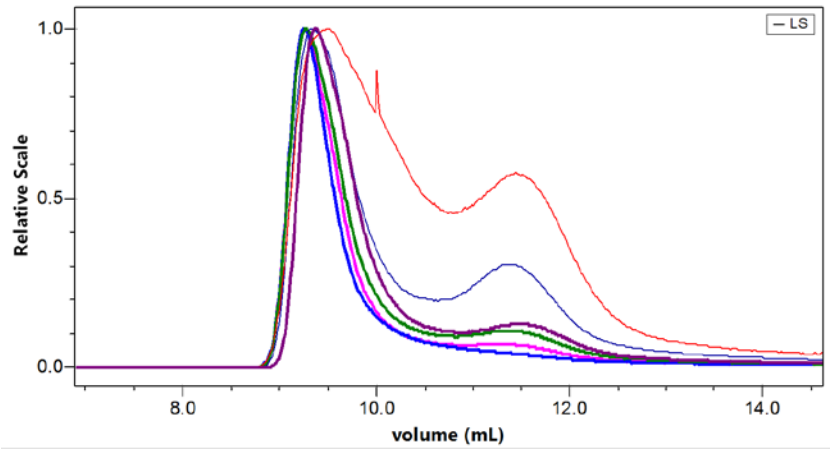


**Figure 2-8** Light Scattering chromatograms of the 85/ 15 wt/ wt% Poly(acrylonitrile-co-methyl acrylate) samples at different time points

### 2.5.2 Viscoelastic Properties of the VHMW PAN-co-MA Dope

Virginia Tech-synthesized VHMW (approximately 1.7 million $M_w$) 97% acrylonitrile, 3% methyl acrylate (by weight) copolymer was provided to UKY CAER for spinning trials. Initial formulation of the polymer-to-solvent concentration for spinning dopes relied on a previously established internal database of experimental data of spinnable solution viscosities. Steady shear viscosities of 150-200 Pa-sec at 1 $s^{-1}$ shear rate and 25 °C were targeted for dry-jet (or air-gap) spinning. As formulation of VHMW polymer dopes continued, a more accurate determination of spinnable viscoelastic property ranges was established for these VHMW polymers by rheological methods.

The results for several spinnable VHMW polymer dopes can be found in Figure 2- 8. The results show shear thinning occurring immediately at very low shear rates, similar to the results found by Jiang [122]. The results also provide a wide target-window for steady state shear viscosity, ranging from 70 to 250 Pa-sec at 1 $s^{-1}$ shear rate at 25 °C.

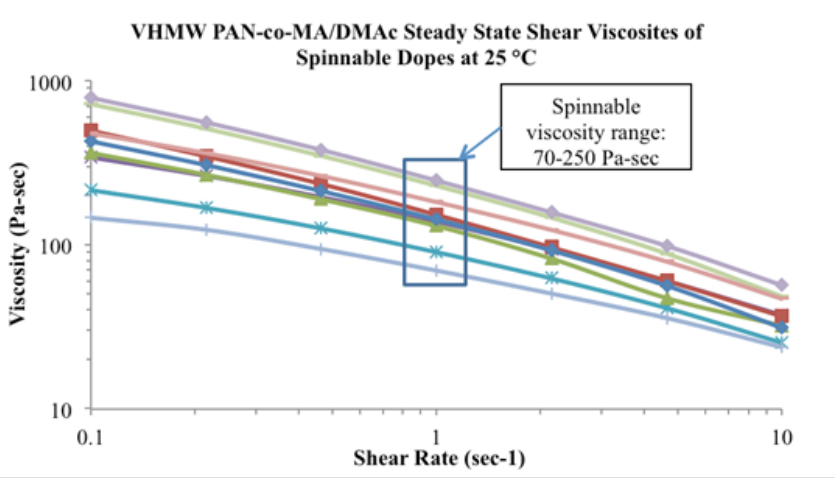


**Figure 2-9. Steady state shear viscosities of VHMW polymer dopes as a function of shear rate at 25 °C**

As dope formulation trials continued, the parameter ranges acceptable for good spinnability for other rheological properties of the dopes emerged, which included the storage and loss shear moduli, $G'$ and $G''$ respectively, as a function of temperature, shown in Figure 2-9. Storage and loss shear moduli decrease with an increase in temperature, as expected based on the results of Jiang [122]. In addition, a crossover point of the storage and loss shear moduli was typically observed for these VHMW PAN-based dopes. At room temperature, the dope behaved as a gel, as the elastic solid-like behavior quantified by the storage shear modulus, $G'$, was larger than the viscous liquid-like behavior quantified by the loss shear modulus, $G''$. However, as the temperature was increased, the dope became increasingly viscous as opposed to elastic, with a crossover occurring at 72 °C and 130 Pa. Similarly, as the temperature decreased below ambient conditions, the dope became increasingly elastic, with the $G'$ further diverging from $G''$.

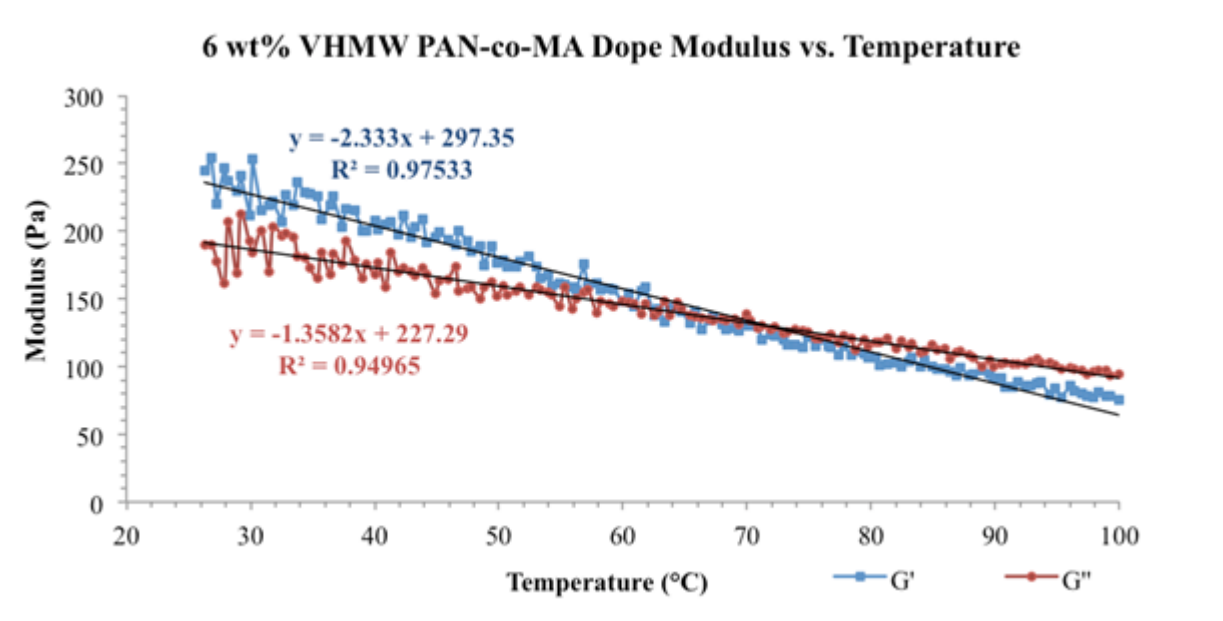


**Figure 2-10. The storage and loss shear moduli as a function of temperature with an angular frequency of 10 rad/s for dope showing the crossover point of G' and G"**

All of the results from these tests were compiled and analyzed, resulting in the summary graph shown in Figure 2-10, which details the average spinnable windows for various rheological properties of the spinning dopes. The average steady shear viscosity at 1 $s^{-1}$ and 25 °C ranged from 250 to 70 Pa-s. The average $G'$ at 10 rad/s and 25 °C was between 380 and 142 Pa, and similarly the average $G''$ was between 280 and 125 Pa. Average moduli were calculated using the linear regression equation from the temperature sweep data, similar to Figure 2-9. The average crossover temperature where $G'$ equaled $G''$ in magnitude was between 118 and 64 °C. The modulus at this crossover point was determined to lie between 138 and 86 Pa. All of these spinnable ranges were important to formulating and developing spinnable dopes.

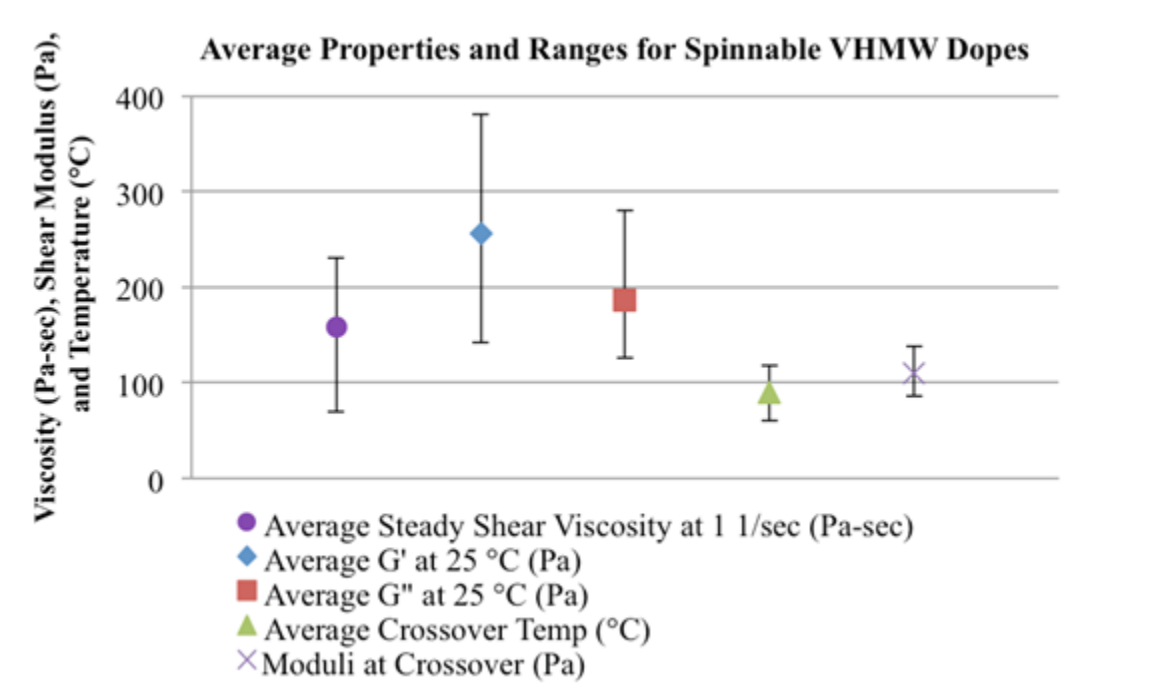


**Figure 2-11. Spinnable windows for rheological properties determined experimentally**

Further rheological analyses on formulated dopes was necessary to diagnose and correct issues related to spinnability. Initial spinning trials with VHMW polymer dope resulted in difficult startup for dry-jet spinning. A 6 wt% solution of VHMW PAN-*co*-MA in DMAc was spun into a 60 wt% DMAc/$H_2O$ coagulation bath maintained at 8°C. Nascent filaments did not properly coagulate and began to fail cohesively under small amounts of process tension in subsequent wash baths. Initial efforts focused on increasing the coagulation bath temperature to speed up coagulation kinetics. Solvent and water diffusion rates out of and into the polymer, respectively, have been shown to increase with bath temperature [109]. However, repeated attempts with the coagulation bath temperature increased to 30 °C resulted in similar failures.

Oscillatory rheology results indicated a relatively high storage (elastic) shear modulus ($G'$), which contributed to the solid-like, or gel behavior (Figure 2-11), particularly at lower temperatures. A spinnable lower molecular weight dope (LMW) ($M_w \approx 200{,}000$) at 20 wt% concentration showed the loss shear modulus ($G''$) well above the storage shear modulus in magnitude, suggesting that the liquid-like behavior of the solution dominated, allowing diffusion to take place more readily (Figure 2-12) [123]. Due to the divergent nature of the storage and loss moduli for VHMW PAN-*co*-MA with decreasing temperature, it was hypothesized that spinning into a chilled coagulation bath should drive the spinning solution towards a more gel-like state, and therefore create a more tenacious nascent filament – better able to withstand the process tensions encountered during the early coagulation and washing processes, during which solvent migration could also occur. Therefore, it was discovered that spinning into a coagulation bath near 0 °C was successful for the VHMW polymer solutions. Spinning polymer solutions into chilled baths to cause a temperature driven phase inversion is often referred to as gel spinning [124, 125]. Previous polyacrylonitrile gel spinning attempts have produced high strength fibers (1.8 GPa), but with large diameters (100 µm). The large diameter hindered thermal treatment and required excessive processing time, as fibers had to remain submerged in a bath for two days to fully solidify, limiting production capabilities [126]. The proposed hybrid method in this work between dry-jet and gel spinning will allow production of small diameter, high strength fibers using VHMW PAN-*co*-MA polymers and processing techniques suited for continuous operation.

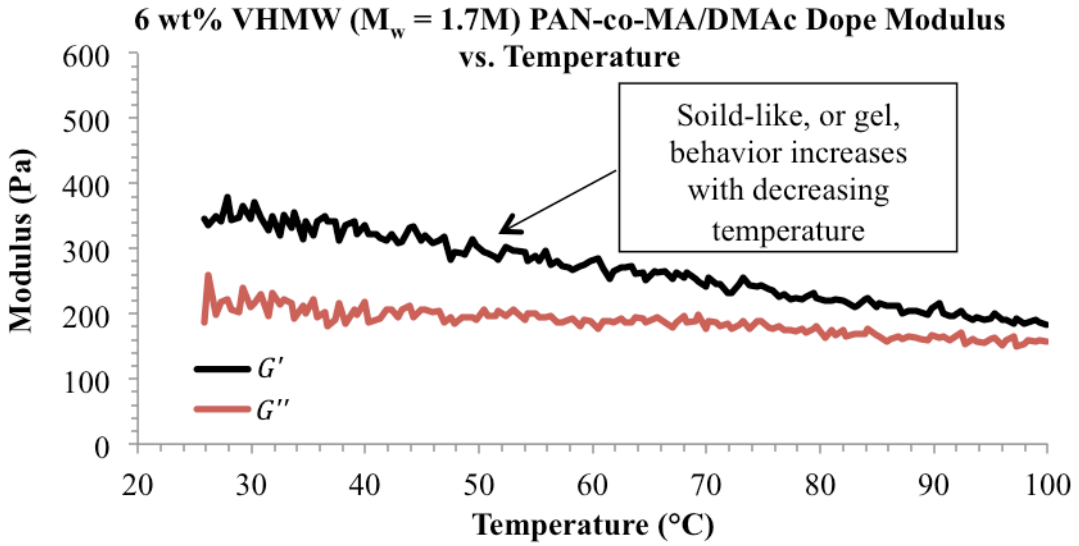


**Figure 2-12. Oscillatory rheology of a VHMW polymer solution ($M_w$ = 1.3M)**

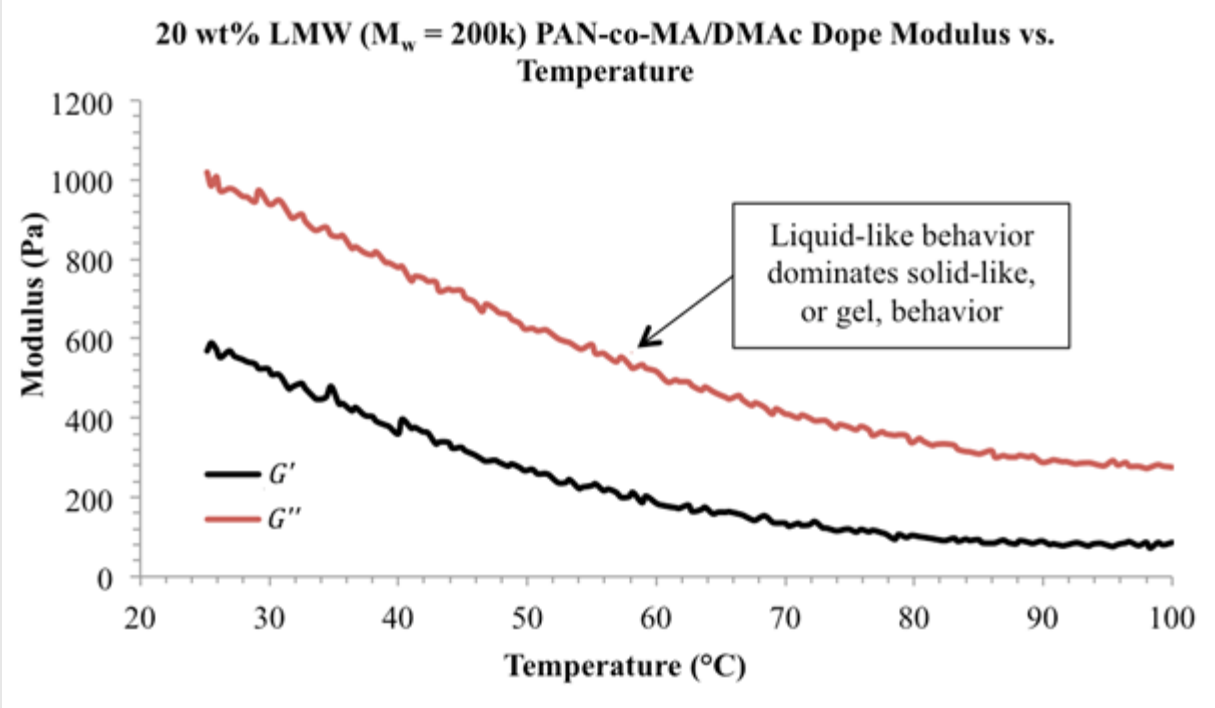


**Figure 2-13. Oscillatory rheology of a LMW PAN-*co*-MA polymer solution ($M_w$ = 200k) showing marked differences in the storage and loss shear moduli as a function of temperature compared to the VHMW PAN (Figure2-11).**

### 2.5.3 VHMW PAN-co-MA Fiber Spinning Conditions

As described previously, a variation of the dry-jet (or air-gap) solution spinning method was used to produce filaments from VHMW polymers, termed “hybrid dry-jet gel spinning”. Low coagulation bath temperatures were used to drive the forming filaments toward a gel state resulting in more tenacious nascent filaments.

The drawdown ratio (DDR) that the fiber tow was subjected to was measured between each set of godet drives (while within the preceding bath). The highest amount of stretching (DDR = 5.75) occurred in the coagulation bath. However, much of this draw occurred in the air gap. The dry-jet spinning method enabled high spin draw of the emerging polymer jets. The gel-like nature of the emerging filaments at this stage in the process also enabled high amounts of stretch, as the PAN molecules retained high mobility in the solution and were not yet set in place by the coagulation process. The forming, gelled filaments were further capable of withstanding a 1.50 DDR in the first wash bath and 1.33 DDR in the second wash bath, after which the fiber was solidified to the point that stretching within the subsequent cool and room temperature wash baths was not possible without producing fiber breakage. After washing, stretching occurred in a hot water bath, and subsequently in a heated glycerol bath, with DDRs of 1.70 and 2.20, respectively. The remaining portion of the line was not used for stretching, but rather for preparing the fiber for take-up. Measurements of residual DMAc showed a gradual, linear decrease in DMAc concentration in the filaments as they progressed through the coagulation/wash baths, resulting in a statistically zero residual content, which confirmed that the number of baths and selection of concentrations was appropriate.

Table 2-4 provides the spin draw (the stretch the fiber encountered in the air gap and coagulation bath), as well as the fiber stretch experienced throughout the remaining portion of the line (this is calculated as the product of the subsequent DDRs). The total DDR is the product of the spin draw and the fiber stretch, and for a representative VHMW PAN-*co*-MA, was determined to be 43.0. This high drawdown ratio [120], coupled with low solids content in the dope, led to precursor filament diameters of approximately 5 µm (equivalent circular diameter). An example of the collected precursor fiber in Figure 2-13 shows a 100 filament count tow, 560 m long, with a 5.7 ± 0.4 µm filament diameter, 1037 ± 101 MPa tensile strength, and 17.9 ± 1 GPa tensile modulus.

| Spin Draw | Fiber Stretch | TOTAL DDR |
|---|---|---|
| 5.75 | 7.5 | 43.0 |

**Table 2-4. The product of spin draw and fiber stretch give the total drawdown ratio (DDR)**

**Figure 2-14. 560 m of hybrid dry-jet, gel spun VHMW PAN-*co*-MA fiber in 100 filament count tow (5.7 ± 0.4 µm filament diameter, 1037 ± 101 MPa tensile strength, and 17.9 ± 1 GPa elastic modulus)**

### 2.5.4 As-Spun Fiber Structure and Physical Properties

As shown in Figure 2-14, the as-spun filaments had a slight kidney bean shape. Bean shapes can be common among solution spun PAN fibers, particularly when spun from dopes with low polymer solids and high $M_w$ polymers [8, 115, 127]. In addition, utilizing a cold coagulation bath, although necessary for this process, favors solvent flux out over water flux into the nascent fibers, also contributing to bean shapes [119, 128-130].

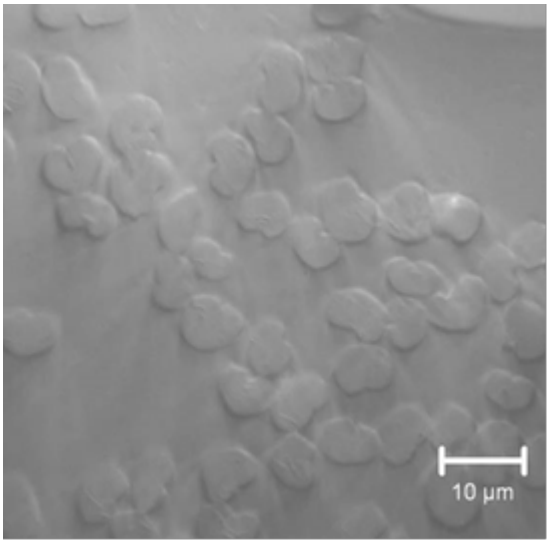


**Figure 2-15. Reflected light optical microscopy of VHMW PAN-*co*-MA fiber ends embedded in epoxy, magnification 1000x**

The fiber cross section shown in Figure 2-15 clearly shows the bean shape of the fibers, as well as some skin formation on the fiber surface, indicated by the arrows. This skin formation is likely a result of moisture-induced phase separation in the air gap.[131-134]

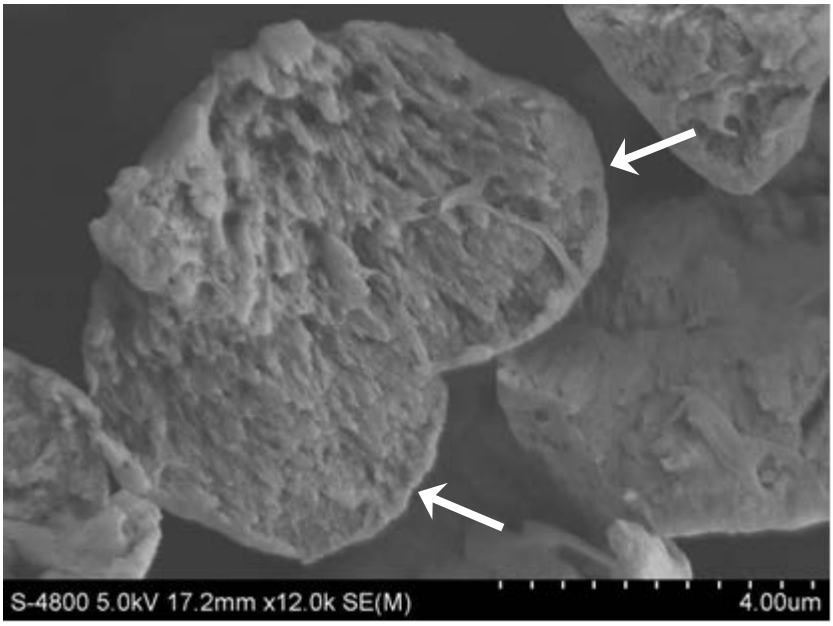


**Figure 2-16. Precursor fiber cross section imaged using SEM (a) Fibers at 1000x magnification (bean-shape highlighted by arrows). (b) Fibers at 3000x magnification (bean-shape highlighted by arrows). (c) 10kx magnification shows smooth fiber surface, typical of dry-jet spun fibers. (d) High magnification (100kx) shows striations in the fiber surface, typical for fibers produced using a diffusion coagulation process**

The images in Figure 16 show the smooth, near defect-free surfaces of fibers spun using the dry-jet gel spinning hybrid technique. It also highlights their bean-shape. In Figure 2-16a and b, the bean-shape is indicated by the arrows, which point to the concavity along the fiber midsection. Figure 2-16c shows the smooth fiber surface, typical of dry-jet spun fibers [135]. Figure 2-16d is a high magnification (100kx) of the fiber surface, showing striations along the fiber surface parallel to the fiber axis. This is characteristic of solution spun fibers which undergo diffusion during the coagulation

process and fibril orientation on the fiber surface [136, 137]. Overall, the filament surfaces were smooth and relatively defect-free, which contributed to their high tensile properties.

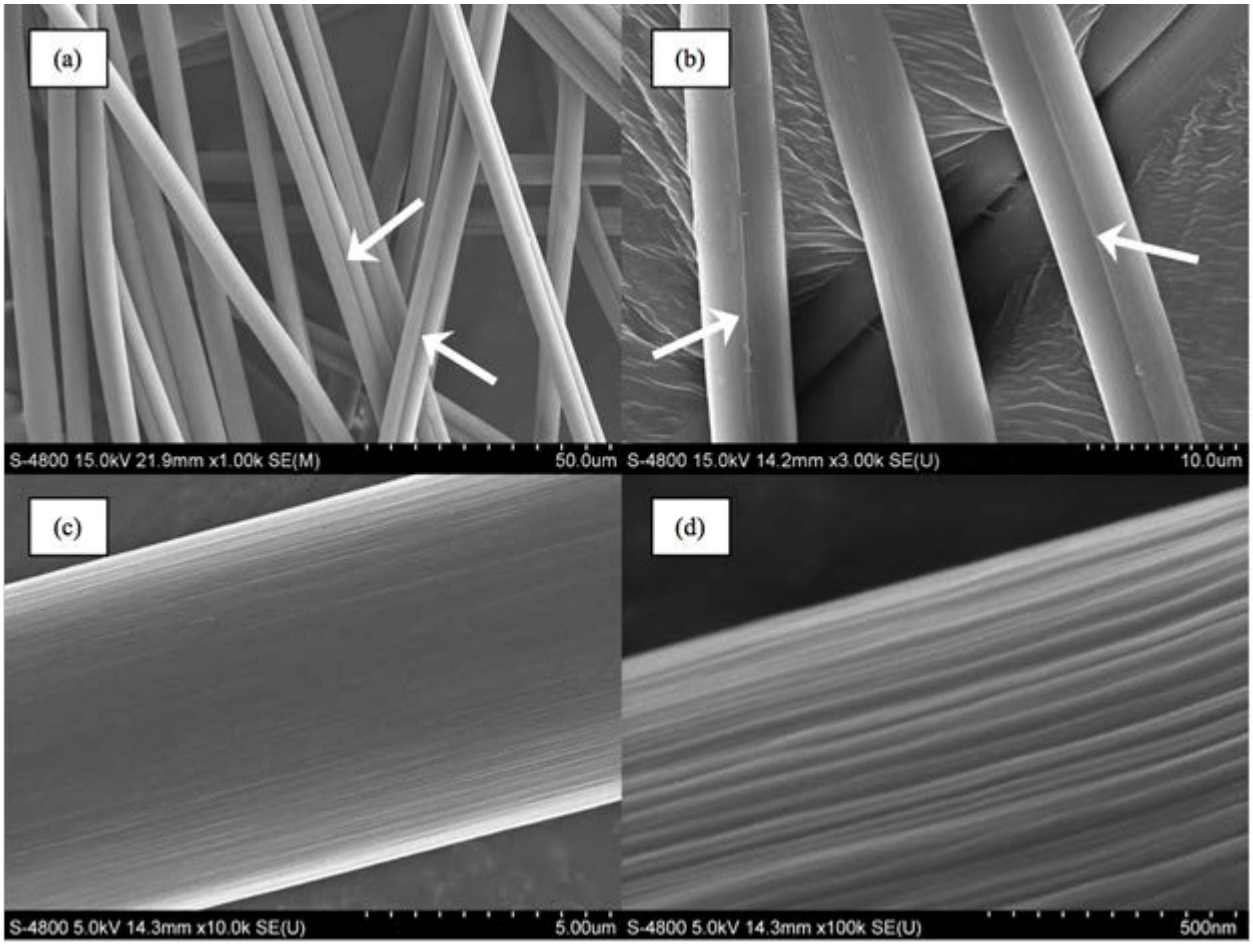


**Figure 2-17. SEM images of dry-jet spun VHMW PAN-*co*-MA fiber.**

(a) Fibers at 1000x magnification (bean-shape highlighted by arrows). (b) Fibers at 3000x magnification (bean-shape highlighted by arrows). (c) 10kx magnification shows smooth fiber surface, typical of dry-jet spun fibers. (d) High magnification (100kx) shows striations in the fiber surface, typical for fibers produced using a diffusion coagulation process

Tensile properties of commercial precursor filaments are not widely available. However, details about tensile strength, elastic modulus, and diameter can be gleaned from literature. For example, Hexcel produced a high performance carbon fiber with a tensile strength of 6.7 GPa and elastic modulus of 324 GPa from a relatively small precursor fiber diameter of 0.6 to 0.8 den, or 8.5 to 9.8 μm [138], assuming a filament density of 1.18 g/cc. Japan Exlan Company produced a PAN fiber having a larger diameter of 50 to 300 μm and a lower tensile strength of 80 to 460 MPa, from a polymer with a $M_w \geq$ 400,000 [139]. Toray Industries produced acrylic precursor fibers with 7.1 g/den strength. They report a resulting carbon fiber with a single filament diameter of 7.0 μm. Assuming a 50% reduction in fiber diameter from acrylic to carbon [140-144], it can be estimated that the precursor fibers had a diameter of approximately 14 μm. Based on this diameter, a 7.1 g/den strength translates to a precursor tensile strength of 456 MPa [145]. Mitsubishi Rayon precursor fibers were reported to have a tensile strength of 579 MPa [146]. Based on a titre of 1.24 dtex, the diameters of those fibers would have been 12.9 μm [146]. A patent by Nikkiso Co., Ltd. described production of a precursor filament with a diameter of 6.3 μm and a tensile strength of 687 MPa by spinning a 5.5 wt% solution of PAN with $M_w$ = 130,000 [147]. Based on these commercial examples, typical precursor fibers are generally no less than 6.3 μm, with a tensile strength no greater than 687 MPa, as summarized in Table 2-5.

| Manufacturer | Precursor<br><br>Fiber Diameter (μm) | Precursor Fiber<br><br>Tensile Strength (MPa) | Reference |
|---|---|---|---|
| Japan Exlan | 50 – 300 | 80 to 460 | [139] |
| Hexcel | 8.5 - 9.8 | | [138] |
| Toray Industries | 14 | 456 | [145] |
| Mitsubishi Rayon | 12.9 | 579 | [146] |
| Nikkiso Co, Ltd. | 6.3 | 687 | [147] |

**Table 2-5. Summary of precursor fiber diameters and tensile strengths produced with reference to commercial manufacturer**

In this work, filament diameter was shown to have a major influence on the tensile properties of the filaments (Figure 2-17). Smaller diameter filaments had higher tensile properties. This is in accordance with Griffith's fracture theory, which is consistent with the statement that at its extreme, a single polymer chain (filament of minimum diameter) would represent the strongest, highest-modulus filamentous form because such a filament could not exist with any defects present [148], and would contain no fraction of misoriented chains.

Figure 2-17 shows a power law relationship between ultimate break stress and fiber diameter, with $R^2$ = 0.91. The tensile strength and elastic modulus of the smaller diameter filaments, measuring from 4 to 6 μm, were averaged in Figure 2-18 and found

to be 954 ± 103 MPa in strength, 15.9 ± 1.8 GPa in elastic modulus (N=296) and 5.1 ± 0.5 um in diameter. Fundamentally, it is suggested that the use of VHMW polymers enabled the production of highly oriented, high tensile performance, small diameter filaments because: a) the very high molecular weight of the PAN-*co*-MA maintained the desired spinning viscosity even at low solids content. Less polymer per unit volume of nascent fiber results in commensurately smaller diameter filaments; b) the high molecular weight of the polymer chains was amenable to high degrees of draw which attenuated the fiber and increased the degree of chain orientation. Therefore, together, increased drawing of the fibers and lower solids content allowed for the production of a precursor filament diameter less than that used commercially, with a high tensile strength approaching 1 GPa (compared to approximately 687 MPa for commercial precursors).

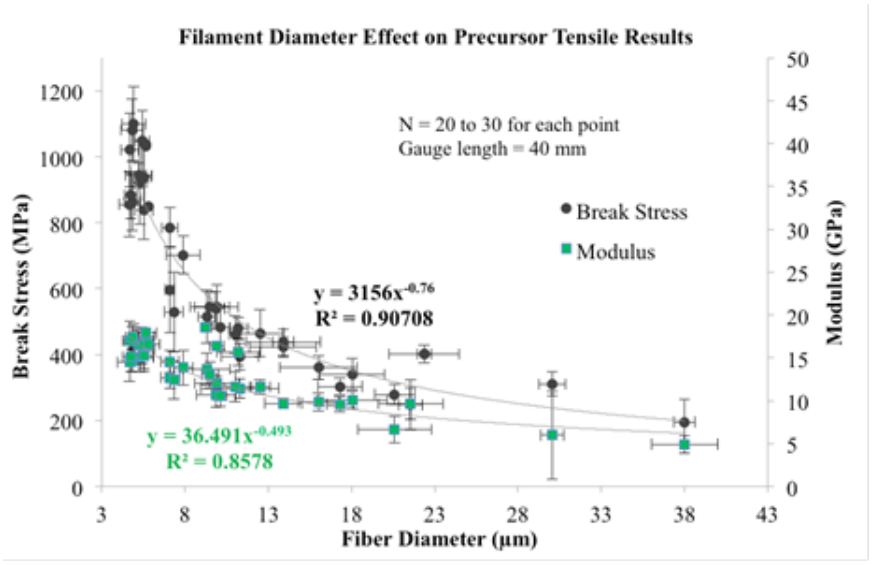


**Figure 2-18. Tensile properties of precursor dry-jet, gel spun fibers in this work from VHMW PAN-*co*-MA**

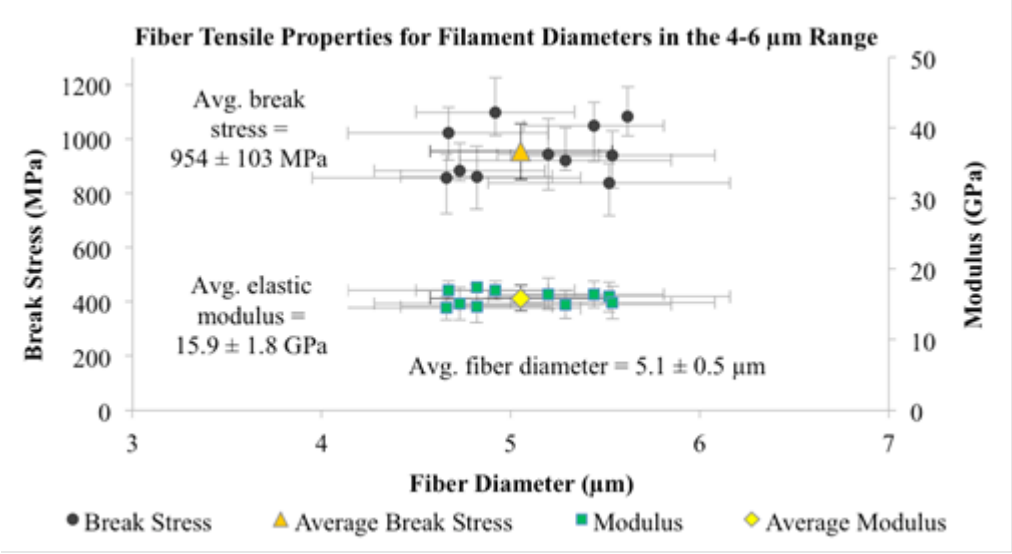


**Figure 2-19. Fiber tensile properties for filament diameters in the 4-6 µm range, showing the average values for break stress and modulus**

### 2.5.5 Effect of Polymer Molecular Weight on As Spun Fiber Properties

To illustrate the effect of molecular weight on fiber tensile properties, Figure 2-19 shows the results from Figure 2-17 separated based on polymer molecular weight, with high molecular weight characterized as being greater than 1 million Daltons (1 M) $M_w$ and low molecular weight being less than 1 M $M_w$. Results indicated an overlap between both modulus and tensile strength for high and low molecular weight. One run consisted of an 18.5 wt% low molecular weight (LMW) polymer in DMAc with a high drawdown ratio of 40x, while another consisted of a 5 wt% VHMW polymer in DMAc, intentionally drawn to a low drawdown ratio of only 5x (compared to a typical DDR = 43). It should be noted that although the VHMW polymer solution was drawn to a much lower drawdown ratio, it achieved the same fiber diameter as the lower molecular weight solution, which was drawn to a higher drawdown ratio. This is due to reduced solids content in the VHMW polymer dope. Therefore, while the runs consisted of differing molecular weights drawn at different ratios, the diameters, tensile strengths, and moduli overlapped, suggesting fiber tensile performance was not completely dependent on molecular weight.

In fact, the results indicated that fiber diameter played a larger role in determining final fiber tensile properties than molecular weight. However, as Figure 2-19 demonstrates, it is the high molecular weight polymer which enabled the production of the smallest filaments. That is, spinning dopes made with high molecular weight polymers could be prepared in a spinnable viscosity and processed at a lower solids content than lower molecular weight polymers. Also, high molecular weight polymers, due to the increased length of polymer chains, tended to have higher drawability [149], thus enhancing

orientation along the length of the fiber. Low solids content in the spinning solution coupled with increased drawability led to smaller precursor fiber diameters, and as a result, precursor fibers with higher tensile performance.

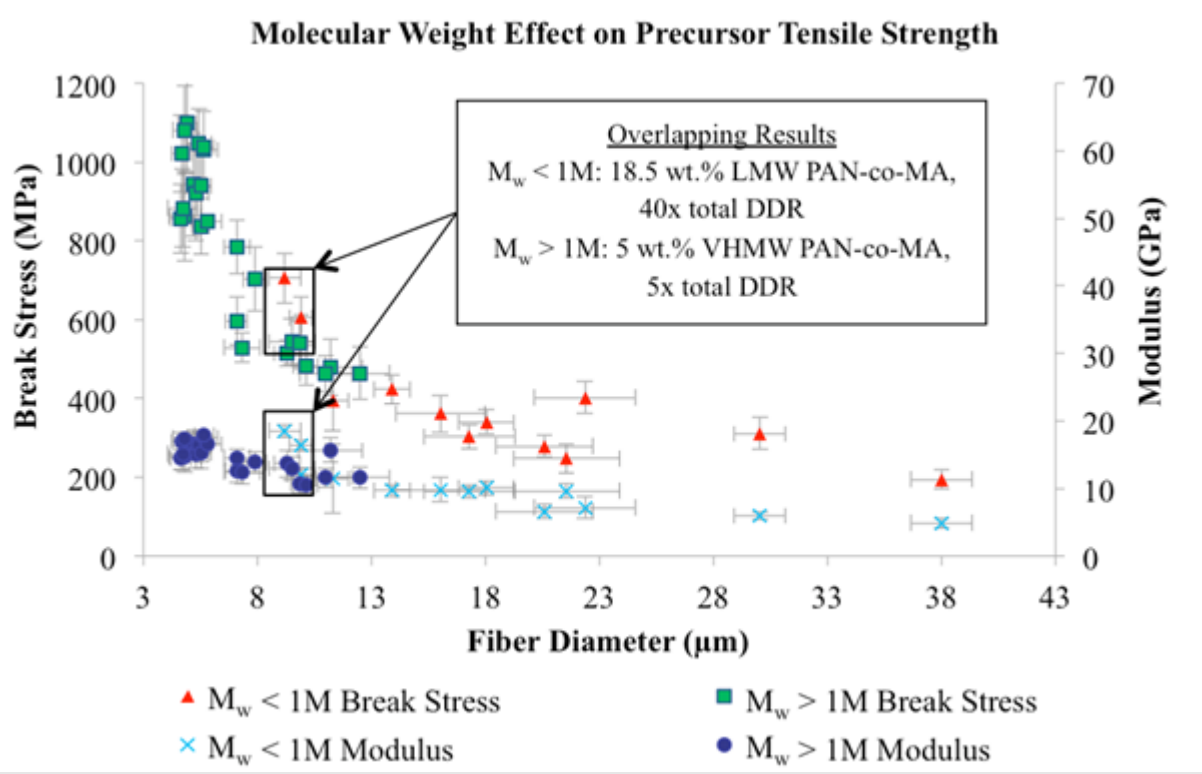


**Figure 2-20. Results shown in Figure 17 separated into high vs. low molecular weight to show the impact of molecular weight on tensile strength**

If higher molecular weight polymers can be synthesized, lower solids content can be utilized to produce spinnable dopes. For example, modifying the following equation derived from the work of Fox [150],

$$\eta_0 = KV_f M_w^{3.4}$$

where $\eta_0$ is polymer solution viscosity based on volume fraction of solids in the solution ($V_f$), molecular weight ($M_w$) of the polymer, and K is a constant related to polymer,

solvent, and temperature [150], allows for extrapolation of the molecular weight necessary for spinnability at low dope polymer concentration (assuming equivalent solution viscosities).

Based on the above equation and experimental results for spinnable polymer solutions, it was extrapolated that a spinnable solution could be produced which required only 1 wt.% solids content at a polymer molecular weight of 2.4 million. Neglecting the effects of die swell and stretch ratio, a change in dope solids content from 6 wt% to 1 wt% would result in approximately a 245% decrease in fiber diameter (from 37 µm to 15 µm). The fiber produced in this study from a 6 wt% solids content resulted in a 5.1 µm fiber diameter, with a tensile strength of 1 GPa, after a DDR = 43. Assuming the decrease in diameter with decrease in solids content to 1 wt% is conserved as the fiber is stretched down the line at the same DDR, the resulting fiber would have an approximate diameter of 2.1 µm. Applying the power law relationship for tensile strength via fiber diameter derived in Figure 2-17 ($R^2$ = 0.91), a precursor filament 2.1 µm in diameter would have a tensile strength of approximately 1.8 GPa. This is a conservative estimate, as the increase in molecular weight to 2.4 M would likely allow for a DDR higher than 43.

Ultimately, this work has shown that the use of VHMW polymers to achieve low solids content in the spinning solution, coupled with the increased drawability of VHMW polymers, led to smaller precursor fiber diameters, and as a result, higher tensile performance of the precursor fiber.

## 2.6 Conclusions

Synthesis of VHMW polyacrylonitrile-*co*-methyl acrylate copolymers with weight average molecular weights of at least 1.7 million g/mole were repeatedly achieved on a laboratory scale using emulsion polymerization, which is achievable in large scale commercial processes. SEC analysis of the VHMW samples in solvent with and without salt to break up aggregation identified the presence of polymer aggregates that are hypothesized to be associated with properties related to the processing of the spinning solution. Future efforts to further characterize the aggregation will be pursued at Virginia Tech.

Difficulties coagulating VHMW polymer-derived nascent filaments were overcome utilizing a hybrid dry-jet gel spinning technique. This hybrid dry-jet gel spinning technique utilized the solvent exchange process common in dry-jet solution spinning, while also utilizing a temperature-induced phase shift towards a gel fiber with tenacity capable of withstanding subsequent processing. Continuous, 100 filament count tows, 100s of meters in length were spun, analyzed, and their fiber form and mechanical properties were characterized. A power law relationship was identified between fiber diameter and fiber break stress and modulus. Experimentally, the hybrid dry-jet gel spinning method, coupled with VHMW polymers, produced precursor fibers with excellent tensile properties, averaging 954 MPa in strength and 15.9 GPa in elastic modulus (N = 296). There was a marked improvement in the ability of VHMW polymers to reach small filament diameters (~ 5 μm) compared to published data on commercial fibers. The higher molecular weight and lower solids content in the dope enabled high drawing and formation of small diameter filaments. In turn, these small diameter fibers

exhibited higher tensile strength and modulus compared to those produced by conventional methods [139, 145-147]. Extrapolation of the power law relationship between fiber diameter and tensile strength shows that a trend toward further increases in precursor tensile strength and modulus should be possible with further increases in precursor polymer molecular weight.

## CHAPTER 3 LOW TEMPERATURE SYNTHESIS AND CHARACTERIZATION OF POLY(ACRYLONITRILE-CO-METHYL ACRYLATE) STATISTICAL COPOLYMERS AND THEIR WATER BLENDS

Co-Authors: Ronald M. Joseph, Judy S. Riffle, James E. McGrath

### 3.1 Introduction

Carbon fibers are increasingly finding applications as reinforcements in composites that are lightweight and have high strength. The global carbon fiber consumption is highest in the industrial segment, with aerospace and sporting goods coming a close second.[151]

| Industry | Carbon Fiber consumption (Tons) | | |
|---|---|---|---|
| | Year 2006 | Year 2007 | Year 2008 |
| Aerospace | 6500 | 7500 | 9800 |
| Sporting | 5700 | 5900 | 6700 |

**Table 3-1** Carbon fiber production in tons[151]

Carbon fibers have also forayed into the automotive industry, since they allow for a significant reduction in weight relative to glass which is necessary for fuel efficiency. However their widespread use is impeded by the high cost of carbon fibers and composite fabrication.

The major precursor of carbon fibers in the market is polyacrylonitrile, while the other sources are pitch[152], and biopolymers like rayon and lignin.[153] Cost reduction of acrylic fibers was achieved in the synthesis step by Mitsubishi Rayon in the 70's by employing a low water- to-monomer technology. It was reported that, higher monomer concentrations and lower activator to initiator ratios of about 4, lead to increased particle

density. This increased particle density lead to lesser water absorption of the polymer slurry and also decreased costs in the drying step as expected.[154-156]

Currently all high performance acrylic fibers with relatively high acrylonitrile content are produced using expensive solution spinning techniques, and highly polar spinning solvents are required to dissolve polyacrylonitrile. Polyacrylonitrile homopolymer has a melting transition well above its degradation temperature, which prevents processing in the melt. This a result of the dipolar interactions between the nitrile groups, the intensity of which depends upon the spatial arrangement of the backbone chains. Hinrici-Olivè and Olivè reported that an antiparallel orientation gives rise to maximum attraction between the nitrile groups, while a parallel arrangement gives rise to maximum repulsion(Figure 3-1).[157]

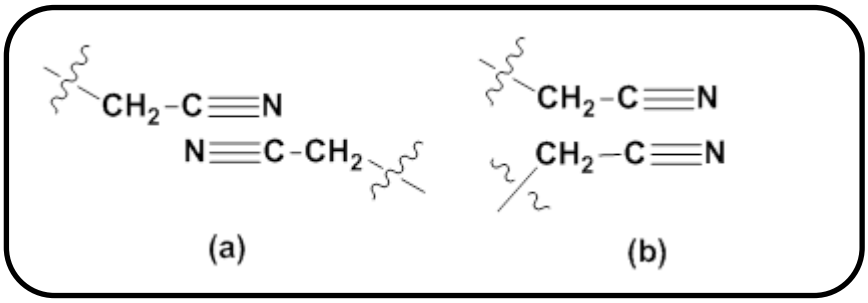


**Figure 3-1. (a) Antiparallel arrangement giving rise to maximum attraction.**

The backbone of the polyacrylonitrile chain thus arranges itself in a helical conformation to achieve the lowest energy state and when several of these chains are stacked, the nitrile groups on neighboring chains orient in an anti-parallel manner, giving rise to the strong attractive interactions.[158] Bohn *et al*[159]. were the first to report that polyacrylonitrile is two dimensional laterally bonded structure, followed by several other researchers who presented strong evidence in favor of the single phase model. However, a number of reports in the literature suggest the possibility of a two-phase morphology for polyacrylonitrile.[160, 161],[162, 163] .

In order to process this material at temperatures below the onset of degradation, melting should be achieved at 200 $^0$C or below. The approaches used to achieve this goal include incorporation of a suitable comonomer and/or benign plasticizers to reduce the melting point.

The first attempt at extruding polyacrylonitrile-water mixtures in the melt was reported by Coxe, where the major caveat was that the processing temperature was above the boiling point of water.[164] However, Frushour was the first to show through differential scanning calorimetry experiments, melting point depression of polyacrylonitrile from 320[165] to 185 $^0$C in the presence of water. Water decouples the dipolar interaction between the nitrile groups through hydrogen bonding. Furthermore, he reported that at a temperature above 185 $^0$C, polyacrylonitrile dissolves in water and forms a single phase, which is reversible upon cooling.[93] Bashir *et al.* analyzed water plasticized PAN films and hypothesized that, association of water with polyacrylonitrile chains, causes it to transform from a hexagonal to an orthorhombic polymorph, to accommodate the water molecule in the crystal lattice.[166]

Furthermore, it was reasoned that water decouples the dipolar interaction by forming hydrogen bonds between the hydroxyl and nitrile group, while the methine proton on the backbone may not be capable of this interaction due to insufficient polarization.

Despite the engineering difficulties that could arise when using water as a melt processing aid, it continues to be of great interest as a potential melting point depressant for polyacrylonitrile copolymers, because it is inexpensive, non-toxic and does not have any recovery costs.

However, along with a reduction in the melting point, It is also necessary to control molecular weight and molecular weight distribution of the poly(acrylonitrile-*co*-methyl acrylate) copolymers, in order to limit the melt viscosity. An important part of determining the molecular weight averages is knowledge of the dn/dc or specific refractive index increment, which is related to molar mass by Equation 1.

$$R(\theta) = K^* McP(\theta)[1 - 2A_2 McP(\theta)] \text{ - - - } (1)$$

where $R(\theta)$ (the excess Rayleigh ratio) is the ratio of scattered and incident light intensity. M is molar mass in g/mole and c is concentration in g/mL. $P(\theta)$ is the scattering function. $A_2$ is the second virial coefficient that defines the interaction between the polymer and solvent. K* is defined by Equation 2.

$$K^* = \frac{4\pi^2 n_0^2}{N_A \lambda_0^4}\left(\frac{dn}{dc}\right)^2 \quad - - - (2)$$

where $n_0$ is the solvent refractive index, $N_A$ is Avogadro's number, $\lambda_0$ is the vacuum wavelength of incident light, and dn/dc is the specific refractive index increment of the solution containing the dissolved polymer.

The dn/dc is dependent on the chemical composition of the polymer, the temperature, and the wavelength of the incident radiation in the light scattering detector.[167] It can be measured using the refractive index detector by two methods. One way is to manually inject a series of polymer samples with different concentrations into the detector using an injection box. The data is plotted on a differential refractive index versus concentration graph. The slope of the line is equal to the dn/dc of the polymer sample in that solvent. The other way is by obtaining a chromatogram of a known

concentration of polymer in solution, assuming 100% mass recovery of the polymer, and then calculating the dn/dc from the peak area. An assumption made in SEC is that the refractive index increment is constant across the molecular weight distribution of a homopolymer. However, in the case of a random copolymer, due to chemical inhomogeneity it can vary across the distribution as the level of comonomer content varies. In this case the dn/dc can generally be expressed as a weight fraction of each component, but this does not lead to accurate SEC molecular weights if it is not constant across the distribution. Hence, online manual dn/dc measurements are necessary in order to accurately determine the molecular weights of these random copolymers.

One objective herein is to develop a synthetic method for poly(acrylonitrile-*co*-methyl acrylate) random copolymers that have high acrylonitrile compositions (at least approximately 93/7 wt/wt % acrylonitrile/methyl acrylate) and where the weight average molecular weight is controlled to be within the targeted range of ~100-200 kg/mole. A challenge has been to establish a method for measuring molecular weight and molecular weight distributions of poly(acrylonitrile-*co*-methyl acrylate) random copolymers. A second goal has been to investigate thermal transitions of the copolymers plasticized with low molecular weight additives to identify copolymer-plasticizer combinations that lower the transition temperatures sufficiently to allow for melt spinning.

## 3.2 Experimental

### 3.2.1 Materials

A 95:5 mole:mole poly(acrylonitrile-co-methyl acrylate) copolymer was kindly provided by Oak Ridge National Laboratories (ORNL). Acrylonitrile monomer (≥ 99+%, AN), methyl acrylate (99%, MA), ammonium persulfate, sodium metabisulfite, 1-dodecanethiol (98+%) and magnesium sulfate were purchased from Sigma-Aldrich. The surfactant (Dowfax 8390) was kindly provided by the Dow Chemical Company. Acrylonitrile and methyl acrylate monomers were passed over activated alumina to remove the stabilizer. Activated alumina, 8-14 mesh, was purchased from Fischer Scientific.

### 3.2.2 Synthesis

#### 3.2.2.1 Emulsion copolymerization procedure

The free radical emulsion copolymerization of acrylonitrile and methyl acrylate was conducted in a 4-necked round bottom reaction flask equipped with a condenser, overhead mechanical stirrer, and nitrogen inlet. The reaction flask was then equipped with an overhead mechanical stirrer, condenser, and sealed. A representative procedure for an emulsion copolymerization of acrylonitrile and methyl acrylate is provided. Deionized (DI) water (200 mL) was boiled immediately prior to the reaction to deoxygenate. Deoxygenated DI water (150 mL) was added to a beaker containing Dowfax 8390 surfactant (5.7145 g, 3 wt% based on water) and the mixture was stirred until the surfactant dissolved, then the surfactant solution was added to the reaction

flask. Nitrogen gas was bubbled through the surfactant solution via a needle for 15 minutes, while the mixture was heated to 40°C. Acrylonitrile (47.5 g, 0.895 mol) and methyl acrylate (2.5 g, 0.029 mol) were added. The chain transfer agent, 1-dodecanethiol (0.3741 g, 0.2 mol % based on total monomers), was added to the flask. The ammonium persulfate initiator (0.2446 g, 0.116 mol % based on total monomers) was dissolved in 15 mL of DI water and added to the flask. Sodium metabisulfite activator (0.0533 g, 0.0315 mol % based on total monomers) was dissolved in approximately 15 mL of DI water and then added to the reaction flask. The remaining 20 mL of DI water was then added to the reaction flask. The reaction was stirred at 40 °C for 24 h. The reaction exotherm was controlled by replacing the oil bath with an ice bath when necessary. The resultant emulsion was added to 1500 mL of a saturated aq. $MgSO_4$ solution at 65 °C and stirred for 24 h, then the solid polymer was filtered. The polymer was washed with 1500 mL of DI water at 65 °C for 24 h. then dried at 70 °C under vacuum.

### 3.2.3 Characterization

#### 3.2.3.1 Composition Analysis by $^1$H NMR

$^1$H NMR in deuterated dimethylsulfoxide (DMSO-$d_6$) was used to measure poly(acrylonitrile-*co*-methyl acrylate) copolymer compositions using a 400 MHz Varian NMR spectrometer.10 mg of the sample was dissolved in 1 mL of the NMR solvent and 32 scans were performed. Copolymer composition was determined by comparing the integrals of the proton signals in the repeat units.

### 3.2.3.2 Molecular Weight Analyses

Absolute molecular weights from size exclusion chromatography (SEC) were measured using an Agilent 1260 infinity multi detector SEC equipped with a Wyatt Heleos II 18 angle SLS detector, a Wyatt Viscostar viscosity detector, and a Wyatt T-rex differential RI detector at 50 $^{0}$C using three PLgel 10 μm mixed-B 200 x 75 mm columns in series. DMAc containing 0.1 M LiCl was used as the elution solvent.

### 3.2.3.3 Differential Refractive Index Increment Measurement

Differential refractive index increment (dn/dc) measurements were made using an Agilent 1260 infinity multi detector SEC equipped with a Wyatt T-rex differential RI detector at 60 $^{0}$C and with a flow rate of 0.5 mL/min.

The following representative procedure was used: 400 mg of the sample was weighed into a vial and dissolved in 20 mL of DMAc containing 0.1 M LiCl. This solution was stirred for approximately 12 h. The sample solution was then diluted to 50 mL in a volumetric flask. This stock solution was used to make 7 new dilutions that were filtered through a 1-μm PTFE filter. The refractive index for each of 8 concentrations was measured and the data points were fit to a straight line (Figure 3-2a).The slopes of the straight lines obtained for each of the 4 copolymers were plotted against the composition of the copolymer to obtain the calibration curve (Figure 3-2b).

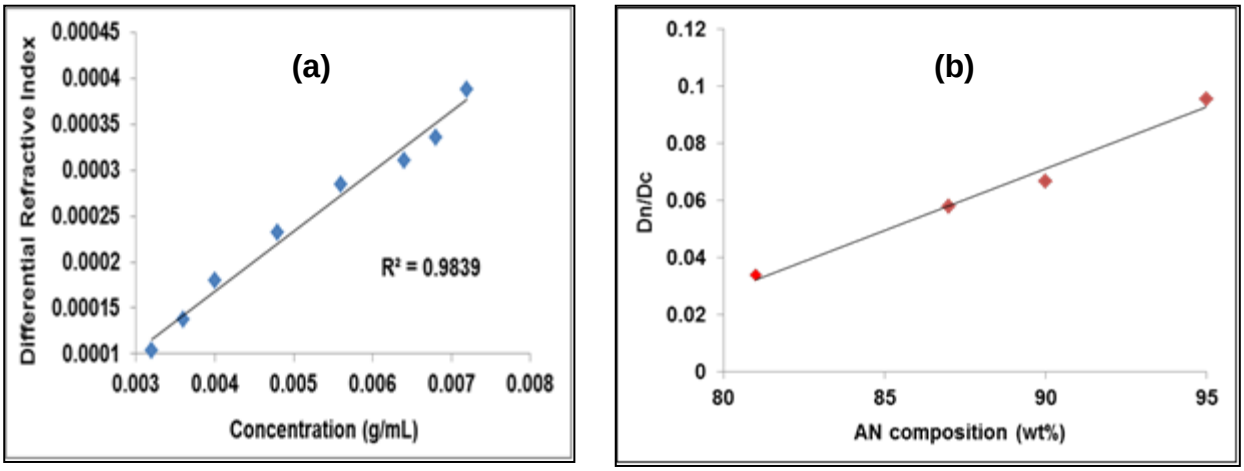


**Figure 3-2. (a) refractive index vs concentration plot of a 93/7 wt/wt % poly(acrylonitrile-co-methyl acrylate) copolymer (b) dn/dc calibration curve as a function of copolymer composition.**

### 3.2.3.4 Thermal Analysis

#### 3.2.3.4.1 Differential Scanning Calorimetry

The glass transition temperatures ($T_g$'s) and the melting temperatures ($T_m$'s) were measured via Differential Scanning Calorimetry (DSC) using a TA Instruments Thermal Analysis Q 1000. A 10 $^0$C/min heating rate was used to determine the $T_g$ and $T_m$ of copolymer-plasticizer blends. High volume pans with O-ring seals were used to prevent volatilization of the plasticizer. A single heating cycle from -20 to 250 $^0$C was performed. A heat scan of 10 $^0$C/ min was used to determine the glass transition temperatures of the pure copolymers in Al hermetic pans. A heat/cool/heat cycle was performed. The pans were heated from -20 to 150 $^0$C, cooled to -20 $^0$C and then heated to 290 $^0$C.

#### 3.2.3.5 X-Ray diffraction measurements

Powder X-ray diffraction (XRD) analyses were performed with a Bruker D8 Discover diffractometer (Bruker AXS, Inc.). Diffractograms were recorded over an angular range of 10–50° with Cu Kα radiation and an anode voltage and current of 40 kV and 40 mA, respectively. The diffractogram intensities were normalized and smoothed using EVA software and then plotted in excel. Hinrichsen's method used to calculate the % crystallinity.[168] The % crystallinity thus calculated, is a value that can be used to compare the relative degree of order in the polyacrylonitrile copolymers of varying comonomer content, but may not be treated as an absolute value.

### 3.2.4 Preparation of the copolymer and plasticizer blends

#### 3.2.4.1 Water blends

A representative procedure for making a 50 mol% (25 wt%) water blend with a poly(acrylonitrile-*co*-methyl acrylate) is as follows :The copolymer powder (0.75 g) was weighed in to a 20 mL scintillation vial and water (0.25 g) was added drop-wise with a syringe. The mixture was vigorously stirred with a spatula at ambient temperature for a few minutes. DSC measurements were made approximately 30 minutes after the samples were prepared.

## 3.3 Results and Discussion

### 3.3.1 Low Temperature Emulsion Synthesis of the Poly(acrylonitrile-co-methylacrylate) Copolymers

An emulsion polymerization method was developed to synthesize random poly(acrylonitrile-*co*-methyl acrylate) copolymers with a target weight average molecular weight range of 150-200 kg/mol. The reaction scheme and reaction components are shown in Table 3-2. The copolymerizations were initiated with ammonium persulfate and dodecanethiol was employed as a chain transfer agent to limit the molecular weights. Table 3-3 shows a series of reactions conducted as this method was developed. Reaction entry #1 was conducted without an activating agent and was begun at 50 $^{0}$C. This process yielded a copolymer with good yield and molecular weight close to the target, but the exotherm was difficult to control.

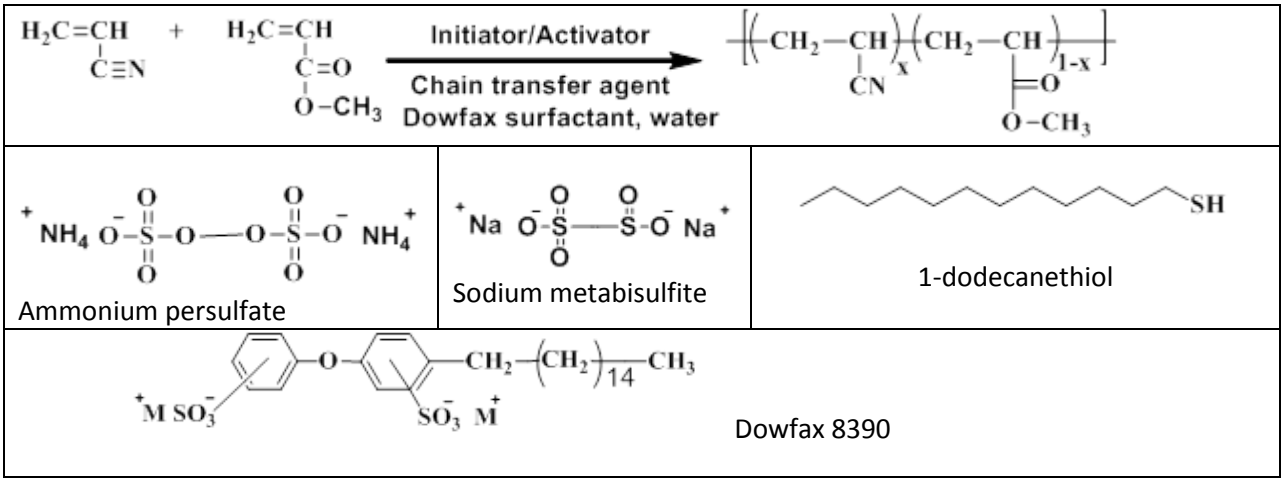


**Table 3-2 Reaction scheme and reaction components**

| Sample ID | AN/MA (wt/wt %) (charged) | AN/MA (wt/wt %) ($^1$H NMR) | Initiator (mol %) | Activator (mol %) | Set Temp - Max Temp (°C) | Reaction Time (h) | Recovered Yield (%) |
|---|---|---|---|---|---|---|---|
| **1** | 95/5 | 94/6 | 0.1 | 0 | 50-60 | 6 | 89 |
| **2** | 95/5 | 96/4 | 0.116 | 0.0630 | 40-52 | 20 | 60 |
| **3** | 95/5 | 95/5 | 0.116 | 0.0473 | 40-56 | 21 | 94 |
| **4** | 95/5 | 95/5 | 0.116 | 0.0315 | 40-47 | 24 | 88 |
| **5** | 95/5 | 96/4 | 0.116 | 0.0200 | 40-41 | 46 | low |
| **6** | 90/10 | 91/9 | 0.116 | 0.0315 | 40-46 | 23 | 97 |
| **7** | 85/15 | 85/15 | 0.116 | 0.0315 | 40-42 | 22 | 89 |
| **8** | 80/20 | 83/17 | 0.116 | 0.0315 | 40-43 | 24 | 76 |
| **9** | 93/7 | 93/7 | 0116 | 0.0315 | 40-41 | 16 | 60 |
| **10 Commercial copolymer** | - | 93/7 | - | - | - | - | - |

**Table 3-3. Synthesis and Characterization of random poly (acrylonitrile-*co*-methylacrylate) copolymers**

Experiments (2-5) were initiated at 40°C and contained systematically varied concentrations of the sodium metabisulfite activator. The goal was to find the lowest concentration of the activator that allowed for the reactions to be run efficiently at lower temperatures without a significant exotherm and with high yields. It was reasoned that this would also allow for potentially scaling up such a reaction. Entry (4) that contained 0.0315 mole percent of ammonium metabisulfite (relative to total monomers) was the most suitable concentration. This approach made the reaction exotherm more controllable. Entry (5) with less of the activator did not yield any copolymer even after a reaction time 46 hours at 40°C, and produced only a limited yield after 48 additional

hours at ~30 $^{0}$C. Additionally, 93/7 and 91/9 wt/wt % poly(acrylonitrile-*co*-methylacrylate) copolymers (9) and (6) were scaled up from 50 to100 g batches and were synthesized in high yields. This demonstrated good reproducibility in terms of control over the exotherm, final copolymer composition, target molecular weight range (100- 200 Kg/mol) and molecular weight distribution.

### 3.3.2 Composition analysis by $^{1}$H NMR

The compositions of the copolymers were confirmed via proton NMR. A representative NMR spectrum is shown in Figure 3-4. A schematic representation of the general copolymerization reaction and the chemical structures of the monomers, chain transfer agent, surfactant, initiator and activator can be found in Table 3-2.The signal at 3.2 ppm (b) corresponds to the backbone methine (CH) protons from acrylonitrile and methyl acrylate in each repeat unit. The signal at 2.1 ppm (a) corresponds to the backbone methylene ($CH_2$) protons from each repeat units. The signal at 3.7 ppm corresponds to the methyl ($CH_3$) protons of the methyl acrylate units. The copolymer composition was calculated from the integral values of the methylene protons using the following equations:

$$\text{Moles MA } \alpha \left(\frac{\int \text{CH}_3}{3}\right)$$

$$(\text{Moles MA}) \times \left(86.04 \frac{g}{mol}\right) = \text{relative weight MA}$$

$$\text{Moles AN } \alpha \left[\left(\frac{\int \text{a}}{2}\right) - \left(\frac{\int \text{CH}_3}{3}\right)\right]$$

$$(\text{Moles AN}) \times \left(53.06 \frac{g}{mol}\right) = \text{relative weight AN}$$

$$\text{Weight Percent AN} = \frac{\text{relative weight AN}}{\text{relative weight AN} + \text{relative weight MA}} \times 100$$

$$\text{Weight Percent MA} = 100 - \text{weight percent AN}$$

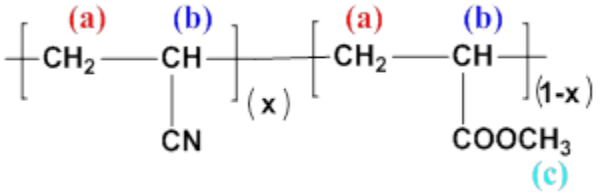


**Figure 3-3. Structure of Poly(acrylonitrile-*co*-methylacrylate)**

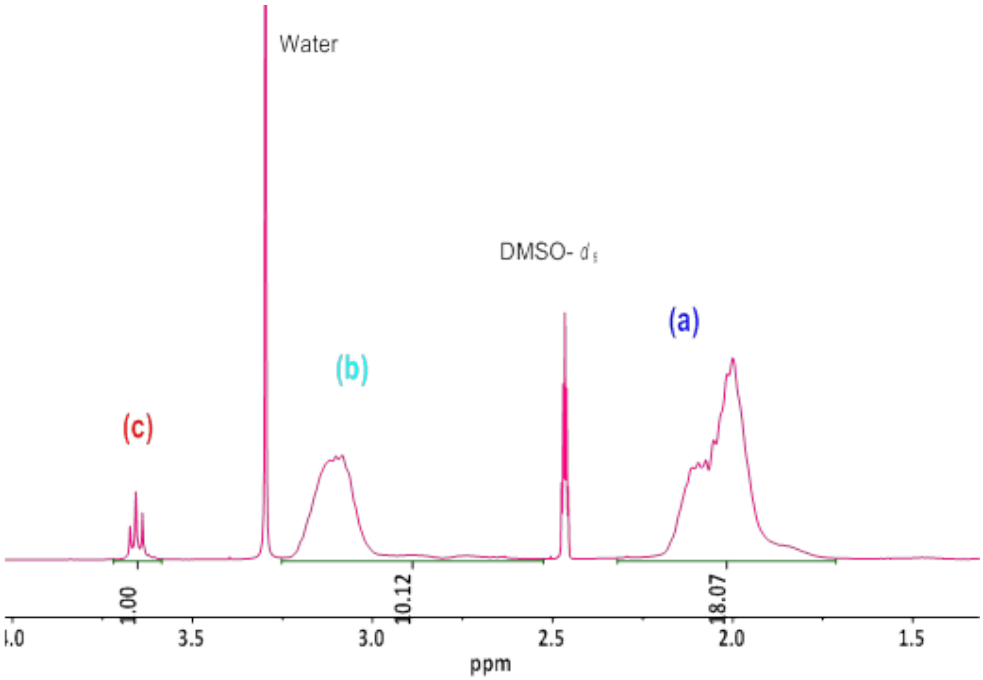


**Figure 3-4.$^{1}$H NMR spectrum of a 94/6 wt/wt % poly(acrylonitrile-co-methyl acrylate)**

All of these copolymers produced SEC chromatograms(Figure 3-5) that were Gaussian in nature and with molecular weight distributions centered around 1.8-2.0.This may be valuable as we investigate melt viscosities related to molecular weights and compositions. Figure 3-5 shows the chromatograms of some of the high acrylonitrile content copolymers i.e. entries 1-4. Entry 2, which employed the highest activator concentration in the series, also has the lowest molecular weight and a relatively broad molecular weight distribution, with a high molecular weight tail. A similar high molecular weight tail is visible in the chromatogram for entry 4.This may not be desirable as it can cause an increase in the viscosity of the polymer melt.

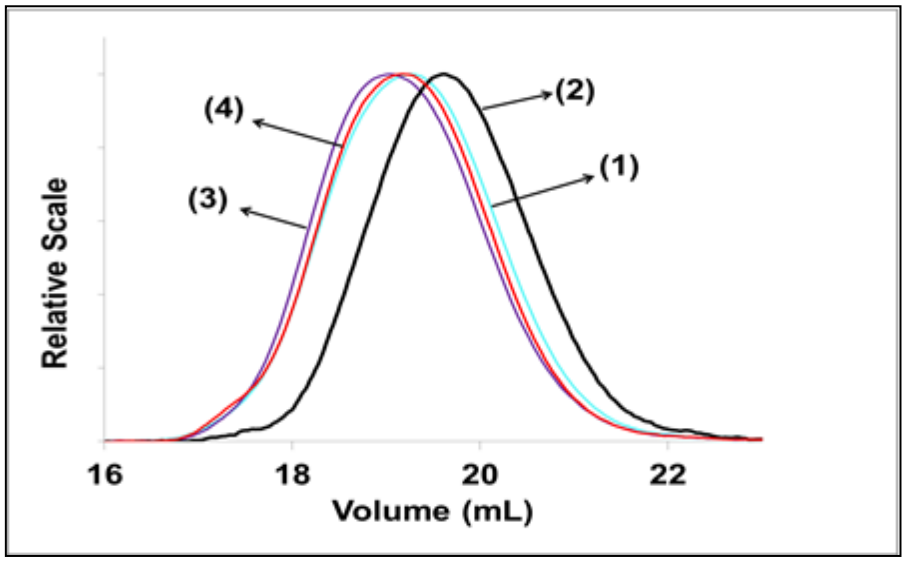


**Figure 3-5. Light scattering chromatograms of poly(acrylonitrile-co-methyl acrylate) entries 1-4**

| Sample ID | AN/MA (wt/wt %) (charged) | AN/MA (wt/wt %) (By $^1$H NMR) | SEC $M_w$ (kg/mol) | PDI | [η] (dL/g) |
|---|---|---|---|---|---|
| **1** | 95/5 | 94/6 | 132 | 1.8 | 0.97 |
| **2** | 95/5 | 96/4 | 82 | 2.2 | 0.62 |
| **3** | 95/5 | 95/5 | 152 | 1.8 | 1.1 |
| **4** | 95/5 | 95/5 | 143 | 1.7 | 1.0 |
| **5** | 95/5 | 96/4 | insoluble | low | -- |
| **6** | 90/10 | 91/9 | 130 | 1.9 | 0.63 |
| **7** | 85/15 | 85/15 | 118 | 1.8 | 1.0 |
| **8** | 80/20 | 83/17 | 135 | 1.8 | 0.82 |
| **9** | 93/7 | 93/7 | 200 | 1.8 | 1.40 |
| **E22B-13 Commercial** | - | 93/7 | 223 | 2.6 | 1.51 |

**Table 3-4 Molecular weight data of the poly (acrylonitrile-*co*-methylacrylate) copolymers**

The reaction entries (6), (7) and (8) were conducted with the activator concentration used in entry (1) but at varying compositions of the methyl acrylate comonomer. These copolymers were used to obtain the dn/dc calibration curve and can later be utilized to assess melt viscosities and transition temperatures as a function of composition.

### 3.3.3 Thermal Analysis of the Poly (acrylonitrile-*co*-methylacrylate) Water Blends

(1), (3) and (4) were of interest to further examine for potential melt processability, because of the desired acrylonitrile content, molecular weight and molecular weight distribution that was achieved. Water blends of the 94/6 wt/wt % poly(acrylonitrile-*co*-

methylacrylate) with 37 and 49 mol% were prepared and the thermal properties were examined. The glass transition temperature was lowered to 74 and 73 $^{0}$C from 96 $^{0}$C. A melting endotherm was observed at about the same peak temperature of about 171 $^{0}$C, however the endotherm was sharper, narrower and more uniform in case of the 49 mol% water blend, compared to the blend with the lower water content (Figure 3-6), which may make it more suitable for further investigation on melt processability.

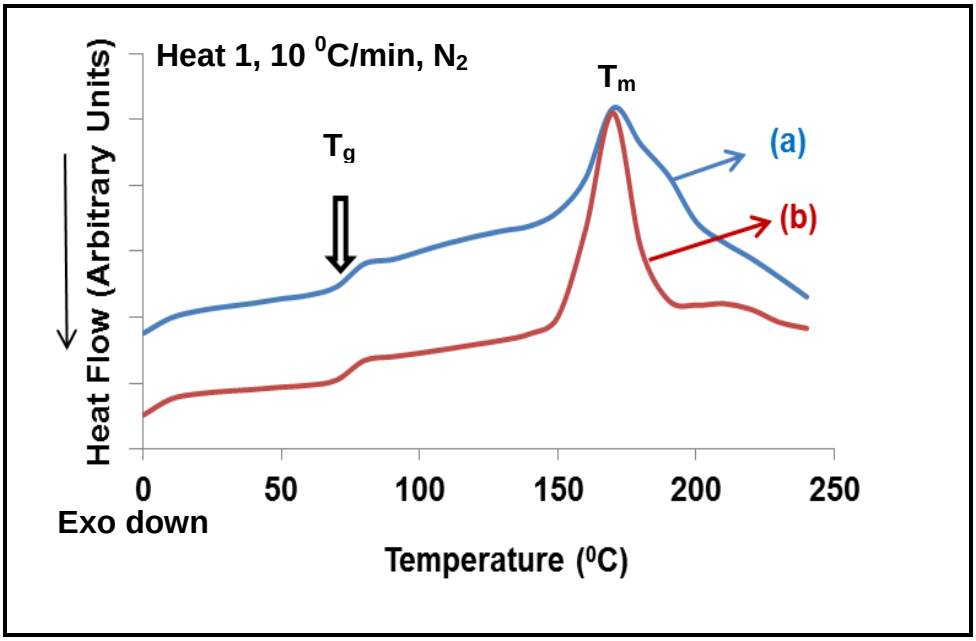


| | Sample ID | $T_g$ ($^{0}$C) | $T_m$ ($^{0}$C) | Mol% water |
|---|---|---|---|---|
| (a) | (1)+ 15 wt% Water | 74.4 | 171.2 | 37 |
| (b) | (1) + 20 wt% Water | 73.2 | 170 | 49 |

**Figure 3-6. Thermal characterization of the 94/6 wt/wt % poly(acrylonitrile-*co*-methylacrylate copolymer**

Frushour reports a critical water content of 33 wt% for polyacrylonitrile homopolymer, which leads to a maximum reduction in $T_m$ to 185 $^{0}$C.[94] This critical water content is

expected to vary with the acrylonitrile content and although it would be useful to determine this threshold, blends with lower water content did not produce reproducible data. Similarly, 50 mol% water blends of the other high acrylonitrile content copolymers (reaction entries 4, 6,9 and 10 in Table 3-3) were prepared, and the thermal properties were examined (Figure 3-7). There was a steady decrease in both the $T_g$ and $T_m$ in all copolymers, with an increase in methyl acrylate content at a fixed mol% water addition, with sharp and well defined endotherms. The shape of the melting endotherm is also expected to be a function of compositional homogeneity[93] or distribution of comonomer sequences in the chain. The final properties of the carbon fiber are highly composition dependent and although the 95/5 wt/wt % poly (acrylonitrile-*co*-methylacrylate) copolymer has a higher % crystallinity[169], the 93/7 and 91/9 wt/ wt % poly(acrylonitrile-*co*-methylacrylate) copolymers are expected to be more easily processable with lower cross-linking due to the presence of a higher comonomer content, that does not entirely disrupt the crystallinity.

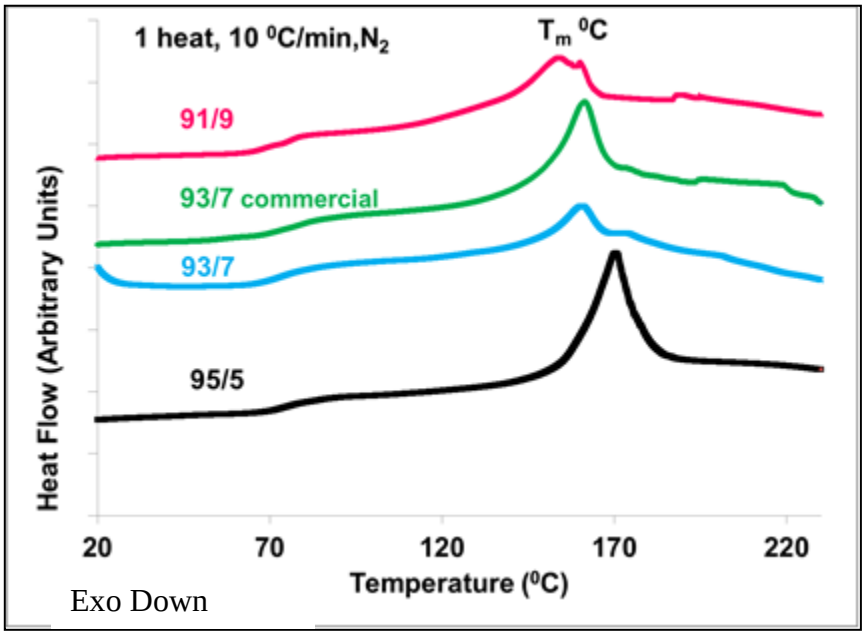


| Sample ID | AN/MA(wt/wt%) (by $^1$H NMR) | $M_w$(Kg/mol) By SEC | PDI | $T_g$($^0$C) | $T_m$($^0$C) |
|---|---|---|---|---|---|
| **(6)** | 91/9 | 130 | 1.9 | 69 | 155 |
| **(9)** | 93/7 | 200 | 1.8 | 73 | 160 |
| **(13)** | 93/7 | 223 | 2.6 | 73 | 160 |
| **(4)** | 95/5 | 143 | 1.7 | 73 | 170 |

**Figure 3-7. Thermal characterization data of the poly(acrylonitrile-*co*-methylacrylate) copolymers**

### 3.3.4 X-Ray Diffraction

The x-ray diffractograms in Figure 3-8 show the difference in crystalline peak intensity of each sample with varying comonomer content. The characteristic diffraction pattern for polyacrylonitrile homo and copolymers is described in terms of two crystalline peaks at $2\theta$ = 17.3 and 29.8, and amorphous scatter in between these two regions, overlapping with the crystalline peak at 29.8.[162, 170-172]

The position of the peak $2\theta$ is a measure of Bragg spacing d of the crystal lattice, as given by the Bragg equation, $2d \sin\theta = n\lambda$, where $\lambda$ is the wavelength of the radiation and n is the order of reflection.[173]

The diffraction pattern for the 95/5 wt/wt % poly(acrylonitrile-*co*-methylacrylate) shows a sharp peak at $2\theta$ =16.5 and the less intense peak at $2\theta$ = 28.7 and this is interspersed by a diffuse broad peak between $2\theta$ = 25 and 27.The slight variation in Bragg's angle from literature values is possibly due to structural differences that arise with different methods of synthesis.[174, 175]

As expected, the 95/5 wt/wt % poly(acrylonitrile-*co*-methyl acrylate) copolymer had the highest crystallinity. Kulshreshtha *et al*. [176] and Bang *et. al*[177] have reported through X-ray diffraction experiments that an increase in the methyl acrylate comonomer content leads to a decrease in the crystalline content as well as the size of the crystallites. This has also been shown to affect the tensile strength of the final carbon fibers.

Similarly, an increase in the comonomer content from 5 wt% to 9 wt%, caused the % crystallinity to drop from 45 to 32 %.(Table 3-5) This is due to the presence of the bulky methyl acrylate comonomer, hindering the chains from packing together in a lateral manner. There also appears to be very little difference in the % crystallinity of that of the 91/9 and 93/7 wt/wt % compositions. The commercial 93/7 wt/wt % (entry 10) poly(acrylonitrile-*co*-methyl acrylate) copolymer has a lower % crystallinity

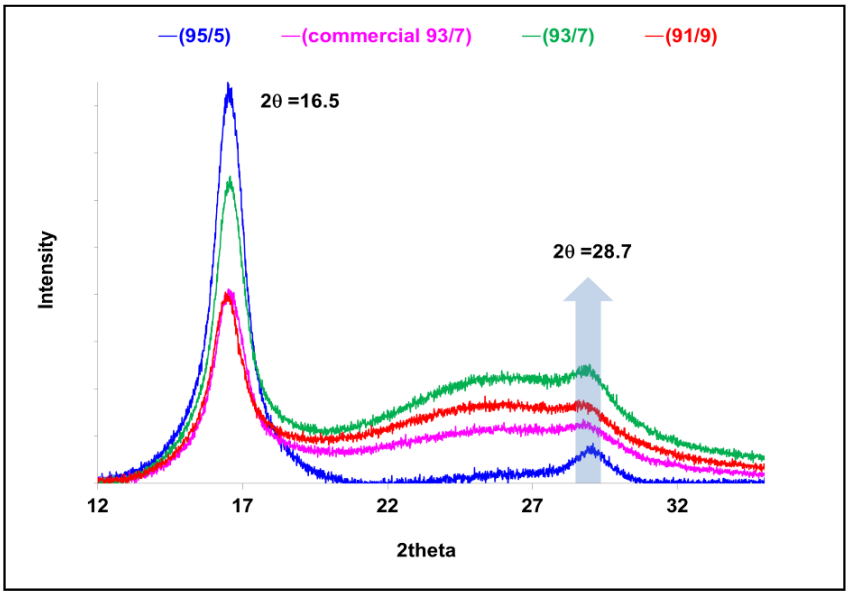


**3-8 (a)**

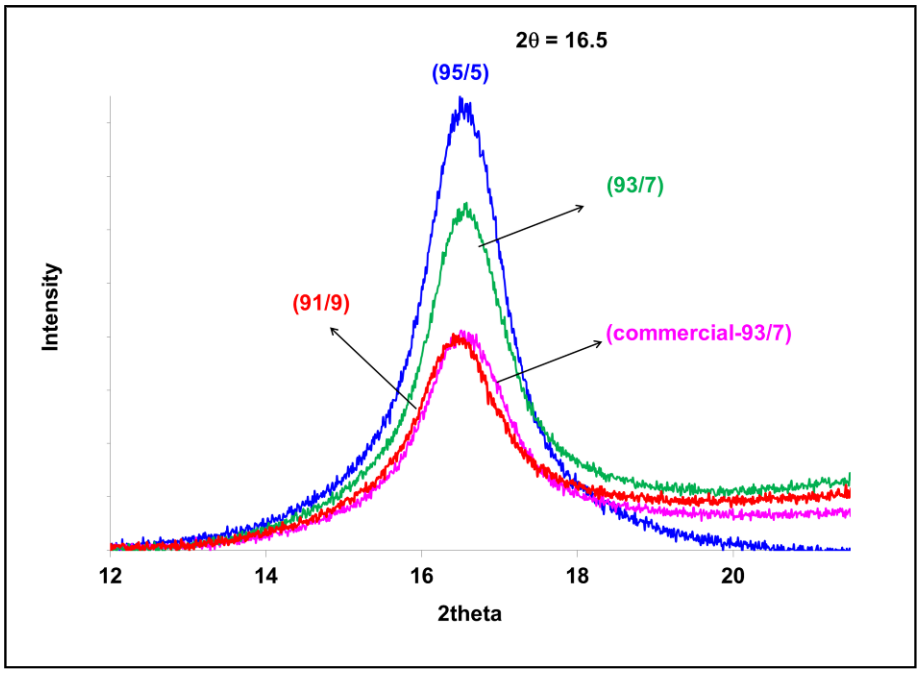


**3-8 (b)**

**Figure 3-8 . X-ray diffractograms of poly(acrylonitrile-co-methylacrylate) copolymers (a)full scale (b) zoomed region between 2$\theta$ = 12 and 20.**

| Sample ID | AN/MA (wt/wt %) (By $^{1}$H NMR) | Relative % crystallinity values |
|---|---|---|
| (4) | 95/5 | 45 |
| (9) | 93/7 | 38 |
| (13) | 93/7 | 29 |
| (6) | 91/9 | 32 |

**Table 3-5. Relative % crystallinity values of the poly (acrylonitrile-*co*-methylacrylate) copolymers**

compared to the copolymer of same composition that was synthesized in lab (entry 9). The % crystallinity in a sample is expected to be a function of the method of synthesis employed, which may result from differences in the distribution of acrylonitrile and methyl acrylate comonomer units in the copolymer, which in turn affects the length of crystallizable sequences.

## 3.4 Conclusions

A low-temperature emulsion polymerization method for preparing poly(acrylonitrile-co-methyl acrylate) copolymers with varied (but high) acrylonitrile contents and targeted molecular weights between ~100-200 kg/mol was developed. Transition temperatures of blends of these materials with water were investigated by conducting DSC in high volume sealed sample pans to determine the extent to which the water functioned as a plasticizer. Water boils below the anticipated melt processing temperatures of these blends, and thus it would be necessary to conduct melt processing under pressure. However, water clearly functions as an excellent plasticizer as melting point depressant for polyacrylonitrile copolymers due its strong hydrogen bonding capabilities. The search for new plasticizers that are inexpensive and environmentally acceptable, easily

recoverable, and high in boiling point remains a goal for developing a cost effective melt spinning process. For this, a clear understanding of the role played by molecular weight, molecular weight distribution, composition, different plasticizers and their interactions with polyacrylonitrile which cause reduction in the melting points are recommended in order to determine an optimum copolymer-plasticizer combination. Preliminary XRD experiments demonstrate a decrease in relative crystallinity in polyacrylonitrile upon copolymerizing with methyl acrylate and suggests that the method of synthesis has an effect on the crystallizability of the polymer. Also, investigation of the melt viscosity of these copolymer–water blends of different compositions as a function of time and temperature is recommended to determine the effectiveness of the plasticizer in imparting melt processability to the copolymer before the onset of thermal cyclization begins.

## CHAPTER 4 THERMAL CHARACTERIZATION OF POLY(ACRYLONITRILE-*CO*-METHYL ACRYLATE) STATISTICAL COPOLYMERS AND THEIR WATER AND ALCOHOL PLASTICIZER BLENDS

Co-authors: Ronald, M. Joseph, Sue J.Mecham, Judy, S. Riffle, James E. McGrath

### 4.1 Introduction

Carbon fibers are of exceptional value due to their unique combination of properties including being lightweight, and having high modulus and a low coefficient of thermal expansion. These fibers are increasingly finding applications in the aerospace industry, as well as for storage tanks, automotive parts and sporting goods such as bike parts. Other uses include electrically conductive[178] fibers. The specific gravity of carbon fibers (1.8-2 g/cm$^3$) is lower than that of glass which is currently the most used high modulus fiber. In addition, carbon fibers have good chemical and thermal resistance, fatigue strength and vibrational damping characteristics. High performance acrylic fibers currently constitute over 95 % of the precursors for carbon fibers, which are derived via a three-step process of spinning, stabilization and carbonization. One obstacle against expanding the utilization of these materials is their high cost of production.

All commercial acrylic fibers are currently wet or dry spun with expensive and environmentally harmful solvents. The second step of stabilization involves heating polyacrylonitrile copolymer fibers under tension in an oxygen atmosphere. In this stage, the polymer chain cyclizes along and across the chain to form a thermally stable and infusible ladder structure. In the third step, the fibers are heated in an inert atmosphere at temperatures between 1000 -1700 $^0$C to form a fused ring graphitic structure, that gives carbon fibers its unique properties. Other carbon fiber precursors include mesophase pitch and rayon which are limited in utility because of the high cost involved

in stabilization (pitch) and low carbon yield (rayon).[179] Pitch also yields relatively brittle carbon fibers due to the non-polymeric nature of the precursors.

Polyacrylonitrile (PAN) is commercially solution spun using polar solvents with a high dipole moment such as dimethylformamide ($\mu$ = 3.82 Debye) and dimethylacetamide ($\mu$ = 3.81 Debye). Melt spinning is expected to be a cost effective process because of the absence of these toxic solvents. Such a process would also eliminate the need for solvent recovery and would simplify post spinning steps including washing and drawing. Also, a higher rate of production could likely be achieved due to the 100% solids used for melt spinning as compared to the 20-30 mole:mole % copolymer concentration in solution spinning. However, spinning in the melt would require thermal stability of the precursors, and polyacrylonitrile has a high melting point of ~320 $^0$C due to molecular stiffness, and it degrades before reaching the melt temperature.

High performance acrylic precursors for carbon fibers are generally very high molecular weight copolymers with high acrylonitrile content. The atactic polyacrylonitrile that is produced via free radical polymerization does not have a three dimensional crystalline structure but rather exhibits lateral order, also known as paracrystallinity.[161,160] Comonomers aid in disrupting this long range order by acting as defects in the chains, thus improving solubility. Flory and Eby have put forth two different theories explaining this phenomenon. Flory[87] suggested that the comonomer is incorporated in the amorphous regions, thus reducing the length of acrylonitrile sequences, while Eby[88] hypothesized that the comonomer becomes incorporated in the crystalline lattice as a defect. The most commonly used comonomers are methyl acrylate and vinyl acetate. Acidic comonomers such as itaconic acid are also used to

lower the exotherm during stabilization. Rangarajan *et al*[89] reported that at a critical methyl acrylate comonomer content of 10 mol%, complete disruption of the paracrystallinity is achieved, enabling melt processability. However, these precursors with high comonomer content relax and/or fuse, rendering them unsuitable for stabilization.

One of the routes used to achieve melt spinnable polyacrylonitrile is the addition of 10-60 mole:mole % of polar low molecular weight additives (plasticizers) that aid in reducing the melting point. It is expected that dipolar interactions between CN groups in the polymer will be decoupled and replaced by interactions between the CN groups and dipoles of the additive.[180] The choice of additive is also governed by practical considerations such as its ease of extraction from the spun fibers, and level of toxicity and boiling point, all of which impact the overall cost of melt spinning.

Water is a well-researched and patented plasticizer for polyacrylonitrile. It has been shown to reduce the melting point of PAN from 320 to 200 $^{0}$C using 20 wt% water, Coxe was the first to report the melt extrusion of PAN hydrates under high pressure.[92] However, since water boils well below the melt processing temperature, the Coxe process failed due to foaming of the fiber at the die end. Frushour showed that a minimum of 0.2 mole:mole % water was sufficient to lower the melting point of polyacrylonitrile to 200 $^{0}$C.[93-95] Porosoff modified the process and developed a melt spinning apparatus for the PAN-water mixtures using a pressurized chamber. However, it was not commercialized because Grove *et al* later found that the fibers contained voids.[96, 97].

Daumit *et al*. at BASF patented a procedure that used 23-48 mole:mole % plasticizer mixtures of water, acetonitrile and a monohydroxy alcohol and successfully achieved melt spun poly(acrylonitrile-*co*-methyl acrylate) (95:5 mole:mole ) precursors.[98] Acetonitrile was later replaced by nitromethane or nitroethane.[99] Although the BASF process used significantly lower amounts of solvents (plasticizers) relative to commercial wet or dry spinning processes (70-80 mole:mole %), the costs associated with solvent extraction and recovery prevented commercialization.

Bashir and Atureliya reported melt extrusion of polyacrylonitrile plasticized with propylene carbonate. In this case, the plasticized polyacrylonitrile crystallized as the fibers were extruded, thus eliminating the additional step of using a coagulation bath. The use of propylene carbonate avoided the need to use a pressure chamber due to the high boiling point of propylene carbonate ($240^0$C). However there was a lack of chain orientation in the fibers that is critical to achieving good mechanical properties. The amount of plasticizer used to generate the polyacrylonitrile melt with good shear thinning behavior was as high as 50 mole:mole %.[100-102] Min *et al.* reported that mixtures of water and ethylene carbonate were synergistic in reducing the melting point, with water being the more effective component.[103]

In the 1990's, British Petroleum developed a series of high acrylonitrile thermoplastic copolymers and claimed that by using a starved comonomer feed. the incorporation of comonomer in polyacrylonitrile could be manipulated to impart melt processability.[104, 105] However, the rate of extrusion was deemed too slow to achieve cost effective production.

Glycerin, a non-toxic alcohol with a high boiling point of 290 $^0$C, was first reported as a plasticizer for polyacrylonitrile by Alves *et al.*[106] Mixtures of glycerin and glycol additives were reported to depress the melting points of a high acrylonitrile content poly(acrylonitrile-*co*-vinyl acetate) copolymer ($M_n$ = 270 kg/mol) to 217 $^0$C, and successful extrusion of fibers with small diameters.[107] It is unclear, however, whether glycerin alone was used to impart melt processability to PAN without the use of other additives. In addition, methyl acrylate is preferred over vinyl acetate as a comonomer for polyacrylonitrile precursors for carbon fibers due to better melt stability of the copolymer. Methyl acrylate also has a more favorable reactivity ratio with acrylonitrile than vinyl acetate, which may enable more uniform distribution of the comonomer in the polymer chain.[67]

We have studied the feasibility of melt processing high acrylonitrile content poly(acrylonitrile-*co*-methyl acrylate) copolymers by blending them with high boiling, non-toxic plasticizers that act as processing aids. Glycerin, glycerin-water solutions and ethylene glycol have been investigated as potential plasticizers. The effect of increasing the plasticizer content on the thermal transitions and the effect of the molecular weight of these copolymers on their melt processability has also been studied. Furthermore, the role played by the molecular weight of the plasticizer and number of moles of hydroxyl groups available for hydrogen bonding, on the melting point depression of the poly(acrylonitrile-*co*-methyl acrylate) copolymers was investigated.

## 4.2 Experimental

### 4.2.1 Materials

A 95:5 mole:mole poly(acrylonitrile-co-methyl acrylate) copolymer was kindly provided by Oak Ridge National Laboratories (ORNL). Two lower molecular weight copolymers of with compositions of 97:3 and 90:10 mole:mole poly(acrylonitrile-co-methyl acrylate) were synthesized by free radical emulsion and suspension copolymerization, respectively. Acrylonitrile ≥ 99+ %), methyl acrylate (99 %), ammonium persulfate initiator (98 %), sodium metabisulfite activator, 1-dodecanethiol (98+ %) as the chain transfer agent, and magnesium sulfate were purchased from Sigma-Aldrich. 2, 2'-Azobisisobutyronitrile (AIBN) was purchased from Sigma-Aldrich and recrystallized from methanol before use. The surfactant (Dowfax 8390, a 35% solution of an alkyldiphenyloxide disulphonate in water) was kindly provided by the Dow Chemical Company. Poly(vinyl alcohol) as the suspending agent was purchased from MP Biomedicals, LLC. Acrylonitrile and methyl acrylate were passed through activated alumina to remove the stabilizer. Activated alumina (8-14 mesh) was purchased from Fischer Scientific.

### 4.2.2. Synthesis

Two lower molecular weight poly(acrylonitrile-*co*-methyl acrylate) copolymers were synthesized via heterogeneous emulsion or suspension copolymerization.

#### 4.2.2.1 Emulsion copolymerization of poly(acrylonitrile-co-methyl acrylate)

The free radical emulsion copolymerization of acrylonitrile and methyl acrylate was conducted in a 4-necked round bottomed flask, equipped with a condensor under nitrogen atmosphere. Deionized (DI) water (300 mL) was boiled immediately prior to the

reaction to deoxygenate. Dowfax 8390 (5.714 g of the aq. Dowfax solution) was diluted with 100 mL of deoxygenated DI water. The surfactant solution was charged to the flask and nitrogen was bubbled through the solution for 15 minutes. Acrylonitrile (95 g, 1.79 mol) and methyl acrylate (5 g, 0.058 mol) were added via syringes, and each syringe was flushed with 40 mL of DI water and this was added to the reaction mixture. The ammonium persulfate initiator (0.212 g, 0.92 mmol, 0.05 mol % based on total monomers), was dissolved in 5 mL of deoxygenated DI water, then added to the flask. 1- Dodecanethiol (2.99 g, 14 mmol, 0.8 mol% based on total monomers) was added to the vessel. The resultant emulsion was added to 2000 mL of a 1 % aq $MgSO_4$ solution at 65 $^{\circ}$C and stirred briefly. The solid polymer was filtered, washed with ~2000 mL of DI water at 65 $^{\circ}$C, and dried at 100 $^{\circ}$C under vacuum to recover the pure copolymer. The yield was 89 %.

#### 4.2.2.2 Suspension copolymerization of poly(acrylonitrile-co-methyl acrylate)

The free radical suspension copolymerization of acrylonitrile and methyl acrylate was conducted in a 4-necked round bottomed reaction flask equipped with a condenser under a nitrogen atmosphere. Deionized (DI) water (350 mL) was boiled immediately prior to the reaction to deoxygenate. Poly(vinyl alcohol) (1.306 g) was dissolved in 100 mL of deoxygenated DI water with vigorous stirring. The aqueous poly(vinyl alcohol) solution was charged to the flask and purged with nitrogen gas for 15 min. Acrylonitrile (28.41 g, 0.535 mol) and methyl acrylate (7.5 g, 0.087 mol) were added via syringe. The AIBN initiator (0.073 g, 1.29 mmol, 0.05 mol % based on total monomers) was dissolved in the remaining acrylonitrile (14.09 g, 0.265 mol) and added to the flask.1-Dodecanethiol (2.157 g, 10.6 mmol, 1.2 mol% based on total monomers), was added to the flask followed by 248 mL of water. The reaction was stirred at 60 $^{\circ}$C for 6 h. The

resultant suspension was added to 2000 mL of water at 65 °C and stirred briefly, then the solid was filtered, washed with another 2000 mL of DI water at 65 °C, and dried at 100 °C under vacuum. The recovered yield was 80%.

## 4.3 Characterization

### 4.3.1 Composition Analysis by 1H NMR

$^1$H NMR in DMSO-$d_6$ was used to measure AN/MA copolymer compositions using a 400 MHz Varian NMR spectrometer. Copolymer composition was determined by comparing the integrals of the proton signals in the repeat units. The signal at 3.2 ppm (b) corresponds to the backbone methine (CH) protons from each repeat unit. The signal at 2.1 ppm (a) corresponds to the backbone methylene ($CH_2$) protons from each repeat unit. The signal at 3.7 ppm (c) corresponds to the methyl ($CH_3$) protons of the methyl acrylate units. The copolymer composition was calculated from the integral values of the methylene protons using the following equations:

$$\text{Moles MA } \alpha \left(\frac{\int \text{CH}_3}{3}\right)$$

$$(\text{Moles MA}) \times \left(86.04 \frac{g}{mol}\right) = \text{relative weight MA}$$

$$\text{Moles AN } \alpha \left[\left(\frac{\int \text{a}}{2}\right) - \left(\frac{\int \text{CH}_3}{3}\right)\right]$$

$$(\text{Moles AN}) \times \left(53.06 \frac{g}{mol}\right) = \text{relative weight AN}$$

$$\text{Weight Percent AN} = \frac{\text{relative weight AN}}{\text{relative weight AN} + \text{relative weight MA}} \times 100$$

$$\text{Weight Percent MA} = 100 - \text{weight percent AN}$$

### 4.3.2 Molecular Weight Analyses

Absolute molecular weight measurements from size exclusion chromatography (SEC) were made using an Agilent 1260 infinity multi detector SEC equipped with a Wyatt Heleos II 18 angle static light scattering detector, a Wyatt Viscostar viscosity detector, and a Wyatt T-rex differential RI detector at 50 $^0$C using three PLgel 10 μm mixed-B 200 x 75 mm columns in series. NMP containing 0.05 M LiBr was used as the elution solvent. The differential refractive index versus composition was measured manually offline.

### 4.3.3 Thermal Analysis

#### 4.3.3.1 Thermogravimetric Analysis

Thermogravimetric analysis was conducted using a TA instruments TGA Q5000**,** to determine the temperature of degradation and was also used to determine the percentage of plasticizer that was incorporated into the polymer. The copolymers and copolymer blends were heated under a nitrogen atmosphere at a rate of 10 $^0$C/min to 500 $^0$C.

#### 4.3.3.2 Differential Scanning Calorimetry

The glass transition temperature ($T_g$) and the melting temperature ($T_m$) values were obtained from Differential Scanning Calorimetry (DSC) measured by a Thermal Analysis Q 1000. A 10 $^0$C/min heating rate was used to determine the $T_g$ and $T_m$ of all

the plasticizer blends. High volume pans with O-ring seals were used to prevent volatilization of the plasticizer. A single heating cycle from -20 to 250 $^0$C was performed. A rapid heat scan of 80 $^0$C/ min was used to observe the melting point of the pure copolymers before degradation occurred in Al hermetic pans. A heat/cool/heat cycle was performed. The pans were heated from -20 to 150 $^0$C, cooled to -20 $^0$C and then heated to 290 $^0$C.

#### 4.3.3.3 Capillary Rheometry

Capillary rheometry was used as a screening method to illustrate the melt processability of these materials. An Instron 3211 single bore capillary rheometer was used. A one-hole die with diameter 1mm and L/D of 30, was mounted on the bottom of the barrel of the rheometer. The barrel and die were heated to the target temperature and purged with nitrogen gas for three minutes. A 3/8" diameter sample pellet was dropped on the barrel and the barrel was sealed with the plunger with the Teflon O-ring from the top. The plunger was driven downward and the sample was allowed to equilibrate to set temperature which took four minutes. The plunger was driven downward to extrude the polymer melt out of the die.

### 4.4 Preparation of copolymer-plasticizer blends

#### 4.4.1 Glycerin, 1,4-butanediol, diethylene glycol blends

The blends of glycerin, 1,4-butanediol and diethylene glycol respectively with the 95:5 mol:mol % poly(acrylonitrile-*co*-methyl acrylate) were prepared in a similar way. A representative procedure for making a 16 mol% (25 wt%) glycerin blend with the copolymer is as follows: The copolymer powder (0.75 g) was weighed in to a 20 mL scintillation vial and glycerin (0.25 g) was added drop-wise with a pipette to produce a

suspension. Isopropyl alcohol (4 mL) was then added to the mixture to reduce the viscosity. The mixture was vigorously stirred with a spatula. The resulting mixture was then maintained under reduced pressure in a vacuum oven at ambient temperature for 12 h, and then at 80 $^{0}$C for 12 h to remove the isopropyl alcohol. Thermogravimetric analysis was used to determine the amount of glycerin that was incorporated in the mixture.

### 4.4.2 Water and Ethylene glycol blends

Water and ethylene glycol blends were made by mixing the reagents with the copolymer at ambient temperature. A representative procedure for making a 50 mol% (25 wt%) water blend with the 95:5 mol : mol % poly(acrylonitrile-*co*-methyl acrylate) is as follows: The copolymer powder (0.75 g) was weighed in to a 20 mL scintillation vial and water (0.25 g) was added drop-wise with a pipette to produce a suspension. Isopropyl alcohol (4 mL) was then added to the mixture to reduce the viscosity. The mixture was vigorously stirred with a spatula.

### 4.4.3 Glycerin-Water Blends

Glycerin was added drop-wise to the copolymer powder. Isopropyl alcohol was then added to the mixture to reduce the viscosity. This mixture was vigorously stirred with a spatula to achieve uniform mixing. The resulting mixture was dried under reduced pressure at ambient temperature for 12h and then at 80 $^{0}$C for 12h. Thermogravimetric analysis was used to determine the amount of glycerin that was incorporated in the blend. Water was then added as needed to obtain the desired proportion of glycerin and water in the mixture.

## 4.5 Results and Discussion

### 4.5.1 $^{1}$H NMR Characterization of the Poly(acrylonitrile-co-methylacrylate) copolymers

Compositions of the poly(acrylonitrile-*co*-methyl acrylate) copolymers were calculated from $^{1}$H NMR spectra (Figure 4-1). The composition of the copolymer that was used for the blends discussed herein was 95:5 mole:mole acrylonitrile to methyl acrylate.

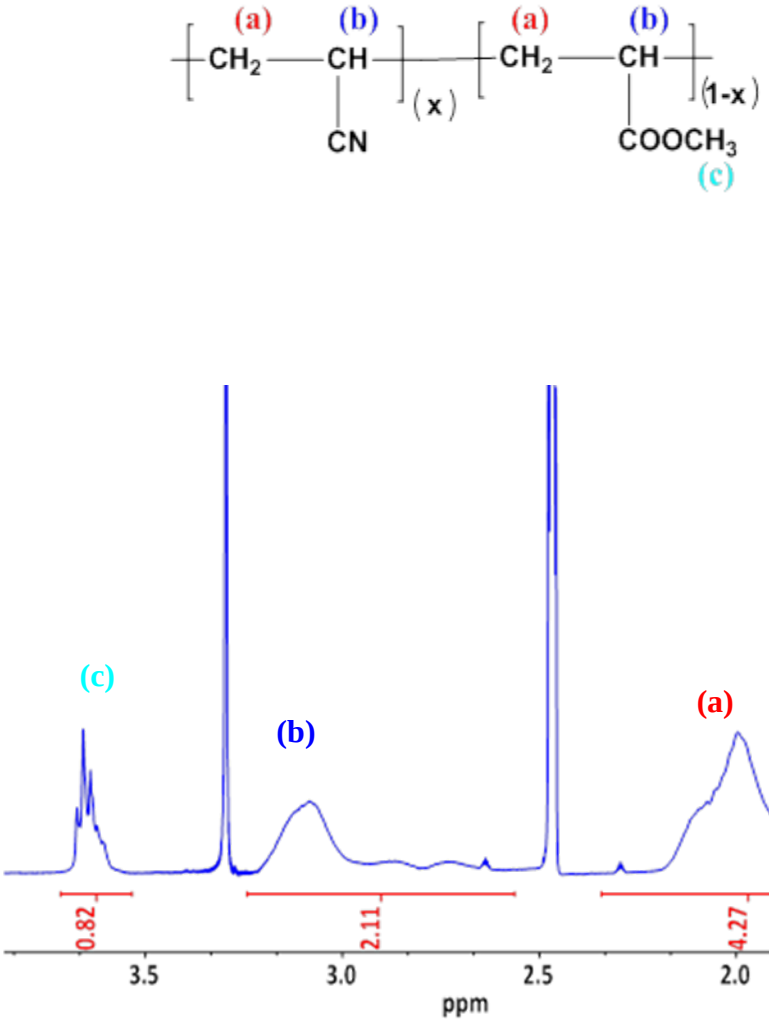


**Figure 4-1. $^{1}$H NMR spectrum of a 95:5 mole:mole % poly(acrylonitrile-*co*-methyl acrylate) copolymer**

### 4.5.2 Thermal properties of blends of poly(acrylonitrile-co-methyl acrylate) with water and alcohol plasticizers

DSC transitions of the 95:5 mole: mole % poly(acrylonitrile-*co*-methyl acrylate) copolymer was performed at two different heating rates. At 10 $^0$C/min, the glass transition temperature ($T_g$) of the copolymer was 100 $^0$C and no melting endotherm was observed (Figure 4-2). At the faster heating rate of 80 $^0$C/min, the $T_g$ shifted upwards to 110 $^0$C. At 287 $^0$C, there is an endotherm, but degradation occurs essentially simultaneously, as evidenced by the rapid drop in the heat flow. The degradation that takes place immediately after the melting point clearly shows that these materials are not melt processible without additives.

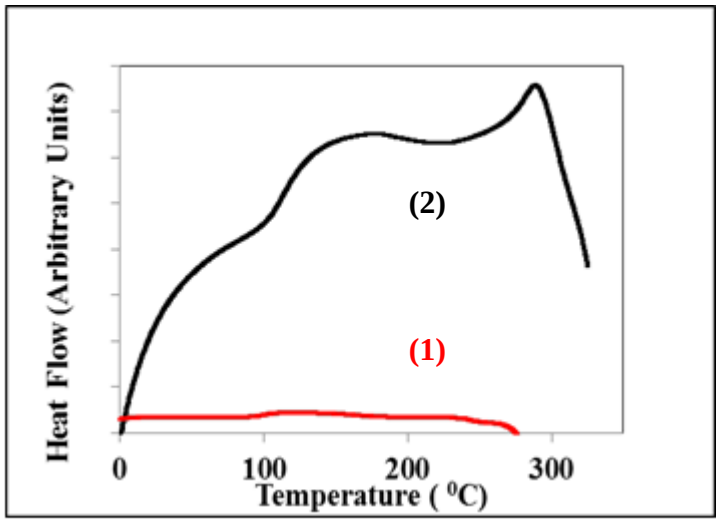


**Figure 4-2. DSC plot of the 95:5 mole:mole % poly(acrylonitrile-*co*-methylacrylate) at two different heat scans: (1) 10 $^0$C/min and (2) 80 $^0$C/min**

The thermal transitions of three copolymer-water blends with differing compositions were examined via DSC (Figure 4-3 and Table 4-1). Water is known to depress the melting point of polyacrylonitrile by decoupling the dipolar interaction between adjacent, pendent nitrile groups in the polymer chain through hydrogen bonds.[166] Addition of 50 mole % water decreased the $T_g$ to 73 $^0$C and the $T_m$ to 160 $^0$C. Upon further increase in the water content to 56 and 75 mole %, no significant change in the glass transition temperature or melting point was observed. The lower limit for achieving a significant depression in melting point is ~50 mole %. and blends with lower water content did not produce consistent data.

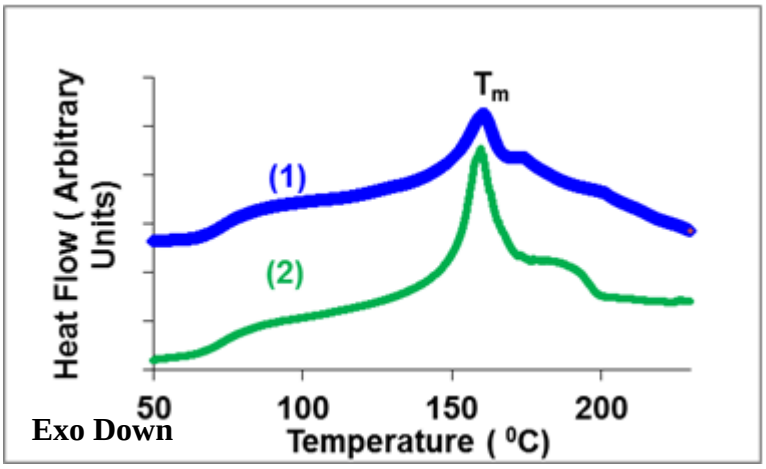


**Figure 4-3. DSC thermogram of the 95:5 mole:mole % poly(acrylonitrile-*co*-methylacrylate) and water blends (1) 50 mole % water (2) 56 mole%water**

The mole percent of water required in each blend to depress the $T_g$ and $T_m$ of the copolymer is reported in Table 1. It is apparent that an equimolar ratio of water to nitrile groups causes a maximum reduction in the $T_g$, thus suggesting that one hydroxyl group participates in hydrogen bonding with one nitrile, Water is able to efficiently penetrate

the chains and disrupt the dipolar interactions between the nitrile groups, and this may occur in both the amorphous and crystalline regions.

| | Additive (mole %) | | Moles (OH/CN group) | | $T_g$ ($^0$C) | $T_c$ ($^0$C) | $T_m$ ($^0$C) |
|---|---|---|---|---|---|---|---|
| Water | 50 | | 1.00 | | 75 | - | 160 |
| | 56 | | 1.30 | | 73 | - | 160 |
| | 75 | | 3.10 | | 73 | - | 160 |
| Glycerin | 16 | | 0.61 | | 96 | 188 | 213 |
| | 23 | | 1.00 | | 96 | 187 | 213 |
| | 30 | | 1.50 | | 96 | 187 | 213 |
| | Glycerin | Water | Glycerin | Water | | | |
| Glycerin-Water | 13 | 15 | 0.56 | 0.26 | 75 | 182 | 171 |
| | 6 | 32 | 0.33 | 0.55 | 79 | - | 178 |
| | 3 | 55 | 0.15 | 0.96 | 90 | - | 204 |
| Ethylene Glycol | 22 | | 0.61 | | 75 | - | 185 |
| | 31 | | 0.99 | | 77 | - | 185 |
| | 41 | | 1.50 | | 75 | - | 185 |

**Table 4-1. Thermal transitions in poly(acrylonitrile-co-methylacrylate) copolymer-water blends**

Glycerin is a high boiling alcohol (290 $^0$C) that has a viscosity of 1410 centipoise at 20 $^0$C, which is significantly higher than that of water (1 centipoise).[181] In the procedure to make the glycerin-copolymer blends, the viscosity of glycerin was reduced with isopropyl alcohol after which the isopropyl alcohol was evaporated in a vacuum

oven. TGA profiles were utilized to assess the final blend compositions. These experiments also confirmed that addition of glycerin did not compromise the onset of weight loss of the copolymer. Addition of 16 mole % of glycerin only reduced the glass transition temperature of the copolymer from 100 to 96 $^0$C. This was followed by a sharp melting endotherm at 213 $^0$C (Figure 4-4). This represented a significant reduction in the melting point since the thermogram of the copolymer alone did not show melting in this temperature region. In addition, a crystallization exotherm occurred right before melting. Crystallization of the copolymer may be a result of glycerin acting as a nucleation center, allowing the polymer chains to pack and crystallize. On increasing the temperature further, the energy barrier to breaking this order in the chains is overcome, thus achieving complete melting of the copolymer. Higher compositions of glycerin in the blend did not cause any further decrease in the melting point of the copolymer, despite an increase in the number of moles of hydroxyl groups available for hydrogen bonding (Table 4-1). This characteristic crystallization behavior disappears in the second heat scan, without changing the $T_g$ or $T_m$.

The minimal reduction in Tg and Tm indicate that glycerin is unable to penetrate both amorphous and ordered domains in polyacrylonitrile. Glycerin could also hydrogen bond with the hydrogen form the methine backbone.

The 16 mol % glycerin blend could not be extruded at either 190 or 215°C, showing no flow from the extruder orifice and significant discoloration after exposure to temperature.

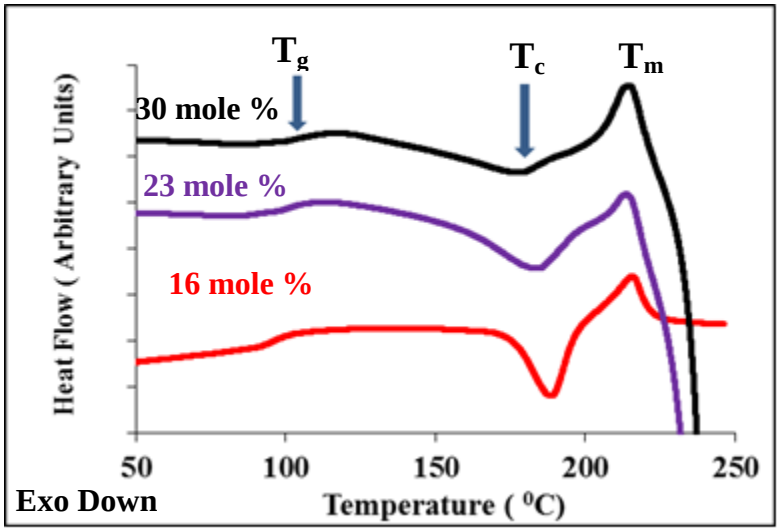


**Figure 4-4. DSC overlay of the (95:5 mole:mole % poly (acrylonitrile-*co*-methylacrylate) + glycerin) blends of various ratios**

Glycerin-water blends with the copolymer were prepared at various compositions of glycerin and water. Table 4-2. shows the boiling point of the glycerin-water solutions as estimated from the Dühring lines.

| Glycerin-Water (mole:mole %) | Boiling point ($^0$C) |
|---|---|
| 13-15 | 121 |
| 6-32 | 105 |
| 3-55 | < 100.6 |

**Table 4-2. Boiling points of glycerin and water solutions estimated from Dühring lines[182]**

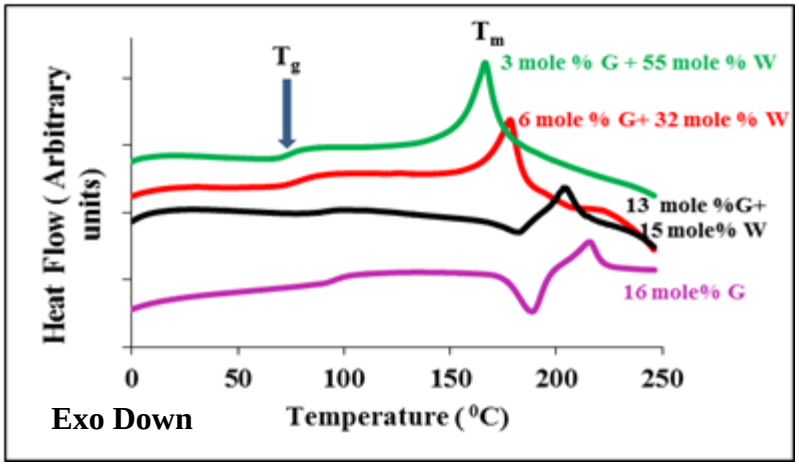


**Figure 4-5. DSC thermograms of the glycerin-water and 95:5 mole:mole %poly(acrylonitrile-*co*-methylacrylate) copolymer blends G= glycerin and W = water**

Figure 4-6 shows the relationship between moles of OH/CN in the glycerin water blends in comparison with the neat copolymer. There is clearly a trend, wherein an increase in the water content led to a decrease in the $T_g$ and $T_m$ of the copolymer. There is also a steady increase in the overall OH molar contribution with an increase in water content. In each of the glycerin-water blends, water has a greater molar contribution of OH groups compared to glycerin. Earlier experiments have shown that water is more effective than glycerin as a plasticizer to reduce the $T_g$ as well as a diluent to reduce the $T_m$. This suggests that the shift in thermal transitions may be mainly due to the effect of addition of water with some contribution from glycerin. The blend of 6 mole % water and 32 mole % glycerin was extruded successfully at 190°C.

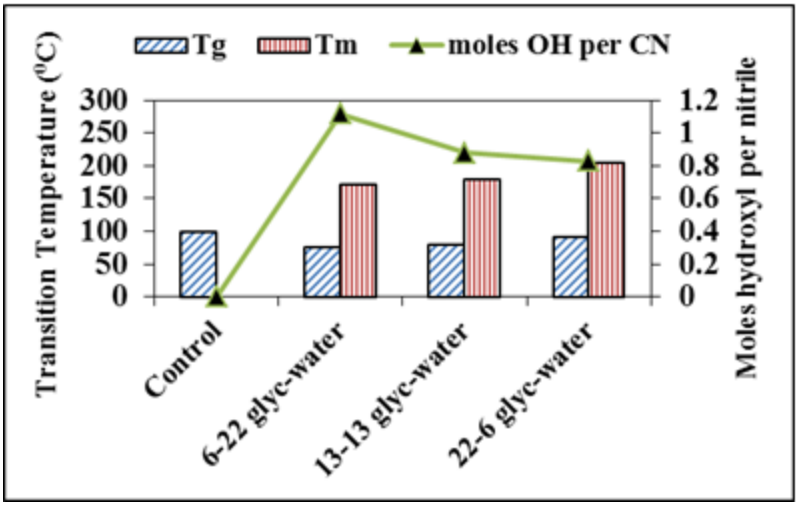


**Figure 4-6. Transition temperatures of glycerin/water (mole:mole % ) blends with the 95:5 mole:mole % poly(acrylonitrile-*co*-methylacrylate)**

The ineffectiveness of glycerin as a diluent to reduce the melting point may be because of its inability to hydrogen bond with the nitrile groups in the polymer chain. Gilli *et al.* correlated pKa's of molecules with their hydrogen bonding strength.[183] Glycerin is a weak acid with a dissociation constant in water of 0.07 x $10^{-13}$. [184] However, the acidities of the other hydroxyl groups of glycerin are not reported in the literature. The hydrogen bonding capability of the 2$^{nd}$ and 3$^{rd}$ hydroxyl groups in glycerin will likely be reduced relative to the 1$^{st}$., and thus the relative capability to form hydrogen bonds is uncertain.

1,4-Butanediol which has two terminal OH groups was chosen for comparison with glycerin which has three OH groups.Two blends of 1,4-butanediol and glycerin with the copolymer were made such that both alcohols had the same contribution of OH/CN moles in the blends and these were analyzed via DSC. A comparison of thermograms (2) and (3) in Figure 4-7 shows a slight shift in the $T_c$, while the $T_g$ and $T_m$ remain constant. Diethyleneglycol blends of the copolymer were also analyzed at 25 and 35 mole % of the alcohol yielding similar results, wherein very little reduction in $T_g$ and $T_m$

was observed, along with a crystallization endotherm. These alcohols are perhaps too hydrophobic to be compatible with the copolymer.

The melting point reduction in the PAN copolymer is expected to depend on the hydrogen bonding capability and dipole moment of the alcohol, but the alcohol needs to be able to penetrate the chains and have proximity to the nitrile groups to effectively hydrogen bond.

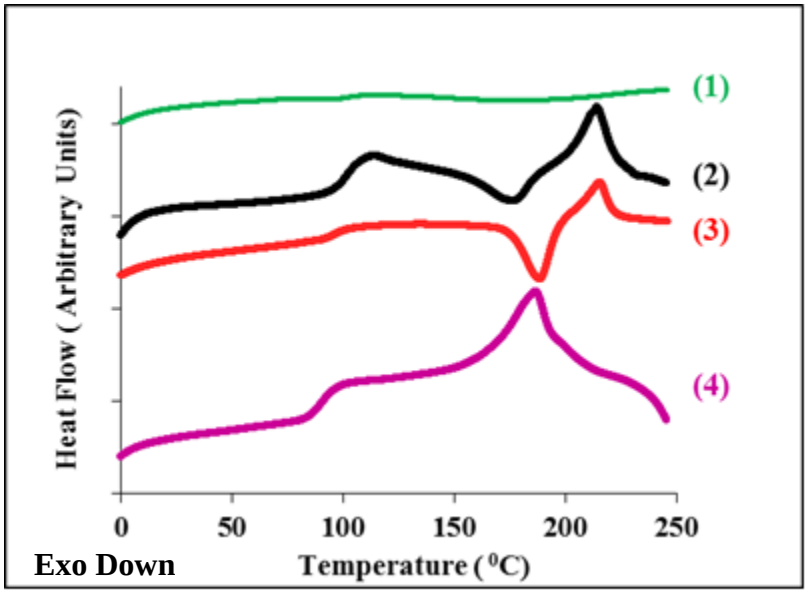


**Figure 4-7. DSC overlay of the 95:5 mole:mole % poly(acrylonitrile-*co*-methyl acrylate) copolymer and plasticizer blends: (1)95:5 mole:mole% copolymer (2) 25 mole % *1,4*-butanediol (3) 16 mole % glycerin(4) 22 mole % ethylene glycol**

Ethylene glycol is a di-hydroxy alcohol with a boiling point of 195 $^0$C, which makes it a potential candidate as a plasticizer for polyacrylonitrile copolymers. At 22 mole % of ethylene glycol, a maximum decrease in the $T_g$ and $T_m$ of the copolymer was observed at 89 and 185 $^0$C respectively. At a fixed mole % incorporation, ethylene glycol showed

a greater reduction in the $T_g$ and $T_m$ of the copolymer than glycerin. Even when ethylene glycol and glycerin have an equal contribution of OH moles/CN group, ethylene glycol shows a greater reduction in the $T_g$ and $T_m$ than glycerin.(Tables 4-1).This indicates that, while the role of the OH interaction with the copolymer in depressing the $T_m$ is evident, the difunctional alcohol is more effective and compatible with the copolymer

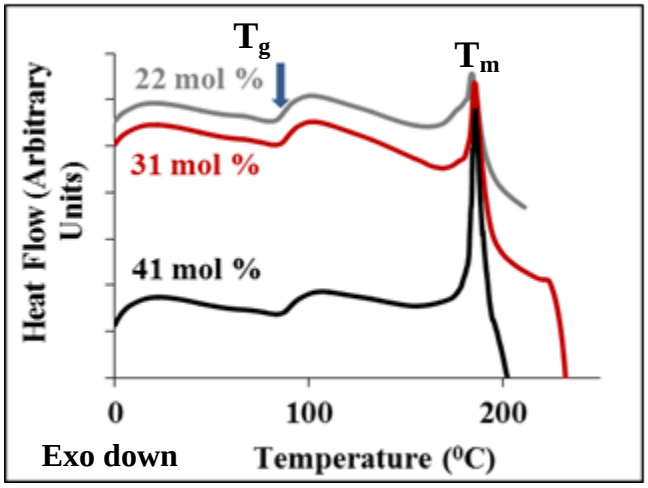


**Figure 4-8. DSC thermogramsof the ethylene glycol blends with the 95:5 mole:mole % poly(acrylonitrile-*co*-methylacrylate)**

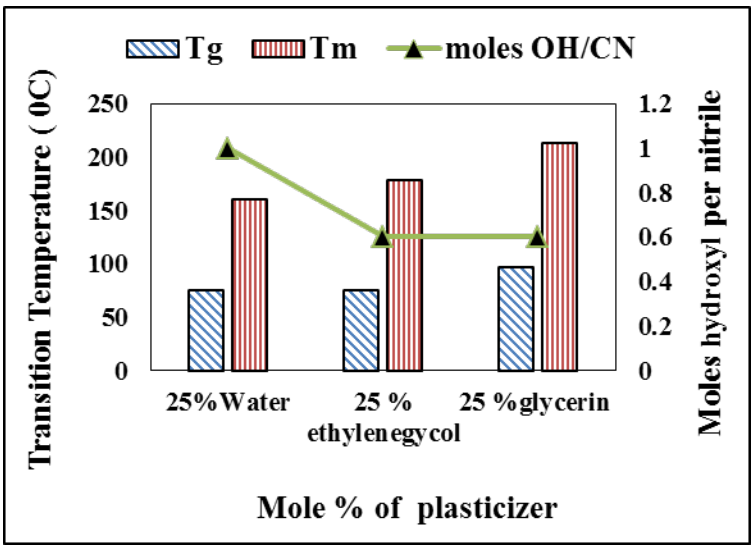


**Figure 4-9. Effect of moles OH/CN ratio on the thermal transitions**

In order to investigate the effect of molecular weight of the copolymer on the melt processability of blended copolymers, lower molecular weight copolymers were synthesized using emulsion and suspension copolymerization. Properties of the copolymers are presented in Table 4-3. Minagawa[185] used inverse gas chromatography to show the dependence of $T_g$ of polyacrylonitrile homopolymers on molecular weight. It is expected, based on the Fox Equation, that higher AN content random copolymers would have a higher $T_g$. However it was found that with the copolymers described in Table 4-3, the low molecular weight copolymer, but with the highest acrylonitrile composition, had the lowest Tg. Thus, it was concluded that the molecular weight had a greater impact on the $T_g$ than the small increase in acrylonitrile content at these high acrylonitrile levels.

| | AN/MA $^1$H NMR ( mol:mol% ) | $M_w$ (g/mol) | $T_g$ [b] ($^0$C) | | $T_m$ ($^0$C) | Melt Extrusion |
|---|---|---|---|---|---|---|
| | | | Control | Blend | Blend | |
| (1) | 95:5 | 200,000 | 100 | 96 | 213 | X |
| (2) | 90:10 | 100,000 | 91 | 88 | 201 | √ |
| (3) | 97:3 | 35,700 | 88 | 85 | 221 | √ |

**Table 4-3. Characteristics of the high AN content copolymers and their 25 mole:mole % glycerin blends**

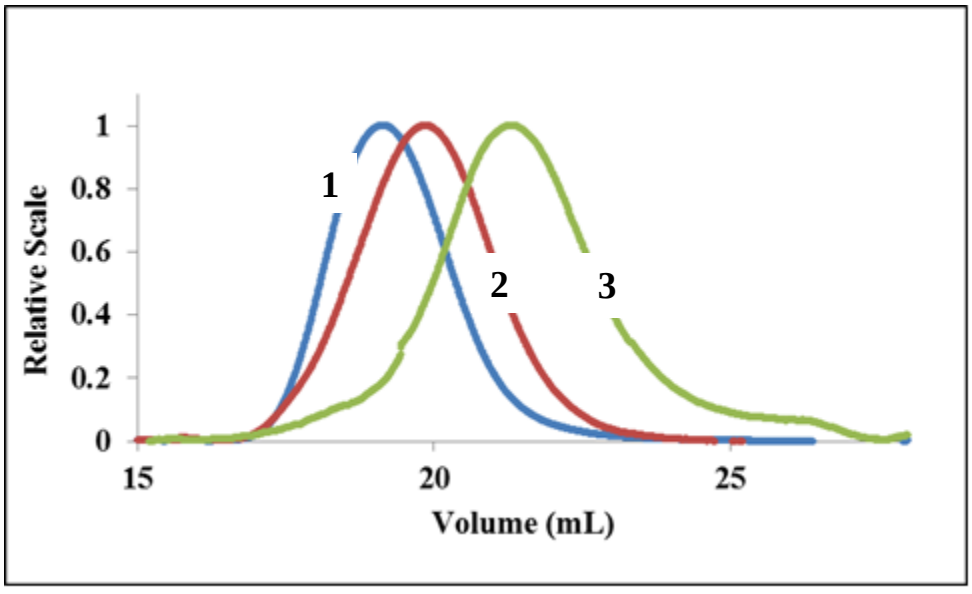


**Figure 4-10. SEC chromatograms of the AN/MA mole:mole % copolymer (1) 95:5 (2) 90:10 (3) 97:3**

The lower molecular weight control copolymer was blended with 16 mol % glycerin to produce a homogeneous powder for comparison to the blend containing the high

molecular weight copolymer. The $T_g$ of the glycerin-low molecular weight polymer blend was reduced slightly, from 90°C for the copolymer alone to 87°C for the blend. This is similar to the behavior observed with the high molecular weight copolymers blended with glycerin. The blend with the low molecular weight polymer crystallizes as observed with an exothermic peak maximum at 189°C, similar also to that seen in the high molecular weight copolymer blended with glycerin. The $T_m$ is somewhat higher at 222°C than for the higher molecular weight copolymer blend which was found to be 213°C. The higher $T_m$ of the low molecular weight copolymer blend is likely due to the higher acrylonitrile content of 97 mole% vs 95 mole % which did not appear to have the same impact on the $T_g$. The 25 mole:mole % glycerin blend with the 97:3 mole:mole % AN/MA 35K copolymer was successfully extruded at 190°C (below the $T_m$).

An 90:10 mole:mole % AN/MA copolymer of 100 kg/mol weight average molecular weight also processed well upon blending with 16 mol % of glycerin. The fiber of this blend was extruded at its $T_m$ (Table 4-3.). It should however be noted that the presence of a low molecular weight fraction in the 97:3 mole:mole % AN/MA copolymer as observed in the light scattering chromatogram (Figure 4-10.) and the lower acrylonitrile content of the 90:10 mole:mole % AN/MA likely contributed significantly contribution towards imparting melt processability to these copolymers.

## 4.5 CONCLUSION

Water and ethylene glycol are most effective in reducing the $T_g$ and $T_m$ of the 95:5 AN/MA mole:mole % copolymer with a molecular weight of 200 kg/mol, making them potential melt processing aids. Glycerin-water solutions with higher glycerin

content prove to be good candidates, with water being the dominant component. High boiling alcohols like glycerin,1,4-butanediol and diethylene glycol were investigated in blends with the 200 kg/mol 95:5 mole:mole % poly(acrylonitrile-*co*-methyl acrylate)copolymer, and those blends showed lower reductions in $T_g$ and $T_m$ compared to using water or ethylene glycol. Those blends also crystallized upon heating whereas this was not observed with water or ethylene glycol blends. Although the higher molecular weight glycerin blend was not melt processable, the 90 and 97 AN mole:mole % copolymers with lower molecular weights could be melt extruded without the use of a pressure chamber. It is evident that a number of parameters such as the type of plasticizer, the nature of its interactions with the polymer, level of plasticizer, composition of the copolymer, molecular weight and molecular weight distribution of the copolymer, all contribute towards imparting the PAN copolymer melt processabiltiy. Further research, where each parameter is varied independently of the other, is hence necessary to better understand the interplay of all these factors.

## CHAPTER 5 : MELT PROCESSABLE POLY (ACRYLONITRILE-CO-METHYL ACRYLATE) COPOLYMERS: EFFECT OF THE COMONOMER CONTENT

Co-authors: Judy S. Riffle, James E. McGrath

### 5.1 Introduction

Polyacrylonitrile is known for its excellent barrier properties against permeation of oxygen and carbon dioxide.[5] This property makes it ideal for packaging applications where barrier properties are required. The strong dipolar interaction between the pendent nitrile groups are partially responsible for the low permeation of gases through these materials. The strong polarity of the nitrile groups also leads to high water sorption due to hydrogen bonding, and this can be a disadvantage. As discussed in the previous chapters, polyacrylonitrile is solution spun from solvents such as dimethylformamide, and inorganic salt solutions such as aqueous sodium thiocyanate and aqueous zinc chloride solution at concentrations of about 20-30 w/v %. Solution spinning also requires the additional steps of solvent recovery, orientational drawing, relaxing, crimping, annealing and solvent recovery which increase the cost of production. In order to reduce this cost, many researchers have tried to replace solution spinning with melt spinning. However, polyacrylonitrile cyclizes to form a six membered ladder-type structure well below its melting temperature of 317 $^{0}$C.[86] The premature formation of this structure increases the viscosity of the material in the melt and inhibits flow.

A considerable amount of research has been conducted utilizing between 30 - 60 wt% of plasticizers in order to melt process PAN with moderate success. However no melt spinning technique has thus far been developed to achieve the fiber quality afforded by wet-spinning PAN-based precursors[100, 101, 103, 186].

In order to lower the melting point by altering the morphology, polyacrylonitrile is copolymerized with a comonomer. Commercially, comonomers such as vinyl acetate and methyl acrylate are used to enable dissolution in spinning solvents for solution spinning.

The comonomer acts as a diluent in the polymer chain and reduces the melting point of the polyacrylonitrile[187]. Flory proposed that the sequence length of the crystallizable repeat units decreases linearly with the addition of comonomer. The correlation between the comonomer content and decrease in the melting point is given by Flory in the following equation:

$$\frac{1}{T_m} - \frac{1}{T_m^0} = \frac{R}{\Delta H_u} \chi_B$$

Where $T_m$ and $T_m^0$ are the melting points of the polymer with comonomer and polyacrylonitrile homopolymer respectively. R is the universal gas constant, $\Delta H_u$ is the heat of fusion per mole of the polyacrylonitrile crystalline repeating unit, and $\chi_B$ is the mole fraction of comonomer (non-crystallizable).[188] The choice of the comonomer is based on its reactivity ratio with acrylonitrile, molar volume of the side chain. Frushour performed DSC experiments on poly(acrylonitrile-*co*-vinyl acetate) copolymers with varying vinyl acetate contents and plotted the reciprocal melting temperatures against the mole fraction of vinyl acetate. He obtained straight lines with a certain slope which he designated as melting point depression constant and observed that upon replacing vinyl acetate with smaller comonomers like vinyl chloride, the slope decreased. He determined that methyl acrylate has a melting point depression constant of $K_b$ = 3.37 x $10^3$ $K^{-1}$ and its side chain has a molar volume of 36 $cm^3$/mole which can sterically

hinder the chains from packing.[93] Although vinyl acetate has a similar molar volume of the side group, methyl acrylate has more commonly been used as a comonomer in polyacrylonitrile due to close reactivity ratios with acrylonitrile[67] ($r_{AN}$ = 1.17 $r_{MA}$= 0.76)[189] and $T_g$ of about 10 $^0$C. The acrylonitrile and vinyl acetate monomer pair on the other hand have reactivity ratios of 4.2($r_{AN}$) and 0.05($r_{VA}$) respectively.[190]

The role of comonomers on the melt processability of polyacrylonitrile and the effect of incorporation of methyl acrylate in acrylonitrile copolymers has been investigated previously.[191-195] It has been demonstrated by parallel plate dynamic rheology experiments in our laboratory that, polyacrylonitrile copolymers containing less that 10 mol% of methyl acrylate exhibit high melt viscosities of the order of magnitude $10^6$ Pa-s at 220 $^0$C.Furthermore, it was shown that increasing the methyl acrylate comonomer content to 10-15 mol%, yielded a melt viscosities in the processible range of 100-1000 Pa-s at 220 $^0$C.[191] However, incorporation of 10-15 mol % of methyl acrylate has also been reported to cause fiber fusion during the oxidative stabilization step of carbon fiber formation,(i.e. the complex reaction involving inter and intramolecular cyclization), possibly due to elimination of crystallinity.[89] To overcome this, the addition of small amounts of UV crosslinkable comonomers like acryloyl benzophenone, in order to partially crosslink the fibers has also been investigated.[196]

One objective herein was to synthesize a series of high molecular weight poly(acrylonitrile-*co*-methyl acrylate) copolymers with sufficient comonomer contents to obtain copolymers that could be melt processed. It was expected that above a certain threshold of methyl acrylate content, the order in the chains would be disrupted and that crystallization would not occur. Requirements for melt processing were that the

materials would flow at a temperature above the glass transition temperature but well before the onset of thermal degradation or cyclization. It was anticipated that this would allow for melt pressing the materials to form films that could be used in conjunction with other polymers in multi-layer films for packaging applications.

## 5.2 Experimental

### 5.2.1 Materials

Acrylonitrile (≥ 99+ %), methyl acrylate (99 %), ammonium persulfate initiator (98 %), sodium metabisulfite activator, 1-dodecanethiol (98+ %) as the chain transfer agent, and magnesium sulfate were purchased from Sigma-Aldrich. 2,2'-Azobisisobutyronitrile (AIBN) was purchased from Sigma-Aldrich and recrystallized from methanol before use. The surfactant (Dowfax 8390, a 35% solution of an alkyldiphenyloxide disulfonate in water) was kindly provided by the Dow Chemical Company. Poly(vinyl alcohol) as the suspending agent was purchased from MP Biomedicals, LLC. Acrylonitrile and methyl acrylate were passed through activated alumina to remove the stabilizer. Activated alumina (8-14 mesh) was purchased from Fisher Scientific.

#### 5.2.2.1 Suspension copolymerization

A free radical suspension copolymerization of acrylonitrile and methyl acrylate was conducted in a 4-neck round bottom reaction flask equipped with a reflux condenser, an overhead mechanical stirrer and a nitrogen inlet. Deionized (DI) water (350 mL) was boiled immediately prior to the reaction to remove oxygen. Poly(vinyl alcohol) (1.306 g, 2.5 wt/wt % based on total monomers) was dissolved in 300 mL of DI water. The aqueous poly(vinyl alcohol) solution was charged to the reaction flask and purged with nitrogen for 15 min. Acrylonitrile (36 g, 0.678 mol) and methyl acrylate (9 g,

0.104 mol), were added to the reaction mixture via separate syringes and each syringe was flushed with 20 mL of water that was added to the reaction mixture. The 1-dodecanethiol chain transfer agent (0.704 g, 0.4 mol % based on total monomers), was added to the reaction mixture via a syringe and the syringe was flushed with 10 mL of water that was added to the reaction. AIBN initiator (0.099 g, 0.05 mol % based on total monomers) was dissolved in the remaining acrylonitrile (4 g, 0.076 mol) and methyl acrylate (1 g, 0.0116 mol) and added to the flask. The reaction was then stirred at 60 °C for 16 h and the reaction exotherm was controlled using an ice water bath. The resultant suspension was added to 2000 mL of water at 65 °C and stirred briefly, then the suspension was filtered. The filtered polymer was washed with another 2000 mL of DI water at 65 °C, then dried at 70 °C under vacuum. The recovered yield was 75%.

**5.2.2.2 Emulsion copolymerization**

A free radical emulsion copolymerization of acrylonitrile and methyl acrylate was conducted in a 4-neck round bottom reaction flask equipped with a condenser, an overhead mechanical stirrer and a nitrogen inlet. DI water (150 mL) was boiled immediately prior to the reaction to remove oxygen. Dowfax 8390 solution (3.33 g) was dissolved in 130 mL of DI water. The surfactant solution was charged to the reaction flask and purged with nitrogen for 15 min. Acrylonitrile (40 g, 0.754 mol) and methyl acrylate (10 g, 0.116 mol) were added via syringes and each syringe was washed with 5 mL of DI water that were added to the flask. The chain transfer agent 1-dodecanethiol (0.176 g, 0.1 mol% based on total monomers), was added to the flask followed by addition of 5 mL of water. Ammonium persulfate initiator (0.099 g, 0.05 mol % based on total monomers) was dissolved in 5 mL of water and added to the flask. The reaction was stirred at 70 °C for 16 h. The reaction exotherm was controlled using an ice water

bath. The resultant emulsion was added to 2000 mL of a 1 % aq $MgSO_4$ solution at 65 $^{\circ}$C and stirred briefly. The solid polymer was filtered, washed with ~2000 mL of DI water at 65 $^{\circ}$C, and dried at 100 $^{\circ}$C under vacuum to recover the copolymer. The recovered yield was 80%.

## 5.3 Characterization

### 5.3.1 Composition analysis by $^1$H NMR

$^1$H NMR in deuterated dimethylsulfoxide (DMSO-$d_6$) was used to measure the copolymer compositions using a 400 MHz Varian NMR spectrometer. Ten mg of sample was dissolved in 1 mL of the NMR solvent and 32 scans were performed. The copolymer composition was determined by comparing the integrals of the proton signals in the repeat units.

### 5.3.2 Thermal analysis

The thermal stability and temperature at which weight loss began was determined using thermogravimetric analysis using a TGA Q500 (TA Instruments) in an atmosphere of nitrogen at a heating rate of 10 $^0$C/min from 25 to 500 $^0$C. The glass transition temperature ($T_g$) was determined using differential scanning calorimetry using a Q200 (TA Instruments). The samples were heated from -20 to 150 $^0$C to eliminate thermal history, and this was followed by cooling to -20 $^0$C and heating again to 290 $^0$C. The second heat was used to obtain the $T_g$ at the midpoint of the step transition.

### 5.3.3 Molecular Weight Analyses

Absolute molecular weight measurements from size exclusion chromatography (SEC) were made using an Agilent 1260 infinity SEC equipped with a Wyatt Heleos II 18-angle static light scattering detector, a Wyatt Viscostar viscosity detector, and a Wyatt T-rex differential RI detector. The chromatograms were acquired at 50 $^{0}$C using three PL gel 10 μm mixed-B 200 x 75 mm columns in series. Dry NMP containing 0.05 M LiBr was used as the elution solvent.

Intrinsic viscosity measurements were performed using a Cannon Ubbelhode viscometer F 519 according to ASTM D445 at 35 $^{\circ}$C in DMF. The DMF was filtered through a 1 μm PTFE filter prior to preparation of the samples. Solutions with a concentration of 1 g/dL were made by dissolving 200 mg of the sample in 20 mL of filtered DMF. The samples were stirred at room temperature for 24 h immediately prior to testing. The solvent time measurements were recorded with 8 mL of DMF in the viscometer. Three solvent times were recorded and averaged. The polymer solutions were not filtered in order to avoid any filtration of high molecular weight fractions. Five solution times for each concentration were recorded and averaged.

### 5.3.4 Melt pressing the poly(acrylonitrile-*co*-methyl acrylate) copolymers

The copolymers were pressed into films using a Carver Hydraulic Unit Model # 3912 melt press instrument using the following representative procedure. The platens were heated to the desired temperature of 170 $^{0}$C and ~0.5-0.7 g of the copolymer was placed between Kapton films between the steel plates. The steel plates were placed between the heated platens and 5000 psi pressure was applied. After 5 min, the platens were separated and the steel plates were placed in cold water, then the copolymer disc was removed.

## 5.4. Results and Discussion

### 5.4.1 Synthesis of 80/20 wt/wt% poly(acrylonitirile-*co*-methyl acrylate) random copolymers

Emulsion and suspension copolymerization routes were used for the synthesis of the poly(acrylonitrile-*co*-methylacrylate). The choice of the route was made following a study of the polymerization reactions that were previously conducted in our laboratory[197-199]. Scheme 5-1 shows the reaction components.

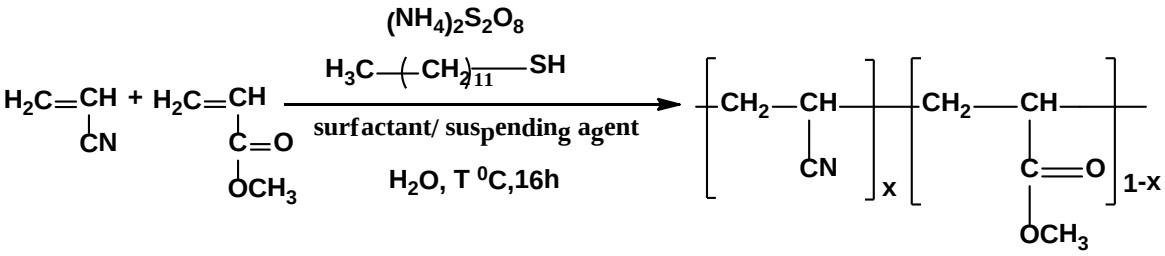


**Scheme 5-1**. Representative reaction scheme and reaction components

| ID | Method | AN/MA (wt/wt %) (charged) | AN/MA (wt/wt %) ($^1$H NMR) | Initiator (mol % relative to monomers) | Chain transfer agent (mol % relative to monomers | Temp – Max Temp (°C) | Time (h) | Yield (%) |
|---|---|---|---|---|---|---|---|---|
| **(1)** | suspension | 80/20 | 82/18 | AIBN 0.05 | 0.4 | 60-65 | 16 | 85 |
| **(2)** | emulsion | 80/20 | 85/15 | Ammonium persulfate 0.05 | 0.1 | 70-75 | 16 | 83 |
| **(3)** | emulsion | 80/20 | 82/18 | Ammonium persulfate 0.05 | 0.1 | 70-80 | 16 | 78 |

**Table 5-1. Synthetic parameters used in the suspension and emulsion copolymerization**

### 5.4.2 Composition and molecular weight analysis

Poly(acrylonitrile-*co*-methyl acrylate) copolymers with a target monomer ratio of 80/20 wt/wt % acrylonitrile/methyl acrylate content were synthesized via suspension and emulsion copolymerization. A representative $^{1}$H NMR spectrum is shown in Figure 1. The signal at 3.2 ppm (b) corresponds to the methine (CH) protons from AN and MA. The signal at 2.1 ppm (a) corresponds to the methylene ($CH_2$) protons from AN and MA repeat units. The signal at 3.7 ppm corresponds to the methyl ($CH_3$) protons of the MA units. The copolymer composition was calculated from the integral values of the methylene protons using the following equations:

$$\text{Moles MA } \alpha \left(\frac{\int \text{CH}_3}{3}\right)$$

$$(\text{Moles MA}) \times \left(86.04 \frac{g}{mole}\right) = \text{relative weight MA}$$

$$\text{Moles AN } \alpha \left[\left(\frac{\int \text{b}}{2}\right) - \left(\frac{\int \text{CH}_3}{3}\right)\right]$$

$$(\text{Moles AN}) \times \left(53.06 \frac{g}{mole}\right) = \text{relative weight AN}$$

$$\text{Weight Percent AN} = \frac{\text{relative weight AN}}{\text{relative weight AN} + \text{relative weight MA}} \times 100$$

$$\text{Weight Percent MA} = 100 - \text{weight percent AN}$$

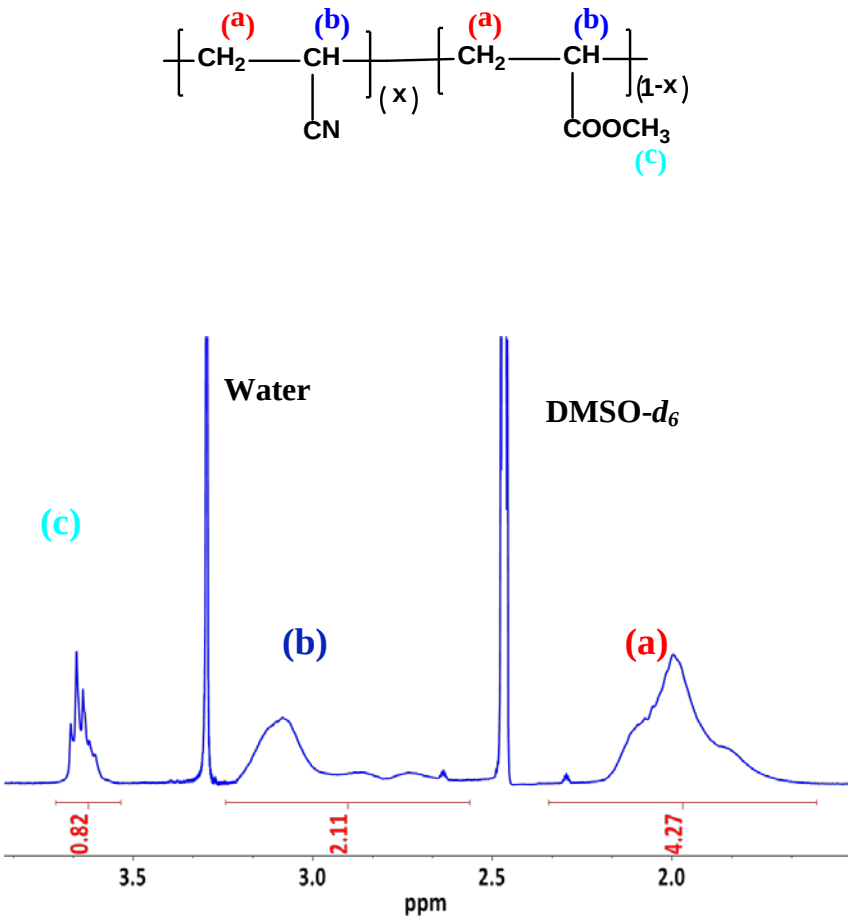


**Figure 5-1. $^{1}$H NMR of an 82/18 wt/wt % poly(acrylonitrile-*co*-methyl acrylate) copolymer prepared by emulsion copolymerization**

The compositions of the copolymers synthesized by both emulsion and suspension techniques were in close agreement with the charged compositions. The minor difference is perhaps due to loss of monomer during the synthesis even under reflux conditions due to the temperature of the reaction being close to the boiling point of the comonomers.

The two emulsion copolymers and the suspension copolymer were all high molecular weight. The molecular weights were analyzed via SEC and dilute solution

viscometry. Figure 2 shows the absolute $M_w$ values obtained using output from the light scattering detector from the SEC chromatograms. The suspension copolymer had a broader molecular weight distribution than the emulsion copolymers. The chromatogram (1) in Figure 5-2 is skewed toward the higher molecular weight end, indicating the presence a high molecular weight fraction.

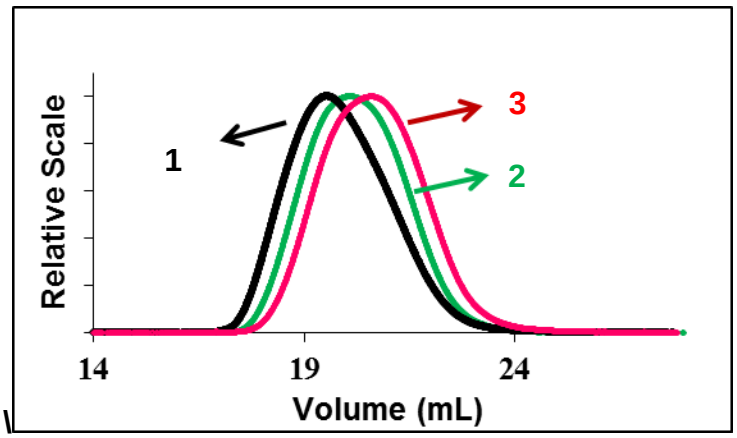


| | AN/MA (wt/wt %) Charged | AN/MA (wt/wt %) by $^1$H NMR | $M_n$ (kg/mol) | $M_w$ (kg/mol) | PDI ($M_w/M_n$) | [η] (dL/g) | $M_v$ (kg/mol) |
|---|---|---|---|---|---|---|---|
| **(1)** | 80/20 | 82/18 | 168.9 | 374.5 | 2.2 | 2.4 | 158 |
| **(2)** | 80/20 | 85/15 | 107.0 | 206.2 | 1.9 | 1.6 | 93 |
| **(3)** | 80/20 | 82/18 | 121.5 | 229.1 | 1.9 | 2.0 | 124 |

**Figure 5-2. Light scattering chromatograms of the poly(acrylonitrile-*co*-methyl acrylate) copolymers**

Dilute solution viscometry was used to determine the intrinsic viscosities of the copolymers using the intercept from a representative plot as shown in Figure 5-3. The viscosity average molecular weights of the copolymers shown in Figure 5-2 were estimated from using Mark-Houwink parameters for polyacrylonitrile homopolymers (K = 3.14 x 10-4, a= 0.746), but there were significant deviations between $M_w$ and $M_v$ with

this approach.[200] K and a parameters depend on polymer and solvent interactions and these values are expected to vary as the composition varies. Intrinsic viscosity measurements are, however, a useful method to compare relative molecular weights of the copolymers.

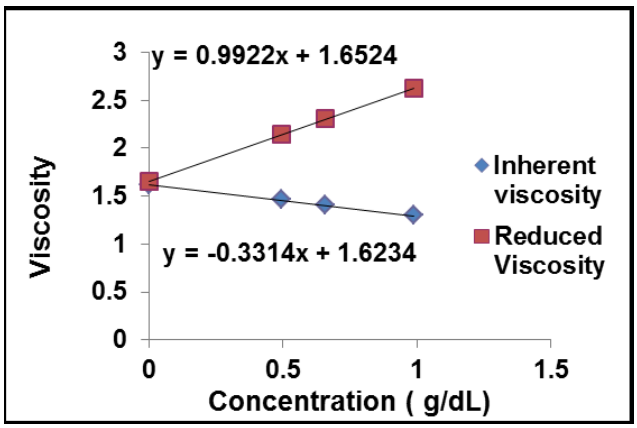


**Figure 5-3. Intrinsic viscosity of the 82/18 wt/wt % poly(acrylonitrile-*co*-methyl acrylate) emulsion copolymer**

### 5.4.3 Thermal Properties

The difference in comonomer content in the compositional range that was studied has a negligible effect on the glass transition temperature of the copolymers (Figure 5-4). The relatively high methyl acrylate content of 15-18 wt% appears to have completely disrupted the order in the predominantly polyacrylonitrile chains, since no melting transitions were observed.

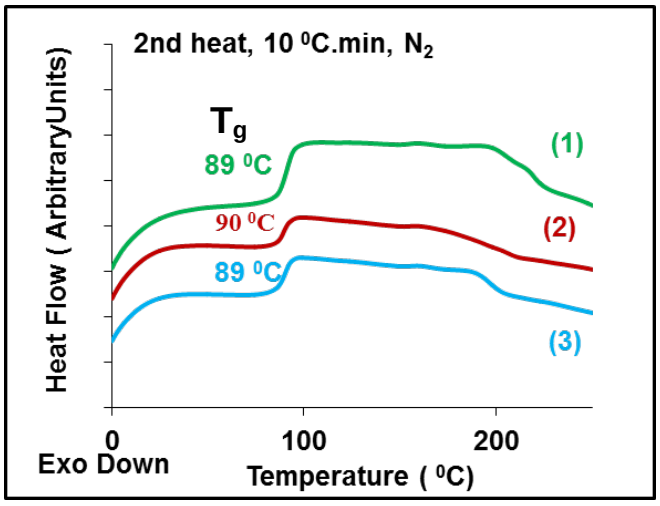


**Figure 5-4 DSC thermograms of the poly(acrylonitrile-*co*-methyl acrylate) copolymers: (1) 82/18 AN/MA wt/wt% suspension, (2) 85/15 wt/wt % emulsion, and (3) 82/18 wt/wt % emulsion**

These 80/20 wt/wt % poly(acrylonitrile-*co*-methyl acrylate) copolymers were successfully melt pressed into transparent discs of about 100 μm thickness. The transparency of the films is likely related to their amorphous morphologies. However, it should be noted that the cooling rate has a significant effect on the crystallite size of the copolymer. The faster the cooling rate, the lesser time the polymer chains have to pack and form crystalline domains. Several authors have reported the complete disruption of crystallinity at methyl acrylate contents over 10-15 wt %[176, 177], but the method of synthesis is expected to affect the relative degree of order or crystallinity in the polymer.[174, 175] Hence, in addition to DSC, complimentary X-ray diffraction experiments on these films as well as films cooled at a slower rate would be necessary to confirm elimination of crystallinity. The relatively high comonomer content and high molecular weight of the copolymers is expected to impart ductility to the films.

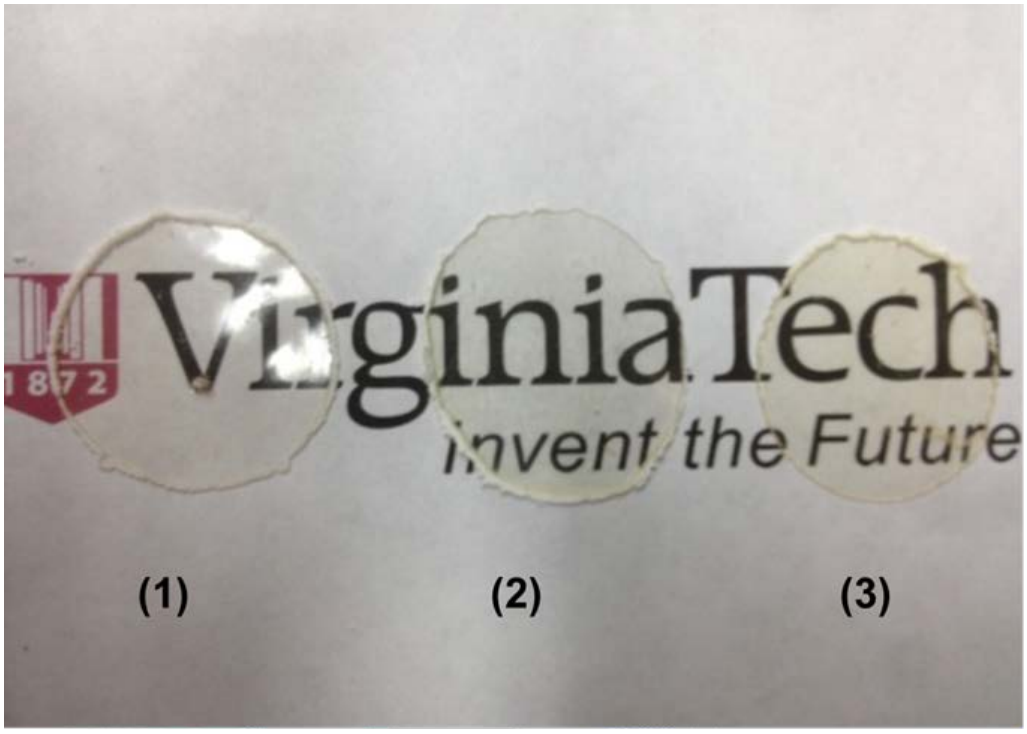


**Figure 5-5. Melt pressed discs of poly(acrylonitrile-*co*-methyl acrylate) copolymers:1) 82/18 wt/wt% AN/MA, suspension (2) 85/15 wt/wt% AN/MA, emulsion (3) 82/18 wt/wt% AN/MA, emulsion. Virginia Tech logo used with the permission of Dr.Larry Hincker, University Relations**

## 5.5 Conclusion

High molecular weight poly(acrylonitrile-*co*-methyl acrylate) copolymers with approximately 80 weight percent of methyl acrylate were synthesized by suspension and emulsion copolymerization. The relatively high reaction temperatures produced exotherms that required careful control. DSC experiments demonstrated that these copolymers did not have an endothermic melting transition before 250°C, suggesting

complete disruption of crystallinity. The transparency of films of these materials combined with high molecular weight is expected to make these materials ideal for packaging applications. The higher acrylonitrile content in these materials compared to commercial PAN packaging material like Barex is expected to enhance its barrier properties.

## CHAPTER 6 CONCLUSIONS AND SUGGESTED FUTURE RESEARCH

The composition (wt % of acrylonitrile), the weight average molecular weight, the molecular weight distribution, level and type of additive added, all play a very important role in imparting melt processability to poly(acrylonitrile-*co*-methyl acrylate) copolymers.Water has shown promise as a potential melt processing aid by reducing the melting point of high acrylonitrile content (91-95 wt%) poly(acrylonitrile-*co*-methyl acrylate) copolymers to well below 200 $^{0}$C. However, its low boiling point (below processing temperature) is still a matter of concern. Water (50 mol%) and ethylene glycol (22 mol%) are most effective in reducing the $T_g$ and $T_m$ of the 95:5 AN/MA mole:mole % copolymer with a molecular weight of 200 kg/mol, making them potential melt processing aids. Glycerin-water solutions with high glycerin content (13 mol% glycerin , 15 mol% water) prove to be good candidates. High boiling alcohols, glycerin and 1,4-butanediol are incompatible with the 200 kg/mol 95:5 mole:mole % poly(acrylonitrile-*co*-methyl acrylate) copolymer, showing lower reductions in $T_g$ and $T_m$ compared to using water or ethylene glycol. A study of the interactions between various solvents and polyacrylonitrile/ polyacrylonitrile copolymers would be necessary in order to understand how these interactions affect the physical properties of PAN such as its melting point.

Wu Qing-Yun and researchers[201] conducted density functional theory studies and a two-dimensional infrared correlation analysis, to study the interaction between polyacrylonitrile and a few polar solvents. They showed that polyacrylonitrile preferentially interacts with the solvents in the order of dimethyl sulfone > dimethyl

sulfoxide > ethylene carbonate > propylene carbonate > dimethyl formamide. They also emphasized the importance of molecular structure of a solvent and how it affects the accessibility of a solvent to interact with polyacrylonitrile and showed that in each of these polymer-solvent systems, the nitrile group and the polar functional group in the solvent were aligned in an anti-parallel fashion. [201]

Bashir *et al.* [166] performed Raman spectroscopy and IR spectroscopy measurements to understand the interactions between water and PAN on the plasticized films and showed that the methine hydrogen in the polymer chain backbone does not hydrogen bond with water. Similar computational modeling studies and the use of FTIR in order to probe the interactions between polyacrylonitrile and solvent need to be conducted for a wider range of solvents and this could perhaps shed light on why polar molecules like ethylene glycol and water impart PAN melt processability while glycerin does not.

Furthermore, investigation of the melt viscosity of these copolymer–plasticizer blends with different compositions as a function of time and temperature is recommended to determine the effectiveness of the plasticizer in imparting melt processability to the copolymer before the onset of thermal cyclization begins.

## BIBLIOGRAPHY


1. Idol, J. D., Jr. Acrylonitrile. US2904580, 1959.
2. Mark, H. F.; Bikales, N. M.; Overberger, C. G.; Menges, G.; Editors, *Encyclopedia of Polymer Science and Engineering, Vol. 1: A to Amorphous Polymers. 2nd Ed*. John Wiley and Sons: 1985.
3. Chanda, M.; Roy, S. K., *Plastics Technology Handbook*. Marcel Dekker, Inc.: 1987.
4. Freeman, B. D.; Park, H. B.; McCloskey, B. D. Water purification membranes with improved fouling resistance. WO2010006196A2, 2010.
5. Allen, S. M.; Fujii, M.; Stannett, V.; Hopfenberg, H. B.; Williams, J. L., The barrier properties of polyacrylonitrile. *J. Membr. Sci.* **1977,** *2*, 153-163.
6. Hungerford, G. P. Flexible film laminates. EP83157A2, 1983.
7. Courtney, J. M.; Park, G. B.; Fairweather, I. A., Polymer structure and blood compatibility evaluation - application of an acrylonitrile copolymer. *Biomater Med Devices Artif Organs* **1976,** *4*, 263-275.
8. Masson, J. C., *Acrylic fiber technology and applications*. M. Dekker: New York, 1995.
9. McIntyre, J. E., *Synthetic fibres : nylon, polyester, acrylic, polyolefin*. CRC Press ; Woodhead Pub.: Boca Raton; Cambridge, England, 2005.
10. Capone, G. J.; Bittle, D. F. Fiber bundles including reversible crimp fibers having improved dyeability. WO9520697A1, 1995.
11. Ebdon, J. R.; Huckerby, T. N.; Hunter, T. C., Free-radical aqueous slurry polymerizations of acrylonitrile: 2. End-groups and other minor structures in polyacrylonitriles initiated by potassium persulfate/sodium bisulfite. *Polymer* **1994,** *35* (21), 4659-4664.
12. Aizenshtein, E. M., Chemical fibers and thread in a crisis year. *Fibre Chem.* **2009,** *41*, 281-293.
13. Donnet, J.-B.; Bansal, R. C., *Carbon fibers*. M. Dekker: New York, 1990.
14. Chung, D. D. L., *Carbon fiber composites*. Butterworth-Heinemann: Boston, 1994.
15. Frank, E.; Steudle, L. M.; Ingildeev, D.; Spörl, J. M.; Buchmeiser, M. R., Carbon Fibers: Precursor Systems, Processing, Structure, and Properties. *Angewandte Chemie International Edition* **2014,** *53* (21), 5262-5298.
16. Liu, Y.; Kumar, S., Recent Progress in Fabrication, Structure, and Properties of Carbon Fibers. *Polymer Reviews* **2012,** *52* (3/4), 234-258.
17. Bashir, Z., A critical review of the stabilisation of polyacrylonitrile. *Carbon* **1991,** *29* (8), 1081-1090.
18. Fitzer, E.; Müller, D. J., The influence of oxygen on the chemical reactions during stabilization of pan as carbon fiber precursor. *Carbon* **1975,** *13* (1), 63-69.
19. Burlant, W. J.; Parsons, J. L., Pyrolysis of polyacrylonitrile. *Journal of Polymer Science* **1956,** *22* (101), 249-256.
20. Grassie, N.; Hay, J. N.; McNeill, I. C., Coloration in acrylonitrile and methacrylonitrile polymers. *Journal of Polymer Science* **1958,** *31* (122), 205-206.
21. Grassie, N.; McGuchan, R., Pyrolysis of polyacrylonitrile and related polymers—II: The effect of sample preparation on the thermal behaviour of polyacrylonitrile. *European Polymer Journal* **1971,** *7* (8), 1091-1104.

22. Tsai, J. S.; Lin, C. H., Effect of comonomer composition on the properties of polyacrylonitrile precursor and resulting carbon fiber. *J. Appl. Polym. Sci.* **1991,** *43*, 679-685.
23. Coleman, M. M.; Sivy, G. T., Fourier transform ir studies of the degradation of polyacrylonitrile copolymers—III: Acrylonitrile/vinyl acetate copolymers. *Carbon* **1981,** *19* (2), 133-135.
24. Grassie, N.; Jenkins, R. H., Photothermal degradation of copolymer of methyl methacrylate and butyl acrylate. *Eur. Polym. J.* **1973,** *9*, 697-716.
25. Grassie, N.; McGuchan, R., Pyrolysis of polyacrylonitrile and related polymers. VII. Copolymers of acrylonitrile with acrylate, methacrylate, and styrene type monomers. *Eur. Polym. J.* **1972,** *8*, 865-878.
26. Watt, W.; Perov, B. V., Handbook of Composites. Vol. 1. Strong Fibres. **1985**.
27. Morgan, P., *Carbon fibers and their composites*. Taylor & Francis: Boca Raton, 2005.
28. Goodhew, P. J.; Clarke, A. J.; Bailey, J. E., A review of the fabrication and properties of carbon fibres. *Materials Science and Engineering* **1975,** *17* (1), 3-30.
29. Watt, W.; Johnson, W., Mechanism of oxidation of polyacrylonitrile fibers. *Nature (London)* **1975,** *257*, 210-212.
30. Young, R. J., Polymers: Fibers and textiles, a compendium Edited by Jacqueline I. Kroschwitz, John Wiley & Sons, New York, 1990. *Polymer International* **1991,** *25* (1).
31. Ismail, A. F.; Rahman, M. A.; Mustafa, A.; Matsuura, T., The effect of processing conditions on a polyacrylonitrile fiber produced using a solvent-free free coagulation process. *Materials Science and Engineering: A* **2008,** *485* (1–2), 251-257.
32. Beniska, J.; Staudner, E., Study of the activity of some sulfur compounds in the modification of vulcanizates by vinyl monomers. *J. Polym. Sci., Polym. Symp.* **1967,** *No. 16*, 1301-1310.
33. Czajlik, I.; Vertes, E., Kinetics of copolymerization. III. Determination of the rate of initiation in the copolymerization system acrylonitrile/methyl acrylate/dimethylformamide. *J. Macromol. Sci., Chem.* **1980,** *A14*, 1243-1254.
34. Gupta, V. B.; Kothari, V. K., *Manufactured fibre technology*. Chapman & Hall: London, 1997.
35. Lewin, M., *Handbook of fiber chemistry*. CRC/Taylor & Francis: Boca Raton, 2007.
36. Odian, G. G., *Principles of polymerization*. Wiley-Interscience: Hoboken, N.J., 2004.
37. Bamford, C. H.; Barb, W. G.; Jenkins, A. D., Vinyl polymerization in heterogeneous systems. *Nature* **1952,** *169*, 1044-1046.
38. Thomas, W. M.; Pellon, J. J., Kinetics of acrylonitrile polymerization in bulk. *J. Polym. Sci.* **1954,** *13*, 329-336.
39. McIntyre, J. E., *Synthetic fibers : nylon, polyester, acrylic, polyolefin*. CRC Press: Washington, DC.
40. Poly(vinyl ether)s, Poly(vinyl ester)s, and Poly(vinyl halogenide)s. In *Handbook of Polymer Synthesis*, CRC Press: 2004.
41. Polymers of Acrylic Acid, Methacrylic Acid, Maleic Acid and their Derivatives. In *Handbook of Polymer Synthesis*, CRC Press: 2004.
42. American Cyanamid, C.; Petrochemicals, D., *The chemistry of acrylonitrile*. New York, 1959.
43. Chain Polymerizaiton of Vinyl monomers. In *Polymer Science: A comprehensive reference*, M.Sawamoto, G. W. C. a., Ed. Elsevier: Vol. 3.

44. Brandrup, J.; Immergut, E. H.; Grulke, E. A., *Polymer handbook*. Wiley: New York, 1999.
45. Schneider, M.; Graillat, C.; Boutti, S.; McKenna, T. F., Decomposition of APS and H2O2 for emulsion polymerisation. *Polymer Bulletin* **2001,** *47* (3-4), 269-275.
46. Bartlett, P. D.; Cotman, J. D., The Kinetics of the Decomposition of Potassium Persulfate in Aqueous Solutions of Methanol. *Journal of the American Chemical Society* **1949,** *71* (4), 1419-1422.
47. Kolthoff, I. M.; Miller, I. K., The Chemistry of Persulfate. I. The Kinetics and Mechanism of the Decomposition of the Persulfate Ion in Aqueous Medium1. *Journal of the American Chemical Society* **1951,** *73* (7), 3055-3059.
48. House, D. A., Kinetics and Mechanism of Oxidations by Peroxydisulfate. *Chemical Reviews* **1962,** *62* (3), 185-203.
49. Kolthoff, I. M.; Meehan, E. J.; Carr, E. M., Mechanism of Initiation of Emulsion Polymerization by Persulfate1. *Journal of the American Chemical Society* **1953,** *75* (6), 1439-1441.
50. Okubo, M.; Mori, T., The decomposition of potassium persulfate used as initiator in emulsion polymerization. *Makromol. Chem., Macromol. Symp.* **1990,** *31*, 143-156.
51. Okubo, M.; Fujimura, M.; Mori, T., The acceleration of decomposition of potassium persulfate in the presence of sodium dodecyl sulfate and polymer particles as a model of emulsion polymerization system. *Colloid Polym Sci* **1991,** *269* (2), 121-123.
52. Thickett, S. C.; Gilbert, R. G., Emulsion polymerization: State of the art in kinetics and mechanisms. *Polymer* **2007,** *48* (24), 6965-6991.
53. Bamford, C. H., *The kinetics of vinyl polymerization by radical mechanisms*. Butterworths: London, 1958.
54. Serra, C., Free Radical Polymerization. In *Micro Process Engineering*, Wiley-VCH Verlag GmbH & Co. KGaA: 2009.
55. Braun, D., Origins and development of initiation of free radical polymerization processes. *Int. J. Polym. Sci.* **2009**.
56. Kopecky, K. R., The Chemistry of Free Radical Polymerization By Graeme Moad and David H. Solomon (University of Melbourne). *Journal of the American Chemical Society* **1997,** *119* (47), 11559-11559.
57. Behrman, E. J.; Edwards, J. O., The thermal decomposition of peroxodisulfate ions. *Rev. Inorg. Chem.* **1980,** *2*, 179-206.
58. Mishra, M. K.; Yagci, Y., *Handbook of vinyl polymers : radical polymerization, process, and technology*. CRC Press/Taylor & Francis: Boca Raton, 2009.
59. Bruyn, H. D.; Gilbert, R. G.; Hawkett, B. S., Retardation by oxygen in emulsion polymerization. *Polymer* **2000,** *41*, 8633-8639.
60. Cunningham, M. F.; Geramita, K.; Ma, J. W., Measuring the effects of dissolved oxygen in styrene emulsion polymerization. *Polymer* **2000,** *41*, 5385-5392.
61. Chern, C. S., *Progress in Polymer Science* **2006,** *31* (5), 443-486.
62. Fukuda, T.; Kubo, K.; Ma, Y.-D., Kinetics of free radical copolymerization. *Progress in Polymer Science* **1992,** *17* (5), 875-916.
63. Van herk, A. M., *Chemistry and Technology of Emulsion Polymerization*.
64. Texter, J., *Reactions and synthesis in surfactant systems*. Marcel Dekker: New York, 2001.
65. van Herk, A. M., Wiley [Imprint]: 2013.

66. Solomon, B. R.; Varanasi, K. K.; Hyder, M. N. Hierarchical porous membrane for emulsion separation. WO2013130893A2, 2013.
67. Wiles, K. B.; Bhanu, V. A.; Pasquale, A. J.; Long, T. E.; McGrath, J. E., Monomer Reactivity Ratios for Acrylonitrile–Methyl Acrylate Free-Radical Copolymerization
*J. Poly. Sci A* **2002,** *44*, 2994-3001.
68. Fordyce, R. G.; Chapin, E. C., Copolymerization. I. The Mechanism of Emulsion Copolymerization of Styrene and Acrylonitrile. *Journal of the American Chemical Society* **1947,** *69* (3), 581-583.
69. Fordyce, R. G.; Ham, G. E., Copolymerization. VIII. Reactivity of Fumaronitrile in Vinyl Copolymerization. *Journal of the American Chemical Society* **1951,** *73* (3), 1186-1189.
70. Sajjadi, S., Particle formation under monomer-starved conditions in the semibatch emulsion polymerization of styrene. I. Experimental. *Journal of Polymer Science Part A: Polymer Chemistry* **2001,** *39* (22), 3940-3952.
71. Smith, W. V.; Ewart, R. H., Kinetics of Emulsion Polymerization. *The Journal of Chemical Physics* **1948,** *16* (6), 592-599.
72. Harkins, W. D., A General Theory of the Mechanism of Emulsion Polymerization1. *Journal of the American Chemical Society* **1947,** *69* (6), 1428-1444.
73. Stuart C. Thickett, R. G. G., Emulsion Polymerization : State of art in kinetics and mechanisms. *Polymer* **2007,** *48*, 27.
74. Halnan, L. F.; Napper, D. H.; Gilbert, R. G., A study of the kinetics of the emulsion polymerization of butyl methacrylate. *Journal of the Chemical Society, Faraday Transactions 1 : Physical Chemistry in Condensed Phases* **1984,** *80*, 2851-2865.
75. Ballard, M. J.; Napper, D. H.; Gilbert, R. G., Theory of emulsion copolymerization kinetics. *J. Polym. Sci., Polym. Chem. Ed.* **1981,** *19*, 939-954.
76. Hawkett, B. S.; Napper, D. H.; Gilbert, R. G., Seeded emulsion polymerization of styrene. *J. Chem. Soc., Faraday Trans. 1* **1980,** *76*, 1323-1343.
77. Fitch, R. M. S., L., Emulsion Polymerization : Kinetics of Radical capture by the particles. *Progress in Colloid and Polymer Science* **1975,** *56*, 1-11.
78. Adams, M. E.; Trau, M.; Gilbert, R. G.; Napper, D. H.; Sangster, D. F., The entry of free radicals into polystyrene latex particles. *Aust. J. Chem.* **1988,** *41*, 1799-1813.
79. Van Berkel, K. Y.; Russell, G. T.; Gilbert, R. G., Entry in Emulsion Polymerization: Effects of Initiator and Particle Surface Charge. *Macromolecules* **2003,** *36*, 3921-3931.
80. Dong, Y. S., D.C., Radical Entry in Emulsion Polymerization : Estimation of the Crtitical Length of Entry Radicals via a Simple Lattice Model. *Macromolecules* **2002,** *35*, 8185-8190.
81. Tauer, K.; Nozari, S.; Ali, A. M. I., Experimental Reconsideration of Radical Entry into Latex Particles. *Macromolecules* **2005,** *38*, 8611-8613.
82. Goicoechea, M.; Barandiaran, M. J.; Asua, J. M., Entry of Hydrophilic Radicals into Latex Particles. *Macromolecules* **2006,** *39*, 5165-5166.
83. Lamb, D. J.; Fellows, C. M.; Gilbert, R. G., Radical entry mechanisms in redox-initiated emulsion polymerizations. *Polymer* **2005,** *46*, 7874-7895.
84. Smith, W. V. E., R. H. J. Chem. Phys., (1948), 16, 592., *J.Chem.Phys.* **1948,** *16*, 592-599.
85. Benson, S. W.; North, A. M., The kinetics of free-radical polymerization under conditions of diffusion-controlled termination. *J. Am. Chem. Soc.* **1962,** *84*, 935-940.
86. Krigbaum, W. R.; Tokita, N., Melting-point-depression study of polyacrylonitrile. *J. Polym. Sci.* **1960,** *43*, 467-488.

87. Flory, P. J., Theory of crystallization in copolymers. *Trans. Faraday Soc.* **1955,** *51*, 848-857.
88. Eby, R. K., First-order transition temperatures in crystalline polymers. *J. Appl. Phys.* **1963,** *34*, 2442-2445.
89. Rangarajan, P.; Yang, J.; Bhanu, V.; Godshall, D.; McGrath, J.; Wilkes, G.; Baird, D., Effect of comonomers on melt processability of polyacrylonitrile. *Journal of Applied Polymer Science* **2002,** *85* (1), 69-83.
90. Bajaj, P.; Roopanwal, A. K., Thermal Stabilization of Acrylic Precursors for the Production of Carbon Fibers: An Overview. *Journal of Macromolecular Science, Part C* **1997,** *37* (1), 97-147.
91. Rangarajan, P. Y., J.; Bhanu, V.A.; Godshall, D.; Wilkes, G.L.; McGrath, J.E.; Baird, D.G., *J Appl Polym Sci* **2002,** *85*.
92. Coxe, C. D. Shaping polyacrylonitriles. US2585444, 1952.
93. Frushour, B. G., New thermal analytical technique for acrylic polymers. *Polym. Bull. (Berlin)* **1981,** *4*, 305-314.
94. Frushour, B. G., Water as a melting point depressant for acrylic polymers. *Polym. Bull. (Berlin)* **1982,** *7*, 1-8.
95. Frushour, B. G., Melting behavior of polyacrylonitrile copolymers. *Polym. Bull. (Berlin)* **1984,** *11*, 375-382.
96. Porosoff, H. Melt-spinning acrylonitrile polymer fibers. US4163770A, 1979.
97. Grove, D.; Desai, P.; Abhiraman, A. S., Exploratory experiments in the conversion of plasticized melt spun PAN-based precursors to carbon fibers. *Carbon* **1988,** *26*, 403-411.
98. Daumit, G. P.; Ko, Y. S.; Slater, C. R.; Venner, J. G.; Wilson, D. W.; Young, C. C.; Zabaleta, H., MSP [melt-spinning precursor] - a domestic precursor for current and future generation carbon fibers. *Int. SAMPE Tech. Conf.* **1988,** *20*, 414-422.
99. Daumit, G. P.; Rector, J. D.; Venner, J. G.; Wilson, D. W.; Young, C. C., Domestic precursor technology - a unique route to current and future generation carbon fibers. *Int. SAMPE Symp. Exhib.* **1990,** *35*, 1-12.
100. Bashir, Z., Thermoreversible gelation and plasticization of polyacrylonitrile. *Polymer* **1992,** *33*, 4304-4313.
101. Bashir, Z., Thermoreversible gels of polyacrylonitrile. *J. Polym. Sci., Part B: Polym. Phys.* **1992,** *30*, 1299-1304.
102. Bashir, Z., Double endothermic and exothermic transitions during heating and cooling of thermoreversible polyacrylonitrile gels. *J. Mater. Sci. Lett.* **1993,** *12*, 598-601.
103. Min, B. G.; Son, T. W.; Kim, B. C.; Jo, W. H., Plasticization behavior of polyacrylonitrile and characterization of acrylic fiber prepared from the plasticized melt. *Polym. J. (Tokyo)* **1992,** *24*, 841-848.
104. Smierciak, R. C.; Wardlow, E., Jr.; Ball, L. E. Process for making a melt-processable acrylonitrile-methacrylonitrile copolymer. CA2134825A1, 1995.
105. Smierciak, R. C.; Wardlow, E., Jr.; Ball, L. E. Process for making a melt processable high nitrile multipolymer of acrylonitrile and olefinically unsaturated monomers. US5618901A, 1997.
106. Alves, N. P. Thermoplastic polyacrylonitrile production process. US20110024939A1, 2011.

107. Brito, C. A. R., Jr.; Fleming, R. R.; Pardini, L. C.; Alves, N. P., Thermal analysis of extruded polyacrylonitrile plasticized by glycerol. *Polim.: Cienc. Tecnol.* **2012,** *22*, 364-368.
108. Mathur, R. B.; Bahl, O. P.; Mittal, J., Advances in the Development of High-Performance Carbon Fibres from PAN Precursor. *Composites Science and Technology* **1993,** *51*, 223-230.
109. Chen, J.; Wang, C.; Ge, H.; Bai, Y.; Wang, Y., Effect of Coagulation Temperature on the Properties of Poly(acrylonitrile-itaconic acd) Fibers in Wet Spinning. *J. Polym. Res.* **2007,** *14* (3), 223-228.
110. Peng, G. Q.; Wen, Y. F.; Yang, Y. G.; Liu, L., A Novel Method for Investigating the Structural Uniformity of Polyacrylonitrile Nascent Fibers. *Int. J. Polym. Anal. Charact.* **2008,** *13*, 369-375.
111. Rahman, M. A.; Ismail, A. F.; Mustafa, A.; Ng, B. C.; Hasbullah, H.; Rahaman, M. S. A.; Abdullah, M. S., The Effect of Coagulation Bath Temperature on the Mechanical Properties of PAN-based Carbon Fiber. *Development in Polymer-Based Carbon Fibre Research in Malaysia*, 169-179.
112. Maslowski, E.; Urbanska, A., High Performance Polyacrylonitrile Fibers - Manufacture, Properties, Applications. *America's Textiles International* **1989,** *18* (FW2).
113. odian, G., *Principles of Polymerization*. Wiley Interscience: New york, U.S.A., 2004.
114. Kwon, Y. D.; Kavesh, S.; Prevorsek, D. C. Method for Preparing Tenacity and Modulus Polyacrylonitrile Fiber. 4,883,628, 1989.
115. Tsai, J. S.; Lin, C. H., The Effect of Molecular Weight on the Cross Section and Properties of Polyacrylonitrile Precursor and Resulting Carbon Fiber. *J. Appl. Polym. Sci.* **1991,** *42*, 3045-3050.
116. Volokhina, A. V., Effect of the Molecular Weight of Fibre-Forming Polymers on the Mechanical Properties of Polymer Fibres (Review). *Fibre Chemistry* **2002,** *34* (1), 1-9.
117. Morris, A.; Weisenberger, M. Tech Facts-Precursor Spinning for Carbon Fiber. http://www.caer.uky.edu/techfacts/TechFacts-CM-Precursor-Spinning-Updated-3June2013.pdf.
118. Baojun, Q.; Ding, P.; Zhenqiou, W., The Mechanism and Characteristics of Dry-Jet Wet-Spinning of Acrylic Fibers. *Adv. Polym. Technol.* **1986,** *6* (4), 509-529.
119. Bajaj, P.; Sreekumar, T. V.; Sen, K., Structure Development during Dry-Jet Wet Spinning of Acrylonitrile/Vinyl Acids and Acrylonitrile/Methyl Acrylate Copolymers. *J. Appl. Polym. Sci.* **2002,** *86*, 773-787.
120. Sen, K.; Bahrami, S. H.; Bajaj, P., High-Performance Acrylic Fibers. *Journal of Macromolecular Science Polymer Reviews* **1996,** *36* (1), 1-76.
121. Konas, M.; Moy, T. M.; Rogers, M. E.; Shultz, A. R.; Ward, T. C.; McGrath, J. E., Molecular Weight Characterization of Soluble High Performance Polyimides. 1. Polymer-Solvent-Stationary Phase Interactions in Size Exclusion Chromatography. *Journal of Polymer Science Part B: Polymer Physics* **1995,** *33* (10), 1429-1439.
122. Jiang, H.; Yin, Q.; Zhou, M.; Pan, D., Effect of Ultra High Molecular Weight Polyacrylonitrile (UHMW-PAN) on the Rheological Behavior of PAN/DMSO Solution. *Adv. Mat. Res.* **2012,** *430-432*, 687-691.
123. Kang, J. S.; Lee, Y. M., Effects of Molecular Weight of Polyvinylpyrrolidone on Precipitation Kinetics During the Formation of Asymmetric Polyacrylonitrile Membrane. *J. Appl. Polym. Sci.* **2001,** *85* (1).

124. Zhang, X.; Liu, T.; Sreekumar, T. V.; Kumar, S.; Hu, X.; Smith, K., Gel Spinning of PVA/SWNT Composite Fiber. *Polymer* **2004,** *45*, 8801-8807.
125. Smith, P.; Lemstra, P. J., Ultra-High Strength Polyethylene Filaments by Solution Spinning/Drawing. *J. Mater. Sci.* **1980,** *15*, 505-514.
126. Sawai, D.; Fujii, Y.; Kanamoto, T., Development of Oriented Morphology and Tensile Properties Upon Superdrawing of Solution-Spun Fibers of Ultra-High Molecular Weight Poly(acrylonitrile). *Polymer* **2006,** *47*, 4445-4453.
127. Tsai, J. S.; Su, W. C., Control of Cross-Section Shape for Polyacrylonitrile Fibre During Wet-Spinning. *J. Mater. Sci. Lett.* **1991,** *10*, 1253-1256.
128. Wang, Y. X.; Wang, C. G.; Yu, M. J., Effects of Different Coagulation Conditions on Polyacrylonitrile Fibers Wet Spun in a System of Dimethylsulphoxide and Water. *J. Appl. Polym. Sci.* **2006,** *104*, 3723-3729.
129. Knudsen, J., The Influence of Coagulation Variables on the Structure and Physical Properties of an Acrylic Fiber. *Text. Res. J.* **1963,** *33* (1), 13-20.
130. Zeng, X.; Chen, J.; Zhao, J.; Wu, C.; Pan, D.; Pan, N., Investigation the Jet Stretch in PAN Fiber Dry-Jet Wet Spinning for PAN-DMSO-H2O System. *J. Appl. Polym. Sci.* **2009,** *114*, 3621-3625.
131. Liu, S.; Tan, L.; Pan, D.; Chen, T., Gel Spinning of Polyacrylonitrile Fibers with Medium Molecular Weight. *Polym. Int.* **2010,** *60*, 453-457.
132. Widjojo, N.; Chung, T. S., Thickness and Air Gap Dependence of Macrovoid Evolution in Phase-Inversion Asymmetric Hollow Fiber Membranes. *Industrial and Engineering Chemistry Research* **2006,** *45*, 7618-7626.
133. Chung, T. S.; Hu, X., Effect of Air-Gap Distance on the Morphology and Thermal Properties of Polyethersulfone Hollow Fibers. *J. Appl. Polym. Sci.* **1997,** *66*, 1067-1077.
134. Tsai, H. A.; Kuo, C. Y.; Lin, J. H.; Wang, D. M.; Deratani, A.; Pochat-Bohatier, C.; Lee, K. R.; Lai, J. Y., Morphology Control of Polysulfone Hollow Fiber Membranes via Water Vapor Induced Phase Separation. *J. Membr. Sci.* **2006,** *278*, 390-400.
135. Morris, A. Bench-Scale, Multifilament Spinning Conditions Effect on the Structure and Properties of Polyacrylonitrile Precursor Fiber. Master's Thesis, University of Kentucky, Lexington, 2011
136. Nohara, L. B.; Filho, G. P.; Nohara, E. L.; Kleinke, M. U.; Rezende, M. C., Evaluation of Carbon Fiber Surface Treated by Chemical and Cold Plasma Processes. *Materials Research* **2005,** *8* (3), 281-286.
137. Wang, Q. F.; Wang, C. G.; Yu, M.; Ma, J.; Hu, X. Y.; Zhu, B., Microstructure of Fibrils Separated from Polyacrylonitrile Fibers by Ultrasonic Etching. *Science in China, Series E Technological Sciences* **2010,** *53* (6), 1489-1494.
138. Leon y Leon, C. A. Carbon Fiber Having Improved Strength and Modulus and an Associated Method and Apparatus for Preparing the Same. 2084314 A2, 2009.
139. Kobashi, T.; Takao, S. High Strength Polyacrylonitrile Fiber and Method of Producing the Same. 4,535,027, 1985.
140. Rahaman, M. S. A.; Ismail, A. F.; Mustafa, A., A Review of Heat Treatment on Polyacrylonitrile Fiber. *Polym. Degrad. Stab.* **2007,** *92*, 1421-1432.
141. Damodaran, S.; Desai, P.; Abhiraman, A. S., Chemical and Physical Aspects of the Formation of Carbon Fibres from PAN-Based Precursors. *Journal of the Textile Institute* **1990,** *81* (4), 384-420.

142. Henrici-Olive, G.; Olive, S., The Chemistry of Carbon Fiber Formation from Polyacrylonitrile. *Adv. Polym. Sci.* **1983,** *51*, 1-60.
143. Gupta, A. K.; Paliwal, D. K.; Bajaj, P., Acrylic Precursors for Carbon Fibers. *J. Macromol. Sci., Part B: Polym. Rev.* **1991,** *C31* (1), 1-89.
144. Farsani, R. E. In *Production of Carbon Fibers from Acrylic Fibers*, International Conference on Chemical, Civil, and Environment Engineering, Dubai, March 24-25; Dubai, 2012; pp 310-312.
145. Matsuhisa, Y.; Kibayashi, M.; Yamasaki, K.; Okuda, A. Carbon Fibers, Acrylic Fibers and Process for Producing the Acrylic Fibers. 6,438,892 B2, 2002.
146. Wangxi, Z.; Jie, L.; Gang, W., Evolution of Structure and Properties of PAN Precursors During their Conversion to Carbon Fibers. *Carbon* **2003,** *41*, 2805-2812.
147. Ohsaki, T.; Imai, K.; Miyahara, N. Process for Preparing a Carbon Fiber of High Strength. 4,925,604, 1990.
148. Griffith, A. A., The Phenomena of Rupture and Flow in Solids. *Philos. Trans. R. Soc. London, A* **1921,** *221*, 163-198.
149. Sawai, D.; Yamane, A.; Takahashi, H.; Kanamoto, T.; Ito, M.; Porter, R. S., Development of High Ductility and Tensile Properties by a Two-Stage Draw of Poly(acrylonitrile): Effect of Molecular Weight. *J. Polym. Sci., Part B: Polym. Phys.* **1998,** *36*, 629-640.
150. Fox, T. G.; Flory, P. J., Further Studies on the Melt Viscosity of Polyisobutylene. *Journal of Physical and Colloid Chemistry* **1951,** *55* (221).
151. Frank, E.; Hermanutz, F.; Buchmeiser, M. R., Carbon Fibers: Precursors, Manufacturing, and Properties. *Macromol. Mater. Eng.* **2012,** *297*, 493-501.
152. Huang, X., Fabrication and properties of carbon fibers. *Materials* **2009,** *2*, 2369-2403.
153. Kubo, S.; Uraki, Y.; Sano, Y., Preparation of carbon fibers from softwood lignin by atmospheric acetic acid pulping. *Carbon* **1998,** *36*, 1119-1124.
154. Ito, S.; Kawai, Y.; Oshita, T., Studies on continuous polymerization of acrylonitrile in aqueous medium at low water-to-monomer ratio. V. Effects of agitation on the polymer properties and polymerization behavior in acrylonitrile polymerization. *Kobunshi Ronbunshu* **1986,** *43*, 345-351.
155. Ito, S.; Plant, O., On loci of acrylonitrile polymerization with bisulfite-persulfate initiators under the conditions of low water/monomer ratio. *J. Appl. Polym. Sci.* **1986,** *31*, 849-859.
156. Ito, S., Studies on continuous polymerization of acrylonitrile in aqueous medium under the condition of low water to monomer ratio. IV. Effects of electrolyte on some properties of polymer in continuous copolymerization of acrylonitrile with vinyl acetate in aqueous medium. *Kobunshi Ronbunshu* **1986,** *43*, 1-8.
157. Henrici-Olive, G.; Olive, S., Molecular interactions and macroscopic properties of polyacrylonitrile and model substances. *Adv. Polym. Sci.* **1979,** *32*, 123-152.
158. Hopfinger, A. J., *Conformational Properties of Macromolecules*. Academic: 1973.
159. Bohn, C. R.; Schaefgen, J. R.; Statton, W. O., Laterally ordered polymers: polyacrylonitrile and poly-(vinyl trifluoroacetate). *J. Polym. Sci.* **1961,** *55*, 531-549.
160. Imai, Y.; Minami, S.; Yoshihara, T.; Joh, Y.; Sato, H., Preparation and chracterization of amorphous polyacrylonitrile. *J. Polym. Sci., Part B* **1970,** *8*, 281-288.
161. Joh, Y., Amorphous polyacrylonitrile: synthesis and characterization. *J. Polym. Sci., Polym. Chem. Ed.* **1979,** *17*, 4051-4067.

162. Gupta, A. K.; Chand, N.; Singh, R.; Mansingh, A., Dielectric study of polyacrylonitrile, poly-2-hydroxyethyl methacrylate and their copolymers. *European Polymer Journal* **1979,** *15* (2), 129-136.
163. Colvin, B. G.; Storr, P., The crystal structure of polyacrylonitrile. *European Polymer Journal* **1974,** *10* (4), 337-340.
164. Coxe, C. D., Preparation of shaped articles from acrylonitrile polymers. Google Patents: 1952.
165. Hinrichsen, G., *Angew Macromol. Chem.* **1974,** *20*.
166. Bashir, Z.; Church, S. P.; Waldron, D., Interaction of water and hydrated crystallization in water-plasticized polyacrylonitrile films. *Polymer* **1994,** *35*, 967-976.
167. Striegel, A. Y., Wallace; Kirkland, Joseph; Bly, Donald, *Modern Size-Exclusion Liquid Chromatography*. 2nd ed.; John Wiley & Sons, Inc: Hoboken, New Jersey, 2009.
168. Hinrichsen, G., Structural changes of drawn polyacrylonitrile during annealing. *Journal of Polymer Science Part C: Polymer Symposia* **1972,** *38* (1), 303-314.
169. Matsuhisa, Y.; Kibayashi, M.; Yamasaki, K.; Okuda, A. Carbon fiber reinforcing materials with increased resin-impregnated strand strength and acrylic fiber precursors therefor and manufacture of them. WO9745576A1, 1997.
170. Holland, V. F.; Mitchell, S. B.; Hunter, W. L.; Lindenmeyer, P. H., Crystal structure and morphology of polyacrylonitrile in dilute solution. *J. Polym. Sci.* **1962,** *62*, 145-151.
171. Minagawa, M.; Taira, T.; Yabuta, Y.; Nozaki, K.; Yoshii, F., An Anomalous Tacticity-Crystallinity Relationship: A WAXD Study of Stereoregular Isotactic (83-25%) Poly(Acrylonitrile) Powder Prepared by Urea Clathrate Polymerization. *Macromolecules* **2001,** *34*, 3679-3683.
172. Hutchinson, S. R.; Tonelli, A. E.; Gupta, B. S.; Buchanan, D. R., An investigation of the structure-property relationships in melt-processable high-acrylonitrile copolymer filaments. *J. Mater. Sci.* **2008,** *43*, 5143-5156.
173. Alexander, L., X-ray diffraction methods in polymer science. *J Mater Sci* **1971,** *6* (1), 93-93.
174. Chapiro, A.; Mankowski, Z., The influence of solvents on molecular association and on the kinetics of acrylonitrile polymerization. Supplementary evidence for the matrix effect. *Eur. Polym. J.* **1981,** *17*, 457-472.
175. Warner, S. B.; Uhlmann, D. R.; Peebles, L. H., Jr., Oxidative stabilization of acrylic fibers. Part 3. Morphology of polyacrylonitrile. *J. Mater. Sci.* **1979,** *14*, 1893-1900.
176. Kulshreshtha, A. K.; Garg, V. N.; Sharma, Y. N.; Dweltz, N. E., Effect of comonomer content and annealing on morphological changes in acrylic copolymers and fibers. *Journal of Applied Polymer Science* **1986,** *31* (5), 1413-1424.
177. Bang, Y. H.; Lee, S.; Cho, H. H., Effect of methyl acrylate composition on the microstructure changes of high molecular weight polyacrylonitrile for heat treatment. *Journal of Applied Polymer Science* **1998,** *68* (13), 2205-2213.
178. Electroconductive acrylic fibers. JP56009426A, 1981.
179. Edie, D. D., *Carbon* **1998,** *36* (4), 7.
180. Selivansky, D., Interaction of water with poly(acrylonitrile): correlation between clustering, phase separation, and the melting point. *Macromolecules* **1985,** *18*, 583.
181. Dorsey, N. E., *Properties of Ordinary Water-Substance*. Reinhold Publishing Corp.
182. Carr, A. R.; Townsend, R. E.; Badger, W. L., Vapor pressures of glycerol-water and glycerol-water-sodium chloride systems. *Ind. Eng. Chem.* **1925,** *17*, 643-647.

183. Gilli, P.; Pretto, L.; Bertolasi, V.; Gilli, G., Predicting Hydrogen-Bond Strengths from Acid-Base Molecular Properties. The pKa Slide Rule: Toward the Solution of a Long-Lasting Problem. *Acc. Chem. Res.* **2009,** *42*, 33-44.
184. Michaulis, L.; Rona, P., The Dissociation Constants of some Very Weak Acids, Particularly the Carbohydrates, Measured Electrolytically. *Biochem. Z.* **1913,** *49*, 232-248.
185. Minagawa, M.; Kanoh, H.; Tanno, S.; Satoh, M., Glass transition temperature (Tg) of free-radically prepared polyacrylonitrile by inverse gas chromatography. 2. Molecular-weight dependence of Tg of two different types of aqueous polymers. *Macromol. Chem. Phys.* **2002,** *203*, 2481-2487.
186. Daumit, G. P. K., Y.S.; Slater, C.R.; Venner, J.G.; Young, C.C. 49355180, 1990.
187. Z, B., *Carbon* **1991,** *29*.
188. Flory, P. J., Thermodynamics of crystallization in high polymers. IV. A theory of crystalline states and fusion in polymers, copolymers, and their mixtures with diluents. *J. Chem. Phys.* **1949,** *17*, 223-240.
189. Iwatsuki, S.; Shin, M.; Yamashita, Y., Radical terpolymerization of dodecyl vinyl ether, fumaronitrile, and β-chloroethyl acrylate. *Makromol. Chem.* **1967,** *102*, 232-244.
190. Dorokhina, I. S.; Klimenkov, V. S.; Abkin, A. D., Study of the copolymerization of acrylonitrile and vinyl acetate in connection with the synthesis of fibrous materials. II. Fiber-forming copolymers of acrylonitrile and vinyl acetate. *Khim. Volokna* **1962**, 16-21.
191. Godshall, D. R., P.; Baird, D.G.; Wilkes, G.L.; Bhanu, V.A.; McGrath, J.E., *Polymer* **2002,** *44*, 17.
192. Rangarajan, P. B., V.A.; Godshall, D.; Wilkes, G.L.; mcGrath, J.E>; Baird, D.G., *Polymer* **2002,** *43*.
193. V.A. Bhanu, p. R., K.Wiles, m.Bortner, M.Sankarpandian, D.Godshall, T.E.Glass, A.K. Banthia, j.Yang, G.Wilkes, d.Baird, J.E. McGrath, Syntheis and characterization of acrylonitrile and methyl acrylate statistical copolymers as melt processible carbon fiber precursors. *Polymer* **2002,** *43*, 10.
194. Bhanu, V. A.; Rangarajan, P.; Wiles, K.; Bortner, M.; Sankarpandian, M.; Godshall, D.; Glass, T. E.; Banthia, A. K.; Yang, J.; Wilkes, G.; Baird, D.; McGrath, J. E., Synthesis and characterization of acrylonitrile methyl acrylate statistical copolymers as melt processable carbon fiber precursors. *Polymer* **2002,** *43* (18), 4841-4850.
195. Rangarajan, P.; Bhanu, V. A.; Godshall, D.; Wilkes, G. L.; McGrath, J. E.; Baird, D. G., Dynamic oscillatory shear properties of potentially melt processable high acrylonitrile terpolymers. *Polymer* **2002,** *43* (9), 2699-2709.
196. Mukundan, T.; Bhanu, V. A.; Wiles, K. B.; Johnson, H.; Bortner, M.; Baird, D. G.; Naskar, A. K.; Ogale, A. A.; Edie, D. D.; McGrath, J. E., A photocrosslinkable melt processible acrylonitrile terpolymer as carbon fiber precursor. *Polymer* **2006,** *47*, 4163-4171.
197. Bhanu, V. A.; Bortner, M.; Mukundan, T.; Glass, T. E.; Baird, D. G.; McGrath, J. E., Study of the accelerating effect of water in the copolymerization of acrylonitrile with methyl acrylate in emulsion and solution processes. *Polym. Prepr. (Am. Chem. Soc., Div. Polym. Chem.)* **2003,** *44*, 1067-1068.
198. Bhanu, V. A. W., K.B.; Banthia, A.K.; Mansuri, A.; Sankarpandian, M.; Rangarajan, P.; Glass,T.E.; Baird, D.G.; Wiles, G.L.; McGrath, J.E., *Polym Prepr* **2001,** *42*.

199. Bhanu, V. A.; Wiles, K. B.; Bortner, M.; Godshall, D.; Glass, T. E.; Baird, D. G.; Wilkes, G. L.; McGrath, J. E., Synthesis and rheological study of polyacrylonitrile copolymer carbon fiber precursors using cost effective water based synthesis routes. *Polym. Prepr. (Am. Chem. Soc., Div. Polym. Chem.)* **2002,** *43*, 674-675.
200. Kwon, Y. D.; Kavesh, S.; Prevorsek, D. C. Acrylic fiber with high tenacity and modulus. EP144793A2, 1985.
201. Wu, Q.-Y.; Chen, X.-N.; Wan, L.-S.; Xu, Z.-K., Interactions between Polyacrylonitrile and Solvents: Density Functional Theory Study and Two-Dimensional Infrared Correlation Analysis. *J. Phys. Chem. B* **2012,** *116*, 8321-8330.